

**MEASUREMENTS OF MOISTURE SUCTION IN  
HOT MIX ASPHALT MIXES**

A Thesis

by

EMAD ABDEL-RAHMAN KASSEM

Submitted to the Office of Graduate Studies of  
Texas A&M University  
in partial fulfillment of the requirements for the degree of

MASTER OF SCIENCE

August 2005

Major Subject: Civil Engineering

**MEASUREMENTS OF MOISTURE SUCTION IN  
HOT MIX ASPHALT MIXES**

A Thesis

by

EMAD ABDEL-RAHMAN KASSEM

Submitted to the Office of Graduate Studies of  
Texas A&M University  
in partial fulfillment of the requirements for the degree of

MASTER OF SCIENCE

Approved by:

Chair of Committee,	Eyad Masad
Committee Members,	Robert Lytton
	Charles Glover
Head of Department,	David Rosowsky

August 2005

Major Subject: Civil Engineering

## ABSTRACT

Measurements of Moisture Suction in Hot Mix Asphalt Mixes. (August 2005)

Emad Abel-Rahman Kassem, B.S., Zagazig University, Zagazig, Egypt

Chair of Advisory Committee: Dr. Eyad Masad

The presence of moisture in hot mix asphalt (HMA) causes loss of strength and durability of the mix, which is referred to as moisture damage. This study deals with the development of experimental methods for measuring total suction in HMA, which can be defined as the free energy state of water in HMA mixes. The total suction is related to the ability of moisture to get into the mix under unsaturated conditions; it is also related to the ability of the mix to retain moisture.

Soil suction has been studied extensively. However, suction in HMA as a porous material and its relationship to moisture damage have not been studied. The development of a procedure to measure the total suction in HMA mixes is the first objective of this research. The second objective is to relate suction measurements to physical and chemical properties of the mixtures. The objectives were achieved in two phases. In the first phase, the total suction was measured in HMA specimens with different types of aggregates (limestone and granite), and with different air void distributions and aggregate gradations. The results of this phase showed that the drying test using a 60 °C temperature-controlled room is the proper setup for measuring the total suction in HMA using thermocouple psychrometers. The characteristics of suction-moisture content curves were found to be related to the air void distribution in HMA. In the second phase, total suction was measured in sand asphalt specimens. These specimens had different

combinations of aggregates and binders with different bond energies and exhibited different field performance in terms of resistance to moisture damage. The suction measurements in sand asphalt specimens were used to calculate the moisture diffusion coefficient. The results revealed that water diffused into sand asphalt specimens that are known to have poor resistance to moisture damage faster than those that are known to have good resistance to moisture damage

**DEDICATION**

To my grandmother for her prayers

To my parents for their patience in my absence

To my brother, Dr. Ahmed Kassem, for his unconditional support

## ACKNOWLEDGEMENTS

I would like to express my sincere appreciation and gratitude to my advisor and committee chair, Dr. Eyad Masad, for his guidance, encouragement, support, patience, and generosity. Dr. Masad's friendly relationship with his students is incomparable, as is his appreciation of their hard work.

I would like to thank Dr. Robert Lytton and Dr. Charles Glover for serving as members of my graduate committee. Dr. Robert Lytton has taught me the basic concepts of my research, and his courses provided me with extensive knowledge in the materials and pavements area.

My gratitude is extended to Dr. Rifat Bulut for his help during the laboratory tests. His guidance and encouragement were really needed during my research.

Special thanks go to Dr. Taleb Al-Rousan for his encouragement throughout my study at Texas A&M University. I deeply value his friendship.

## TABLE OF CONTENTS

	Page
ABSTRACT.....	iii
DEDICATION.....	v
ACKNOWLEDGEMENTS.....	vi
TABLE OF CONTENTS.....	vii
LIST OF TABLES.....	x
LIST OF FIGURES.....	xii
 CHAPTER	
I INTRODUCTION.....	1
1.1 Overview.....	1
1.2 Problem Statement and Objectives.....	1
1.3 Research Tasks.....	3
1.4 Organization of the Study.....	5
II LITERATURE REVIEW.....	6
2.1 Introduction.....	6
2.2 HMA Moisture Damage.....	6
2.3 Suction Concept.....	7
2.4 Soil Suction Measuring Devices.....	12
2.5 Measurements of Suction Using Psychrometers.....	13
2.5.1 Concept and Experimental Procedure.....	13
2.5.2 Psychrometer Calibration.....	20
2.6 The Tube Suction Test.....	23
III EXPERIMENTS AND RESULTS.....	27
3.1 Introduction.....	27
3.2 Development of a Procedure for Measuring the Total Suction in HMA Mixes.....	27
3.2.1 Psychrometer Calibration.....	27
3.2.2 Measuring Suction Using the Wetting Protocol.....	33
3.2.3 Measuring Suction Using the Drying Protocol.....	38
3.2.3.1 Drying Test under Room Temperature.....	38
3.2.3.2 Drying Test Using Temperature-Controlled Room.....	40

CHAPTER	Page
3.3 Results and Analysis .....	44
3.3.1 Wetting Protocol .....	44
3.3.2 Drying Test under Room Temperature .....	50
3.3.3 Drying Test Using Temperature-Controlled Room .....	50
3.3.3.1 Description of HMA Specimens .....	50
3.3.3.2 Interpretation of Microvolt Outputs .....	56
3.3.3.3 Total Suction Results .....	59
3.3.3.4 Water Content .....	60
3.3.3.5 Analysis of Total Suction Measurements .....	62
3.3.3.6 The Relationship between Total Suction and Moisture Damage .....	66
3.4 Using TST to Assess the Moisture Susceptibility in HMA Mixes .....	68
3.4.1 Results of the TST .....	72
 IV DETERMINATION OF THE DIFFUSION COEFFICIENT .....	 74
4.1 Introduction .....	74
4.2 The Moisture Diffusion Concept .....	74
4.3 Determination of Diffusion Coefficient, $\alpha$ .....	79
4.3.1 The Soaking Test Procedure for Determination of $\alpha$ .....	79
4.4 Determination of the Diffusion Coefficient in Sand Asphalt .....	80
4.4.1 Specimens Preparation .....	80
4.4.2 Testing Apparatus and Measurement Setup .....	85
4.4.3 Results and Analysis .....	88
4.4.3.1 Suction Measurements .....	88
4.4.3.2 Analysis of Suction Measurements .....	89
4.4.3.3 Relationship of Suction and Diffusion Coefficient to Surface Energy and DMA Results .....	92
 V CONCLUSIONS AND RECOMMENDATIONS .....	 98
5.1 Conclusions .....	98
5.2 Recommendations .....	99
 REFERENCES .....	 100
 APPENDIX A .....	 103
 APPENDIX B .....	 105
 APPENDIX C .....	 110
 APPENDIX D .....	 117



	Page
APPENDIX E .....	131
VITA.....	135

## LIST OF TABLES

	Page
Table 1. Devices Used to Measure Total, Matric, and Osmotic Suctions in Soils .....	12
Table 2. Osmotic Coefficients of Several Salt Solutions.....	22
Table 3. Osmotic Suctions of Several Salt Solutions .....	23
Table 4. NaCl Osmotic Suctions for Psychrometer Calibration .....	28
Table 5. Granite Mixture Gradation.....	51
Table 6. Limestone Mixture Gradation.....	51
Table 7. Quartiles of Air Void Size Distribution.....	52
Table 8. Average Total Suction Values in Bar for Limestone Specimens .....	60
Table 9. Average Total Suction Values in Bar for Granite Specimens .....	60
Table 10. Water Content in Percent in Limestone Specimens.....	61
Table 11. Water Content in Percent in Granite Specimens .....	61
Table 12. Mixture 4 Gradation.....	82
Table 13. Mixture 7 Gradation.....	83
Table 14. Mixture 8 Gradation.....	83
Table 15. Mixture Descriptions .....	84
Table 16. Aggregate Gradation for Sand Asphalt Mixtures 7 and 8 .....	84
Table 17. Aggregate Gradation for Sand Asphalt Mixture 4.....	84
Table 18. Aggregate Composition of Test Specimens.....	85
Table 19. The Average Elapsed Time for Total Suction to Drop to Psychrometer's Range .....	90
Table 20. Diffusion Coefficient $\alpha$ for Mixes 8, 7, and 4.....	92

	Page
Table 21. Surface Energy Components of Aggregates.....	93
Table 22. Surface Energy Components of Asphalts for Wetting.....	93
Table 23. Mixture Rankings According to Adhesive Wetting Bond Energy under Both Dry and Wet Conditions.....	94
Table 24. Mixture Rankings According to Average Fatigue Life in Both Dry and Wet Conditions .....	94

## LIST OF FIGURES

	Page
Fig. 1. Total Suction versus Relative Humidity.....	10
Fig. 2. Total Suction and Relative Humidity Relationship.....	10
Fig. 3. Total, Matric, and Osmotic Suctions for Glacial Till.....	11
Fig. 4. Seebeck Effect.....	14
Fig. 5. Peltier Effect.....	14
Fig. 6. Stainless Steel Screen Thermocouple Psychrometer.....	16
Fig. 7. Cover Materials and Equilibration Times for Thermocouple Psychrometer .....	16
Fig. 8. HR-33T Microvoltmeter.....	17
Fig. 9. CR-7 Datalogger.....	19
Fig. 10. Percometer Device.....	24
Fig. 11. TST Setup and TST Results .....	26
Fig. 12. Thermocouple Psychrometer.....	28
Fig. 13. Psychrometers Suspended in Calibration Solution.....	30
Fig. 14. Temperature Controller to Maintain Temperature during Calibration.....	31
Fig. 15. Relationship between Microvolt Outputs and Total Suction.....	32
Fig. 16. Calibration Curve of Thermocouple Psychrometer.....	32
Fig. 17. HMA Specimen with Three Holes for Psychrometers .....	34
Fig. 18. Inserting Psychrometer in HMA Hole.....	34
Fig. 19. Filling Holes with Filler .....	35
Fig. 20. Covering Holes with Plastic Tape .....	35
Fig. 21. Three Psychrometers Inserted in HMA Specimen. ....	36

	Page
Fig. 22. Wrapping HMA Specimen with Two Layers of Plastic Clear Wrap .....	36
Fig. 23. Wrapping HMA Specimen with Aluminum Foil and Supported with Plastic Tape.....	37
Fig. 24. Placing HMA Specimens in Bath of Water.....	37
Fig. 25. Box Used in Drying Test.....	39
Fig. 26. HMA Specimen with One Uncovered Surface Covered with Packing Foam Material.....	39
Fig. 27. HMA Specimen Placed in Plastic Mold.....	41
Fig. 28. Temperature-Controlled System (Temperature Regulator, Water in Ice Chest, and Plastic Mold).....	42
Fig. 29. CR-7 Datalogger with 40 Openings for Psychrometers .....	42
Fig. 30. Psychrometers Connected to CR-7 Datalogger.....	43
Fig. 31. Computer Connected to CR-7 Datalogger.....	43
Fig. 32. Wetting Test Setup .....	44
Fig. 33. Total Suction versus Time (Specimen 1) .....	45
Fig. 34. Total Suction versus Time (Specimen 2) .....	45
Fig. 35. Total Suction versus Time (Specimen 3) .....	46
Fig. 36 Total Suction versus Time (Specimen 4) .....	46
Fig. 37. Total Suction versus Time (Specimen 5) .....	47
Fig. 38. Total Suction versus Time (Specimen 6) .....	47
Fig. 39. Microvolt Outputs Recorded by Psychrometer 1 .....	48
Fig. 40. Microvolt Outputs Recorded by Psychrometer 2 .....	49

	Page
Fig. 41. Microvolt Outputs Recorded by Psychrometer 3 .....	49
Fig. 42. Quartile Air Void Size Difference between Granite and Limestone.....	53
Fig. 43. Distributions and Three Dimensional Visualization of Air Voids (a) WR-C1 and (b) GA-C1 .....	54
Fig. 44. $N_f$ Ratio and Average Diameter: (a) Limestone and (b) Granite.....	55
Fig. 45. Microvolt Outputs after Stage 1 .....	57
Fig. 46. Microvolt Outputs after Stage 2 .....	57
Fig. 47. Microvolt Outputs after Stage 3 .....	58
Fig. 48. Microvolt Outputs after Stage 4 .....	58
Fig. 49. Microvolt Outputs after Stage 5 .....	59
Fig. 50. Weights of Absorbed Water, Lost Water, and Stored Water in Mixes .....	62
Fig. 51. Relationship between Water Content and Total Suction in Limestone Specimens .....	64
Fig. 52. Relationship between Water Content and Total Suction in Granite Specimens .....	65
Fig. 53. Effect of Tube Radii on Radius of Curvature.....	65
Fig. 54. Relationship between Moisture Damage and Total Suction in Limestone Mixes.....	67
Fig. 55. Relationship between Moisture Damage and Total Suction in Granite Mixes.....	67
Fig. 56. Specimen Wrapped with Plastic Wrap .....	69
Fig. 57. Specimen Wrapped with Aluminum Foil.....	69

	Page
Fig. 58. Plastic Tape Is Used to Fasten the Wrap .....	70
Fig. 59. Porous Stones Placed in Bath of Water .....	70
Fig. 60. HMA Mixes Placed over Porous Stones in Bath of Water.....	71
Fig. 61. Percometer Used to Record Dielectric Values .....	71
Fig. 62. TST Results of HMA Mixes.....	73
Fig. 63. Incremental Section with Dimensions $\Delta x$ , $\Delta y$ , and $\Delta z$ .....	76
Fig. 64. Soaking Test Setup for Determination of $\alpha$ .....	79
Fig. 65. Gyrotory Specimen after Coring of Test Specimens.....	85
Fig. 66. Sand Asphalt Specimens after Coring Gyrotory Compacted Mixes .....	86
Fig. 67. Schematic View of Drilled Sand Asphalt Specimen.....	86
Fig. 68. Cross Section at Center of Drilled Sand Asphalt Specimen.....	87
Fig. 69. Inserting Psychrometer .....	87
Fig. 70. Sealing Hole and Covering Upper Side with Silicon Glue .....	87
Fig. 71. Microvolt Outputs from Soaking Test versus Time .....	89
Fig. 72. Elapsed Time for Total Suction to Drop to Psychrometer's Range, and Average Diffusion Coefficient, $\alpha$ .....	95
Fig. 73. Asphalt Sand Specimen Mounted in DMA .....	95
Fig. 74. Elapsed Time, Diffusion Coefficient ( $\alpha$ ), and Adhesive Wetting Bond Energy .....	96
Fig. 75. Elapsed Time, Diffusion Coefficient ( $\alpha$ ), and DMA Results .....	97

# CHAPTER I

## INTRODUCTION

### 1.1 Overview

The presence of moisture in hot mix asphalt (HMA) causes loss of strength and durability, which is referred to as moisture damage. Moisture damage can be caused by the debonding between asphalt binder and aggregate, referred to as adhesive failure. Moisture damage is also associated with cohesive failure, which refers to the loss of bond within the binder.

Suction is a measure of the free energy state of water in materials. Suction is a well-known term in soil science and geotechnical engineering. The change in soil's suction due to the variation of the water content causes swelling or shrinking of soils. The movement of moisture through unsaturated soils is a function of the diffusion coefficient. However, the concept of suction in HMA is fairly new. Suction in HMA is believed to be a function of all factors that influence the presence of moisture in HMA. These factors include air void distribution, particle size distribution, binder cohesive energy, and aggregate-binder adhesive energy. This study looks at the effect of these factors on the total suction in HMA by measuring suction and determining the diffusion coefficient of different HMA mixes and sand asphalt.

### 1.2 Problem Statement and Objectives

Moisture damage deteriorates the pavement structures as it causes loss of strength

---

This thesis follows the style and format of the *Journal of Materials in Civil Engineering*.



and durability of the mix. Many studies have been conducted to develop methods to characterize and minimize moisture damage in asphalt pavements. This study focuses on the assessment of HMA moisture susceptibility using the suction concept. The development of an experimental procedure to measure HMA suction is the first objective of this research. Several different experimental setups were evaluated, and a new procedure for measuring moisture suction in HMA was developed.

The second objective is to investigate the relationship between suction, material physical and chemical properties, and moisture damage. This objective was achieved in two phases. In the first phase, suction was measured in HMA specimens with two different aggregate types (limestone and granite) with different gradations. Field experience has shown that the limestone mix has very good resistance to moisture damage, while the granite mix has poor resistance to moisture damage. Also, experimental measurements of moisture damage that were conducted at the University of Florida identified the relationship between the aggregate gradations of these mixes and moisture damage. In the second phase, sand asphalt specimens were prepared from combinations of aggregate and binders with different bond energies and field performance in terms of resistance to moisture damage. The suction measurements were used to calculate the diffusion coefficient, which quantifies the movement of the moisture in sand asphalt. These diffusion coefficients were related to the resistance of sand asphalt specimens to moisture damage.

### 1.3 Research Tasks

The tasks carried out in this study can be summarized as follows:

- Task 1: Literature Review

A comprehensive literature review was conducted to determine the proper methods to measure suction in HMA. This literature review focuses on the methods that have been used to measure soil suction. The discussion focuses on the accuracy of these methods, their applicability to HMA mixes, the components of suction that can be measured, and finally the range of suction that can be measured.

- Task 2: Measuring Moisture Content in HMA Using the Tube Suction Test (TST)

Based on the findings of the literature review, the ability of the tube suction test to assess moisture susceptibility in HMA was evaluated in the second task of this study. TST is used to evaluate the moisture susceptibility of granular bases in pavements.

- Task 3: Measuring Suction in HMA Using Psychrometers

The ability to measure HMA suction using psychrometers in conjunction with different drying and wetting mechanisms was evaluated in this study.

- Sub-task 3.1: Psychrometer Calibration

Before the suction in HMA mixes could be measured, psychrometers needed to be calibrated. The calibration of a psychrometer consists of

determining the relationship between microvolt outputs from the thermocouple psychrometers and a known total suction value.

- Sub-task 3.2: Experimental Measurements

Psychrometers were used to conduct two sets of measurements. The first set was on HMA specimens with two different aggregate types (limestone and granite) and a number of gradations with known field and laboratory performance in terms of resistance to moisture damage. The second set of measurements was conducted on sand asphalt specimens that were prepared from combinations of aggregate and binders with different bond energies and resistance to moisture damage. These suction measurements were used to calculate the diffusion coefficient, which quantifies the movement of the moisture in sand asphalt specimens.

- Task 4: Results and Analysis

The results of task 3 were analyzed in order to determine:

- the relationship of suction to air void distribution, aggregate size distribution, and aggregate type in HMA mixes;
- the relationship of total suction to the resistance to moisture damage;
- the influence of binder cohesive energy and aggregate-binder adhesive energy on suction and moisture damage; and
- the relationship between the diffusion coefficient and moisture damage.

## 1.4 Organization of the Study

Chapter I of this thesis presents an overview of this study. It includes the problem statement, objectives, tasks, and study organization. Chapter II documents the literature review of the methods used to measure suction in soils. In this chapter the thermocouple psychrometer, which is used to measure the suction in soils, and TST, which is used to evaluate the moisture susceptibility of granular bases in pavements, are discussed.

Chapter III includes the test procedures that were used in this study for measuring suction in HMA specimens with two different aggregate types (limestone and granite) and different gradations. In addition, this chapter includes the analysis of the total suction measurements. Chapter IV presents the test setup for measuring suction in sand asphalt specimens. It also includes the calculations of the diffusion coefficient  $\alpha$  in sand asphalt specimens.

Chapter V summarizes the results of measuring the total suction in HMA mixes and sand asphalt, and of calculating the diffusion coefficient in sand asphalt. It also presents a summary of findings in regard to the effect of different factors on suction; these factors include air void distribution, particle size distribution, binder cohesive energy, and aggregate-binder adhesive energy. Finally, recommendations are presented based on the results of the study.

## CHAPTER II

### LITERATURE REVIEW

#### 2.1 Introduction

Although suction has been studied in soils for a long time, it is a fairly new concept in HMA mixes. Suction in HMA is believed to be a function of a number of factors that influence the presence of moisture in HMA. These factors include air void distribution, particle size distribution, binder cohesive energy, aggregate-binder adhesive energy, and fluid composition. While some methods have been used to measure suction in soils, there is no established method to measure suction in HMA. In this chapter, the causes of moisture damage, definition of suction, and methods that have been used to measure suction will be presented.

#### 2.2 HMA Moisture Damage

Moisture damage can be defined as the loss of strength and durability of HMA. The presence of moisture between the aggregate and binder could break down the adhesive bond causing stripping; this type of failure is known as adhesive failure. Moisture can break the bonding within the binder itself causing cohesive failure.

There are some ways to reduce moisture damage. Providing the pavement structure with an adequate drainage system will reduce the moisture in the pavement structure. Compaction is an important factor in reducing moisture damage, as the infiltrated water to the mix can be decreased with an adequate compaction level. The surface energies of aggregate and binder are very important factors that influence the HMA resistance to fracture due to moisture damage. Lytton (2005a) showed that in order

to provide adequate cohesive and adhesive bond strengths in the HMA, the surface energies of both the aggregate and the binder should be well matched to show this kind of strength.

### 2.3 Suction Concept

Soil suction can be defined as the free energy state of soil water (Edlefsen and Anderson 1943). HMA, as a porous material, like soils has the ability to attract and retain moisture. There are two components of soil suction, matric and osmotic suction (Fredlund and Rahardjo 1993). Matric or capillary suction comes from the capillary phenomenon as a result of water surface tension of the water. The matric suction ( $u_a - u_w$ ) can be defined as “the equivalent suction derived from the measurement of the partial pressure of the water vapor in equilibrium with the soil water, relative to the partial pressure of the water vapor in equilibrium with a solution identical in composition with the soil water” (Aitchison 1965). The matric suction has a negative sign, as the capillary water is under a negative stress with respect to the air pressure, which in general equals to the atmospheric pressure ( $u_0 = 0$ ).

The osmotic suction is a result of the presence of dissolved salts in water, as it is known the presence of dissolved salts in the water decreases the relative humidity. The osmotic suction can be defined as “the equivalent suction derived from the measurement of the partial pressure of the water vapor in equilibrium with the solution identical with the soil water, relative to the partial pressure of the water vapor in equilibrium with free pure water” (Aitchison 1965). Thus the sum of the matric and osmotic suction is the total suction, as shown in Eq. (1). The total suction can be defined as “the equivalent suction

derived from the measurement of the partial pressure of the water vapor in equilibrium with a solution identical in composition with the soil water, relative to the partial pressure of water vapor in equilibrium with free pure water” (Aitchison 1965)

$$h_t = (u_a - u_w) + h_\pi \quad (1)$$

where

$h_t$  = total suction

$(u_a - u_w)$  = matric suction

$u_a$  = pore-air pressure

$u_w$  = pore-water pressure

$h_\pi$  = osmotic suction

The total suction in soils can be measured by calculating the partial vapor pressure of the soil water. The relationship between the partial vapor pressure of the pore-water vapor and the total suction is given as (Fredlund and Rahardjo 1993):

$$h_t = -\frac{RT}{v_{w0} \omega_v} \ln \left( \frac{\bar{u}_v}{\bar{u}_{v0}} \right) \quad (2)$$

where

$h_t$  = total soil suction

$R$  = universal gas constant

$T$  = absolute temperature

$v_{w0}$  = specific volume of water

$w_0$  = molecular mass of water vapor

$$\frac{\bar{u}_v}{\bar{u}_{v0}} = \text{relative humidity}$$

$\bar{u}_v$  = partial pressure of pore-water vapor

$\bar{u}_{v0}$  = saturation pressure of water vapor over a flat surface of pure water at the same temperature

At a reference temperature 25 °C, the relationship between total suction and relative humidity can be written as follows (Bulut et al. 2001):

$$h_t = -137182 \times \ln \left( \frac{\bar{u}_v}{\bar{u}_{v0}} \right) \quad (3)$$

The relationship between relative humidity and suction at a 25 °C is shown in Fig. 1 (Bulut et al 2001). From Fig. 1, it can be seen that there is a linear relationship between total suction and relative humidity over a small range of relative humidity. If relative humidity is less than 100 percent (full saturation), it indicates the presence of suction in soil.

Suction is commonly measured in pF units,  $pF = \log_{10} |h|$ , where h is the total suction in centimeters. The logarithmic scale is used to reflect the high suction values. Fig. 2 shows the relationship between the suction in log kPa [ $\log kPa \approx (Suction \text{ in } pF \text{ units} - 1)$ ] and the relative humidity. From Fig. (2), it is clear that suction becomes very sensitive to relative humidity as relative humidity approaches 100 percent.



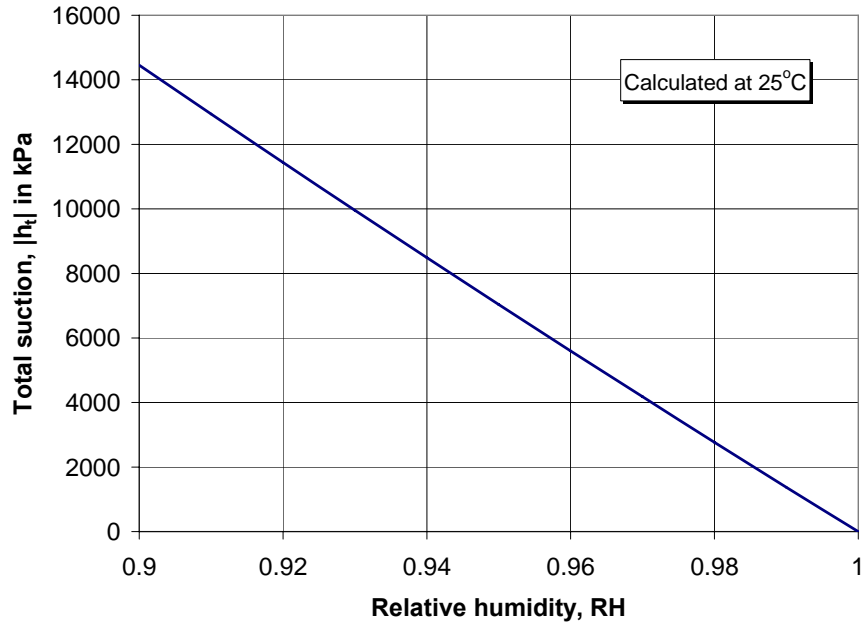


Fig. 1. Total Suction versus Relative Humidity (Bulut et al. 2001).

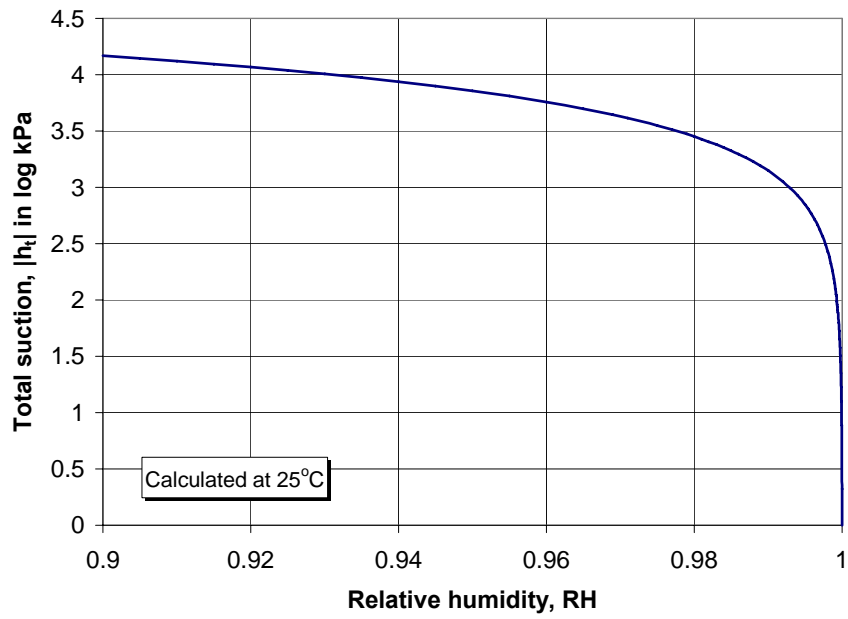


Fig. 2. Total Suction and Relative Humidity Relationship (Bulut et al. 2001).

Fig. 3 shows the relationship between water content, total suction, and its components. The matric suction has an inversely proportional relationship with water content and is sensitive to any change in water content, while the osmotic suction looks insensitive to the change in water content. Secondly, with any change in the matric suction, the measured total suction measured by psychrometers is considered good representative of the change of the matric suction measured. At the high suction range, the matric suction is difficult to measure; thus, the measurement of total suction is important (Fredlund and Rahardjo 1993).

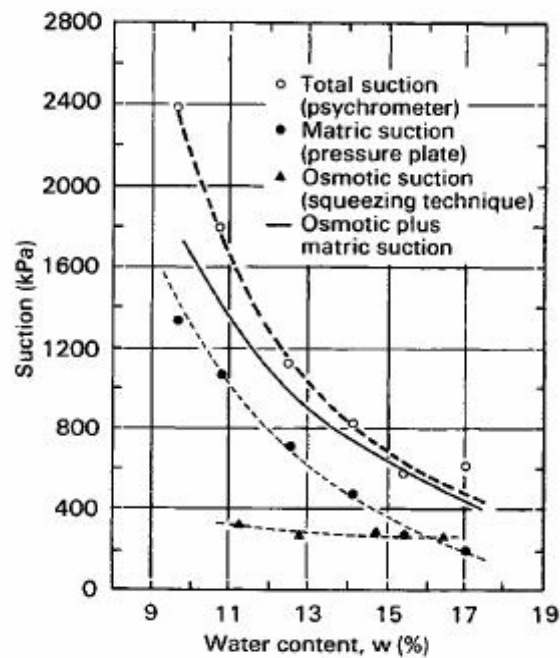


Fig. 3. Total, Matric, and Osmotic Suctions for Glacial Till (Krahn and Fredlund 1972)

## 2.4 Soil Suction Measuring Devices

Total suction and its components have been measured by several devices as presented in Table 1. This table includes the suction range for each device (Fredlund and Rahardjo 1993).

The total suction can be calculated by determining relative humidity. The following sections will focus on suction measurements using the thermocouple psychrometers and give a discussion of the tube suction test.

Table 1. Devices Used to Measure Total, Matric, and Osmotic Suctions in Soils  
(Fredlund and Rahardjo 1993)

Name of Device	Suction component measured	Range (kPa)	Comments
Psychrometers	Total	100 <sup>a</sup> -8000	Constant temperature environment required
Filter paper	Total	(entire range)	May measure matric suction when in good contact with the moist soil
Tensiometers	Negative pore-water pressure or matric suction when pore-air pressure is atmospheric	0-90	Difficulties with cavitations and air diffusion through ceramic cup
Null-type pressure plate (axis translation)	Matric	0-1500	Range of measurement is a function of the air entry value of the ceramic disk
Thermal conductivity sensors	Matric	0-□ 400+	Indirect measurement using a variable pore size ceramic sensor
Pore fluid squeezer	Osmotic	(Entire range)	Used in conjunction with a psychrometer or electrical conductivity measurement

<sup>a</sup>Controlled temperature environment to  $\pm 0.001$  °C

## **2.5 Measurements of Suction Using Psychrometers**

### **2.5.1 Concept and Experimental Procedure**

The thermocouple psychrometer is used to measure the total suction by measuring the relative humidity in the air phase of pores. The suction range measured by the psychrometers is from 3.67 pF to 4.68 pF (Fredlund and Rahardjo 1993). The psychrometer device is very sensitive to the temperature fluctuations, and therefore temperature control should be provided to the system during suction measurements. There are two types of thermocouple psychrometers. The first one is called wet loop and the second one is called Peltier psychrometer. Both of them measure the relative humidity based on the temperature difference between two surfaces, the nonevaporating surface (dry bulb) and the evaporating surface (wet bulb) (Fredlund and Rahardjo 1993). The Peltier psychrometer is commonly used to measure suction in soils. The operation of this psychrometer depends on two principles, the Seebeck effect, and the Peltier effect (Fredlund and Rahardjo 1993).

When Seebeck studied the closed circuit, shown in Fig. 4, that consists of two dissimilar metals and has two different junction temperatures, he noticed generating electromotive force through the circuit. Based on this discovery, temperature can be measured by using two different metals or wires. One junction of the circuit will be a reference, while the second will be used to assess the change in temperature. The electromotive force can be calculated by installing a microvoltmeter in the circuit, and it is known from the Seebeck circuit that the electromotive force is a function of the temperature difference through the circuit (Fredlund and Rahardjo 1993).

When Peltier studied the circuit shown in Fig. 5 that consists of two dissimilar metals passing a small current, he noticed different thermal conditions being generated for both junctions, where one gets cool while the second gets warm. When Peltier reversed the current, the thermal condition for both junctions reversed (Fredlund and Rahardjo, 1993).

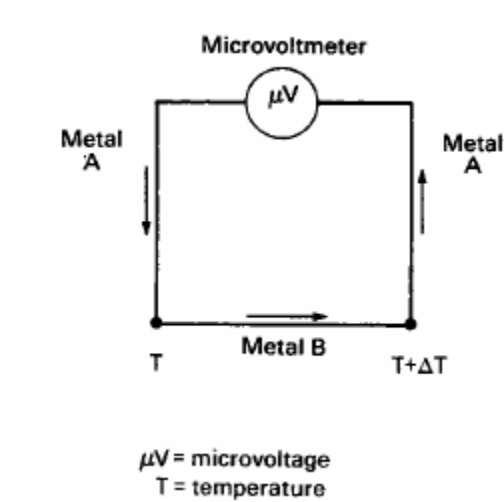


Fig. 4. Seebeck Effect (Fredlund and Rahardjo 1993)

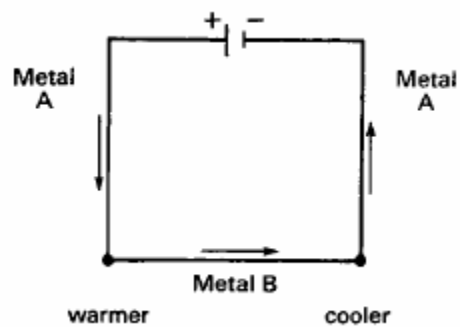


Fig. 5. Peltier Effect (Fredlund and Rahardjo 1993)

The thermocouple psychrometer uses the Peltier effect to cool its junction until it reaches the dewpoint; therefore, water vapor condenses on this junction. Once the passing current is stopped, the condensed water starts to evaporate, leaving a temperature difference between the junction and the surrounding atmosphere. The temperature reduction of the junction depends on the evaporation rate, which is influenced by water vapor pressure in the atmosphere (Fredlund and Rahardjo 1993). By measuring the ambient temperature and the temperature reduction, the relative humidity can be calculated and hence the suction can be measured. Each thermocouple has its minimum dewpoint temperature that affects the maximum cooling or the lowest relative humidity, which in turn affects the maximum suction that can be measured by each psychrometer.

The thermocouple psychrometer used in measuring the total suction in soils is called the Peltier psychrometer, which is shown in Fig. 6. This psychrometer is used in this study to measure the total suction in HMA mixes. The psychrometer consists of two different wires, the first made from constantan (copper-nickel) and the second made from chromel (chromium-nickel). The diameter of each wire is 0.025 mm. The two wires are welded together at one end, forming the measuring junction, while the other ends are subjected to a wire gauge forming, a reference junction. The thermocouple psychrometer used in this study has a stainless steel screen as a cover. The stainless steel screen cover requires less time for water vapor equilibration compared to a ceramic cup cover, as shown in Fig. 7 (Fredlund and Rahardjo 1993).

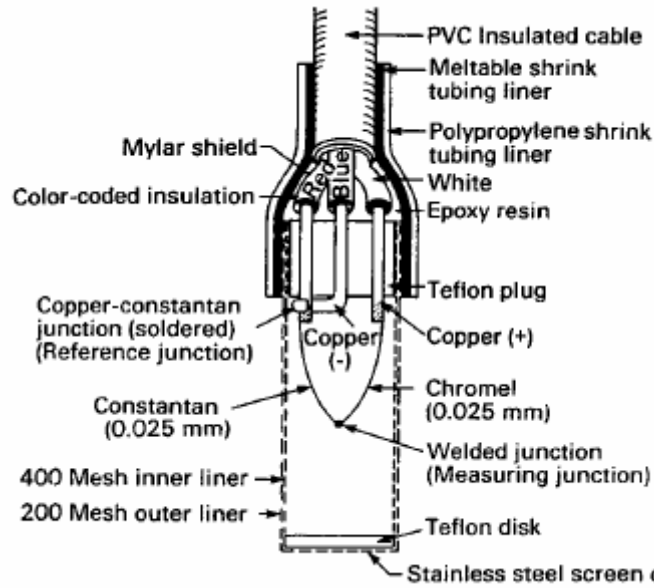


Fig. 6. Stainless Steel Screen Thermocouple Psychrometer (Fredlund and Rahardjo 1993)

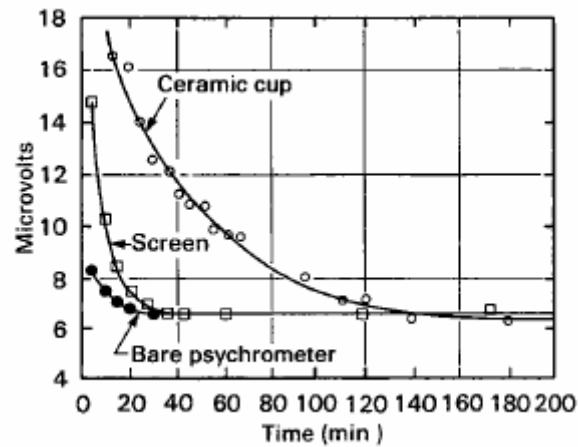


Fig. 7. Cover Materials and Equilibration Times for Thermocouple Psychrometer (Fredlund and Rahardjo 1993)

In this study, two microvoltmeters have been used to measure the generated electromotive force during the evaporation process. The HR-33T shown in Fig. 8 is used to measure water potential in soils. There are two operational modes, dewpoint mode and

psychrometric mode. The dewpoint mode is less influenced by the surrounding temperature (Wescor, Inc. 2001).



Fig. 8. HR-33T Microvoltmeter

The operational procedure of the HR-33T dewpoint microvoltmeter is outlined briefly below based on the information from Wescor, Inc., (2001) and Sood (2005):

- 1) Set the function switch on input short, turn on the HR-33T and allow it to warm up.
- 2) Connect the thermocouple psychrometer to the HR-33T microvoltmeter.
- 3) Turn the function switch to the read position and adjust the pointer to zero by moving the zero offset coarse and zero offset fine.
- 4) Switch the  $^{\circ}C / \mu V$  (temperature/microvolts) button to  $^{\circ}C$  (temperature mode) to record the temperature.



- 5) If the recorded temperature is less than 25 °C, the cooling coefficient should be adjusted by using Eq (4):

$$\pi_v = 0.7 * (T_1 - T_0) + \pi_{v_0} \quad (4)$$

where

$\pi_v$  = adjusted cooling coefficient

$T_1$  = the recorded temperature in step number 4

$T_0$  = the temperature at which the psychrometer is calibrated, in this study = 25 °C

$\pi_{v_0}$  = the cooling coefficient of the psychrometer (every psychrometer has its  $\pi_{v_0}$ )

- 6) Switch the °C /  $\mu V$  (temperature/microvolts) button to the microvolt mode, and set it at the adjusted  $\pi_v$  from step 5 by pressing ( $\pi_v$  read) button and rotating the ( $\pi_v$  set) button.
- 7) Adjust the zero offset control to zero by moving the zero offset coarse and zero offset fine.
- 8) Switch the function button to cool and leave it for 45 seconds.
- 9) Switch the function button to the dewpoint position and take the reading.
- 10) Use the range switch button to adjust it to the proper range of the reading.

The CR-7 datalogger shown in Fig. 9 is used for measuring the water potential in soils, and it is also used in this study to measure the total suction in HMA mixes. The CR-7 datalogger is an automated multi-channel device. It records readings of 40 psychrometers every 10 minutes, which makes CR-7 much easier to use than HR-33T. The PC208W software program is used to exchange the data between a computer and the CR-7 datalogger. The PC208W software has interactive widows to communicate with the

datalogger, edit programs, retrieve stored data in CR-7, view and graph real-time data, and process the data (Campbell Scientific, Inc. 2001)

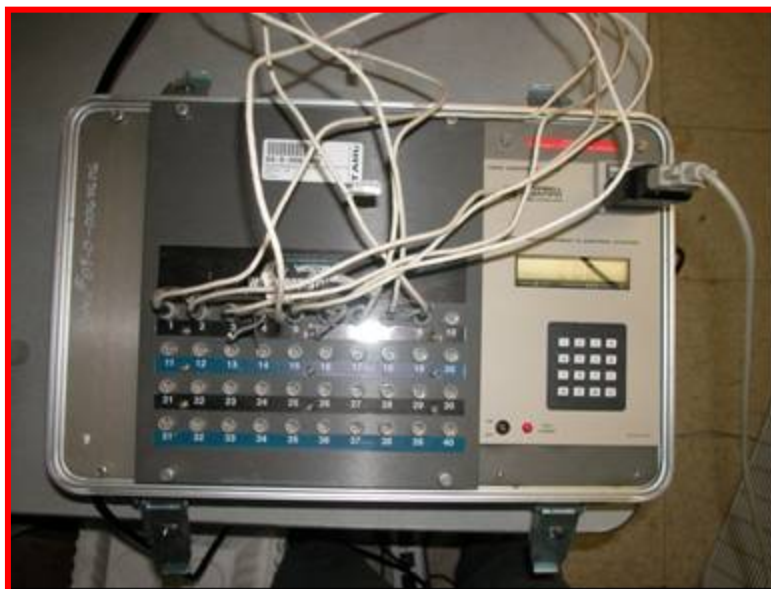


Fig. 9. CR-7 Datalogger

The operational procedure for the CR-7 datalogger is discussed briefly below based on the information from Campbell Scientific, Inc., (1997) and Sood (2005):

- 1) Turn the device on, and connect the psychrometers to the datalogger.
- 2) Connect the datalogger to a computer equipped with the PC208W software.
- 3) Open the interactive windows of the PC208W program, and press the connect icon to interact with the datalogger.
- 4) The time between the readings can be entered by using the interactive PC208W's windows.

- 5) The program starts to download the data from the datalogger to the computer every 10 minutes. It can also be changed to the desired time.
- 6) The recorded data can be collected by pressing the collect button.
- 7) The outputs are .dat files that can be easily transferred to a Microsoft Excel file for analysis

The CR-7 datalogger records three values for each psychrometer: temperature, offset, and microvolt without any corrections (Sood 2005). Eq. (5) is used for the correction of the microvolt readings:

$$\mu v = (\mu v_o / (0.325 + 0.027T)) - offset \quad (5)$$

where

$\mu v$  = the corrected microvolt reading

$\mu v_o$  = the initial microvolt reading

$T$  = the temperature

### 2.5.2 Psychrometer Calibration

The microvolt values recorded by HR-33T or CR-7 are converted to suction values by using the calibration curve for each psychrometer. In the calibration process of the psychrometers, the osmotic suction of the electrolyte solution is used. The osmotic suction can be measured by obtaining the osmotic coefficient of the salt solution, which is represented in Table 2 for different salt solutions. The osmotic coefficients for different salts can be calculated using Eq. (6) (Lang 1967):

$$\phi = -\frac{\rho_w}{vmw_0} \ln \left( \frac{\bar{u}_v}{\bar{u}_{v0}} \right) \quad (6)$$

where

$\phi$  = osmotic coefficient

$v$  = number of ions from one molecule of salt

$m$  = molality

$w_0$  = molecular mass of water vapor

$\rho_w$  = density of water

$\frac{\bar{u}_v}{\bar{u}_{v0}}$  = relative humidity

Eq. (7) is a result of the combination of Eq. (2) and Eq. (6), which can be used to calculate the osmotic suction (Bulut et al. 2001).

$$h_\pi = vRTm\phi \quad (7)$$

Eq. (7) is used to calculate the osmotic suction for different salt solutions, as presented in Table 3.

Table 2. Osmotic Coefficients of Several Salt Solutions (Bulut et al. 2001)

Osmotic Coefficients at 25 °C							
Molality (m)	NaCl	KCl	NH <sub>4</sub> Cl	Na <sub>2</sub> SO <sub>4</sub>	CaCl <sub>2</sub>	Na <sub>2</sub> S <sub>2</sub> O <sub>3</sub>	MgCl <sub>2</sub>
0.001	0.9880	0.9880	0.9880	0.9608	0.9623	0.9613	0.9627
0.002	0.9840	0.9840	0.9840	0.9466	0.9493	0.9475	0.9501
0.005	0.9760	0.9760	0.9760	0.9212	0.9274	0.9231	0.9292
0.010	0.9680	0.9670	0.9670	0.8965	0.9076	0.8999	0.9106
0.020	0.9590	0.9570	0.9570	0.8672	0.8866	0.8729	0.8916
0.050	0.9440	0.9400	0.9410	0.8229	0.8619	0.8333	0.8708
0.100	0.9330	0.9270	0.9270	0.7869	0.8516	0.8025	0.8648
0.200	0.9240	0.9130	0.9130	0.7494	0.8568	0.7719	0.8760
0.300	0.9210	0.9060	0.9060	0.7262	0.8721	0.7540	0.8963
0.400	0.9200	0.9020	0.9020	0.7088	0.8915	0.7415	0.9206
0.500	0.9210	0.9000	0.9000	0.6945	0.9134	0.7320	0.9475
0.600	0.9230	0.8990	0.8980	0.6824	0.9370	0.7247	0.9765
0.700	0.9260	0.8980	0.8970	0.6720	0.9621	0.7192	1.0073
0.800	0.9290	0.8980	0.8970	0.6629	0.9884	0.7151	1.0398
0.900	0.9320	0.8980	0.8970	0.6550	1.0159	0.7123	1.0738
1.000	0.9360	0.8980	0.8970	0.6481	1.0444	0.7107	1.1092
1.200	0.9440	0.9000	0.8980	...	...	...	...
1.400	0.9530	0.9020	0.9000	...	...	...	...
1.500	...	...	...	0.6273	1.2004	0.7166	1.3047
1.600	0.9620	0.9050	0.9020	...	...	...	...
1.800	0.9730	0.9080	0.9050	...	...	...	...
2.000	0.9840	0.9120	0.9080	0.6257	1.3754	0.7410	1.5250
2.500	1.0130	0.9230	0.9170	0.6401	1.5660	0.7793	1.7629

Table 3. Osmotic Suctions of Several Salt Solutions (Bulut et al. 2001)

Osmotic Suctions in kPa at 25 °C							
Molality (m)	NaCl	KCl	NH <sub>4</sub> Cl	Na <sub>2</sub> SO <sub>4</sub>	CaCl <sub>2</sub>	Na <sub>2</sub> S <sub>2</sub> O <sub>3</sub>	MgCl <sub>2</sub>
0.001	5	5	5	7	7	7	7
0.002	10	10	10	14	14	14	14
0.005	24	24	24	34	34	34	35
0.010	48	48	48	67	67	67	68
0.020	95	95	95	129	132	130	133
0.050	234	233	233	306	320	310	324
0.100	463	460	460	585	633	597	643
0.200	916	905	905	1115	1274	1148	1303
0.300	1370	1348	1348	1620	1946	1682	2000
0.400	1824	1789	1789	2108	2652	2206	2739
0.500	2283	2231	2231	2582	3396	2722	3523
0.600	2746	2674	2671	3045	4181	3234	4357
0.700	3214	3116	3113	3498	5008	3744	5244
0.800	3685	3562	3558	3944	5880	4254	6186
0.900	4159	4007	4002	4384	6799	4767	7187
1.000	4641	4452	4447	4820	7767	5285	8249
1.200	5616	5354	5343	...	...	...	...
1.400	6615	6261	6247	...	...	...	...
1.500	...	...	...	6998	13391	7994	14554
1.600	7631	7179	7155	...	...	...	...
1.800	8683	8104	8076	...	...	...	...
2.000	9757	9043	9003	9306	20457	11021	22682
2.500	12556	11440	11366	11901	29115	14489	32776

## 2.6 The Tube Suction Test

TST is used to evaluate the moisture susceptibility of granular bases in pavements. This test was developed by the Finnish National Road Administration (Syed et al. 2000). A number of research studies demonstrated that moisture susceptibility is related to the suction of aggregates (Scullion and Saarenketo 1997). TST is used to rank an aggregate according to its moisture susceptibility. An aggregate can be classified as good, or poor according to the final dielectric values of compacted specimens placed to

soak water for 10 days. The dielectric constant represents the free or unbound water within the aggregate sample. The percometer device shown in Fig. 10 has been used to measure the dielectric values of the specimens. An increase in the dielectric value, which associated with the matric suction, is used as an indication of moisture content and moisture susceptibility (Syed et al. 2000).



Fig. 10. Percometer Device

The three main elements in a soil specimen have different dielectric values. The aggregates' dielectric values vary from 4 to 6, while the dielectric value of air is 1. The dielectric value of the water depends on its bonding state with the aggregate; the tightly bounded water has a dielectric value of 3 to 4, while the dielectric value of unbounded water is 81 (Scullion and Saarenketo 1997).

The tube suction test testing procedure for the aggregates is as follows (Scullion and Saarenketo 1997):

- 1) Discard any aggregates with a size more than 25 mm.
- 2) Compact samples in test molds at the optimum moisture content (Fig. 11). The optimum moisture content can be determined from the standard or modified Proctor procedure.
- 3) Place the sample in a room that has a 50 °C temperature for drying for 3-4 days.
- 4) Place the samples in a bath with a 20 mm height of water. The water level should be maintained at 20 mm throughout the test.
- 5) Use the percometer device (Fig. 10) to take surface dielectric measurements. At least six dielectric readings should be taken on each specimen surface.
- 6) The measuring intervals are 0, 15, 30, 60, and 120 minutes and then 6, 12, 24, 48, and 72 hours. One measurement daily needs to be taken afterward until a constant dielectric value is achieved.
- 7) Drop the highest and lowest values and take the average of the remaining measurements.
- 8) Plot the dielectric values versus time.

Scullion and Saarenketo (1997) demonstrated that the maximum acceptable dielectric values for the granular materials are 16, and if the dielectric values are greater than 16, poor performance is expected for these materials.



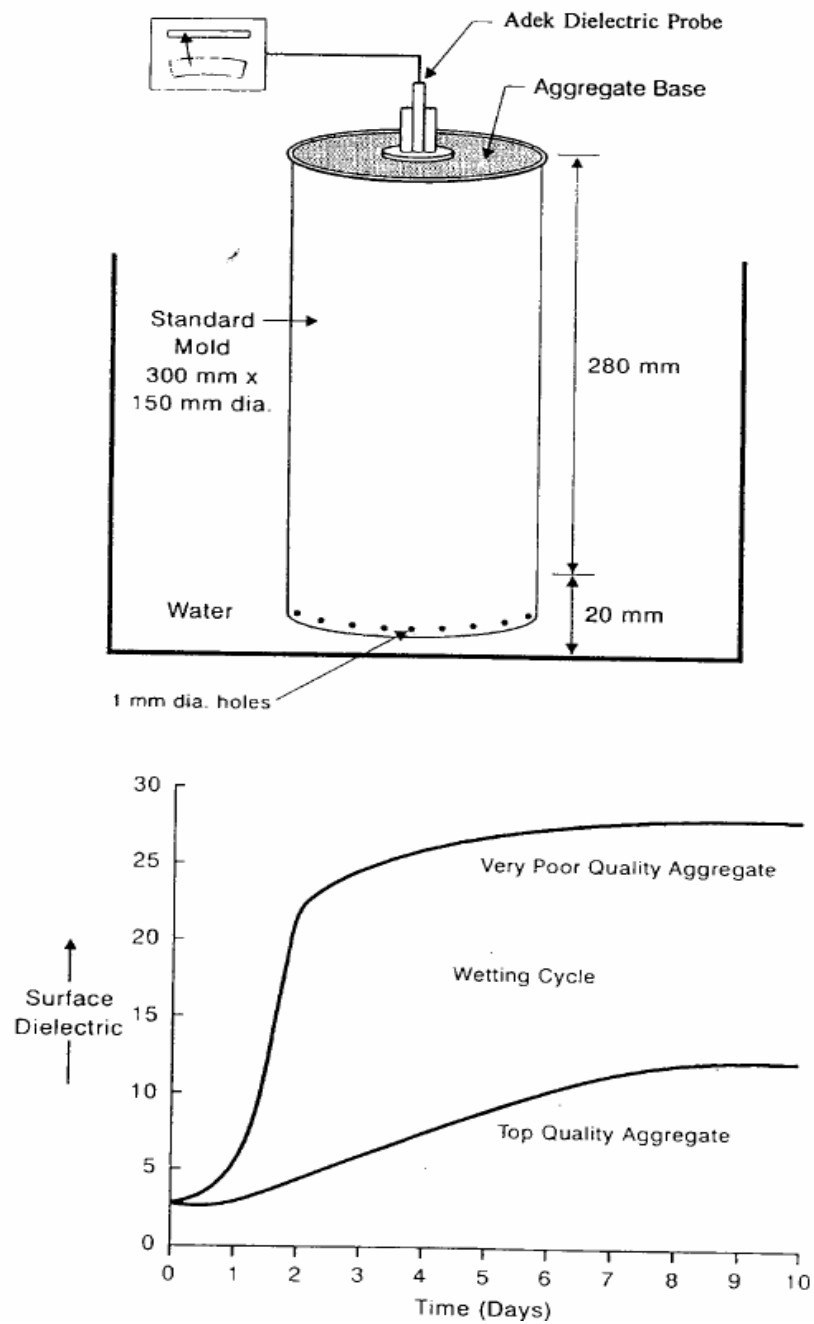


Fig. 11. TST Setup and TST Results (Scullion and Saarenketo 1997)

## **CHAPTER III**

### **EXPERIMENTS AND RESULTS**

#### **3.1 Introduction**

This chapter discusses the results of using the thermocouple psychrometers to measure the total suction in HMA mixes. The different protocols that were used to measure the total suction in HMA mixes using psychrometers are discussed in detail. The results and analysis section documents the relationship between suction measurements using the psychrometers, aggregate size distribution, aggregate type, air void distribution, and moisture damage. Finally, the results of the TST to assess moisture susceptibility in HMA mixes are documented.

#### **3.2 Development of a Procedure for Measuring the Total Suction in HMA Mixes**

Two main protocols with different experimental setups were followed to measure the total moisture suction in HMA mixes. The first is referred to as the wetting protocol, and the second is referred to as the drying protocol. The following sections discuss psychrometer calibration, the drying and the wetting protocols, and the main findings in regard to their suitability for measuring HMA suction.

##### **3.2.1 Psychrometer Calibration**

The first step in measuring the total suction in HMA mixes is the calibration of psychrometers shown in Fig. 12. The calibration process means determining the relationship between the recorded microvolts and a known total suction value. The calibration is conducted by using a salt solution with different concentrations (molalities).

The sodium chloride (NaCl) solution is used in this study to calibrate the psychrometers over a range of suction from 3.0 pF to 5.0 pF. The required amount of NaCl to prepare the solution of different molalities is illustrated in Table 4.



Fig. 12. Thermocouple Psychrometer

Table 4. NaCl Osmotic Suctions for Psychrometer Calibration (Bulut et al. 2001)

Molality	NaCl amount (grams/liter)	Osmotic suction(bar)	Osmotic suction (pF)	Osmotic suction (kPa)
0.02	1.1688	0.95	2.99	95.02
0.05	2.9221	2.34	3.38	233.90
0.10	5.8442	4.62	3.67	462.32
0.20	11.6885	9.16	3.97	916.08
0.50	29.2212	22.86	4.37	2286.15
0.70	40.9097	32.17	4.52	3216.82
1.20	70.1310	56.26	4.76	5626.15
2.20	128.5734	108.87	5.05	10887.35
1 Mole NaCl = 58.442468 grams				

The calibration process is outlined briefly below:

- 1) Calculate the required amount of the NaCl in grams/liter using Table 4 that corresponds to the targeted total suction value.
- 2) Add one liter of pure water to each amount of the salt, and shake the flask well until the salt is dissolved in the water.
- 3) Put a small amount of this solution in a jar as shown in Fig. 13, where the top level of the solution covers the head of the psychrometers.
- 4) Seal the top cover of the jar as shown in Fig. 13 with silicone glue and plastic tape.
- 5) Put the jar in a plastic bag and keep all in a bath of water at 25 °C. The temperature should be maintained at 25 °C by using a temperature controller as shown in Fig. 14.
- 6) Connect the psychrometers to CR-7 or HR-33T to record the microvolt readings.
- 7) Keep the datalogger to record the readings for one day.
- 8) After downloading the data from the CR-7 using the PC208W software, clean the psychrometers well with distilled water and air dry them.
- 9) Repeat the previous steps with different molalities corresponding to different total suction value.



Fig. 13. Psychrometers Suspended in Calibration Solution (Sood 2005)

In order to deal with the massive recorded data, a simple macro Excel file was developed in this study to analyze the recorded data. This macro is located in Appendix A. After collecting the data from the datalogger using the PC208W software, one can transfer these data to Excel files. The macro in Appendix A uses Eq. (5) to calculate the corrected values in separated columns for each psychrometer reading.



Fig. 14. Temperature Controller to Maintain Temperature during Calibration

The relationship between the total suction and the microvolt outputs is presented in Fig. 15. If the total suction value is less than 3.5 pF, the recorded microvolts are negative values or equal to zero as shown in part 1 of Fig. 15. If the total suction value is between 3.5 pF to 4.70 pF, there is a proportional relationship between the recorded microvolts and total suction as illustrated in part 2 of Fig. 15. Part 2 is taken to be the calibration curve of the psychrometer. For the total suction higher than 4.70 pF, the microvolts tend to decrease until it reaches zero or given negative values as shown in part 3 of Fig. 15. Each psychrometer has its own range of total suction that it can measure. On average, this range is between 3.67 pF (4.5 bar) and 4.68 pF (47 bar), where  $pF = \log (1019.8 \times \text{suction in bar})$ .

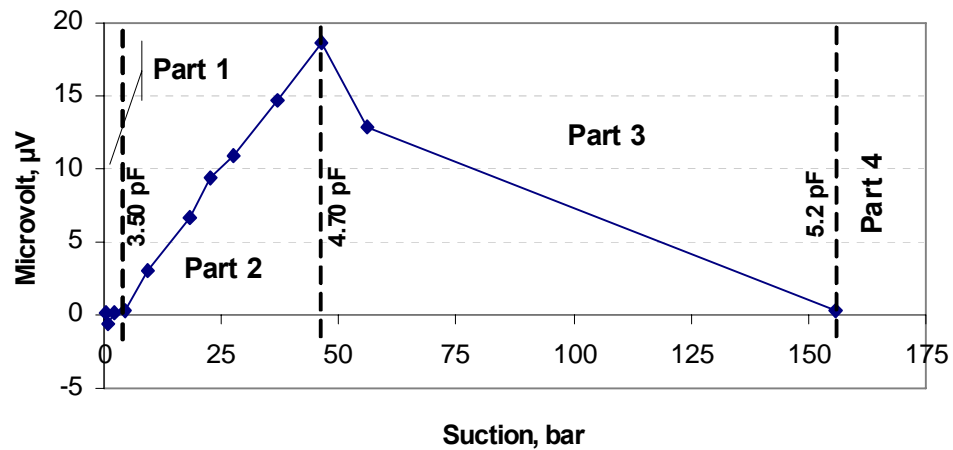


Fig. 15. Relationship between Microvolt Outputs and Total Suction

Part 2 of Fig. 15 is used to generate the calibration curve of a thermocouple psychrometer as shown in Fig. 16. The calibration curves for the thermocouple psychrometers used in this study are given in Appendix B.

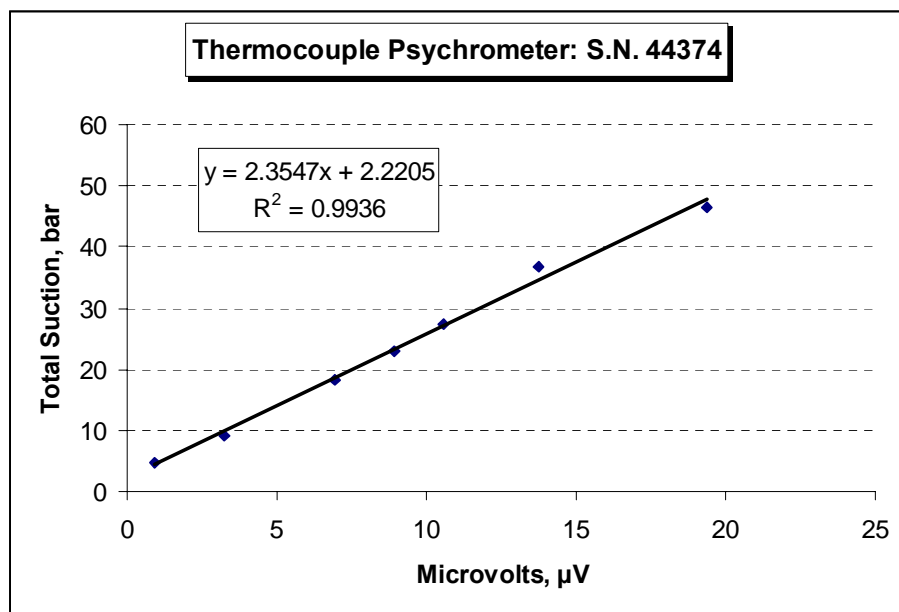


Fig. 16. Calibration Curve of Thermocouple Psychrometer

### 3.2.2 Measuring Suction Using the Wetting Protocol

In the first protocol, the change in total suction was measured when a dry HMA specimen was placed in a 2.55 cm bath of water. The main concept of this protocol is that water rises in a sample under capillary action, leading to an increase in moisture content and a decrease in total suction. The experimental procedure followed in this protocol was as follows:

- 1) HMA specimens were kept to dry in a temperature-controlled room (TCR) for 2 days at 60 °C.
- 2) Three holes were drilled in each HMA specimen. The diameter and the depth of the hole were 0.95 cm and 5 cm (half of a specimen's diameter), respectively. The distance between holes was 3.8 cm. A drilled HMA specimen is shown in Fig. 17.
- 3) Thermocouple psychrometers were inserted in the holes as shown in Fig. 18.
- 4) Holes were filled with plastic filler as illustrated in Fig. 19. Plastic tape was then used to cover the hole as shown in Figs. 20 and 21.
- 5) A specimen was wrapped with two layers of clear plastic wrap, as shown in Fig. 22, and with one layer of aluminum foil. Plastic tape was used to support the wrap as shown in Fig. 23. The top surface was kept uncovered.
- 6) HMA specimens were placed over a porous stone in a 2.50 cm height of water as illustrated in Fig. 24. The diameter of the porous stone was equal to the specimen's diameter (4 inches or 10.16 cm), and its thickness was 1/4 inch or 0.65 cm.
- 7) Thermocouple psychrometers were connected to a microvoltmeter to record the microvolt outputs.





Fig. 17. HMA Specimen with Three Holes for Psychrometers



Fig. 18. Inserting Psychrometer in HMA Hole



Fig. 19. Filling Holes with Filler



Fig. 20. Covering Holes with Plastic Tape



Fig. 21. Three Psychrometers Inserted in HMA Specimen



Fig. 22. Wrapping HMA Specimen with Two Layers of Plastic Clear Wrap



Fig. 23. Wrapping HMA Specimen with Aluminum Foil and Supported with Plastic Tape



Fig. 24. Placing HMA Specimens in Bath of Water

### **3.2.3 Measuring Suction Using the Drying Protocol**

In this protocol, suction was measured during the drying process of specimens that were initially saturated with water. At first, drying took place under room temperature. However, this was found to be a very slow process; consequently, a TCR at 60 °C was used in order to speed up the drying of HMA specimens.

#### **3.2.3.1 Drying Test under Room Temperature**

This protocol consisted of the following steps:

- 1) Specimens were fully saturated with water using vacuum saturation for 20 minutes, and then specimens were kept in water for 2 hours.
- 2) Specimens were removed from the water and then placed for 1 hour in a room at a controlled temperature of 25 °C.
- 3) Thermocouple psychrometers were inserted into the specimens as shown in Fig. 18.
- 4) Specimens were wrapped with two layers of plastic wrap and one layer of aluminum foil from all sides except the top surface.
- 5) Each specimen was placed in a box as shown in Fig. 25. The purpose of placing specimens in this box was to reduce temperature fluctuations; hence fluctuations in suction measurements can also be reduced. The uncovered top surface of a specimen was exposed to the outside as shown in Fig. 26. Each specimen was covered by packing foam material to help in reducing temperature fluctuations.
- 6) Thermocouple psychrometers were connected to a microvoltmeter to record microvolt outputs.



Fig. 25. Box Used in Drying Test



Fig. 26. HMA Specimen with One Uncovered Surface Covered with Packing Foam Material

### 3.2.3.2 Drying Test Using Temperature-Controlled Room

In this protocol, the TCR was used to accelerate water loss from HMA specimens and to cause change in suction measurements. The steps of this approach can be summarized as follows:

- 1) Specimens were fully saturated with water using vacuum saturation for 20 minutes, and then specimens were kept in water for 2 hours.
- 2) HMA specimens were placed and removed from the TCR in five stages. The durations of placing specimens in TCR were as follows:
  - I. Stage one = 60 minutes
  - II. Stage two = 75 minutes
  - III. Stage three = 180 minutes
  - IV. Stage four = 300 minutes
  - V. Stage five = 480 minutes
- 3) After each stage, specimens were placed in 25 °C room to cool down.
- 4) Thermocouple psychrometers were inserted into the specimens.
- 5) Specimens were totally wrapped with two layers of plastic wrap and one layer of aluminum foil.
- 5) Specimens were placed in a plastic mold at a constant temperature of 25 °C as shown in Fig. 27. In this protocol, a simple system was developed to provide specimens with isothermal conditions throughout the testing period. This system contains a temperature regulator adjusted to 25 °C, water surrounding all specimens' molds, and plastic molds filled with packing foam to decrease the temperature fluctuations as illustrated in Figs. 27 and 28.

- 6) Thermocouple psychrometers were connected to the CR-7 datalogger as shown in Figs. 29 and 30. The CR-7 datalogger has advantages over the HR-33T microvoltmeter. The CR-7 datalogger is an automated multi-channel device, and it can take reading of 40 psychrometers at the same time every 10 minutes. A computer is used to download the data from CR-7, as shown in Fig. 31.
- 7) Total suction of each psychrometer was recorded for 1500 minutes for every stage. This time was found sufficient for the suction to reach a constant value.



Fig. 27. HMA Specimen Placed in Plastic Mold





Fig. 28. Temperature-Controlled System (Temperature Regulator, Water in Ice Chest, and Plastic Mold)

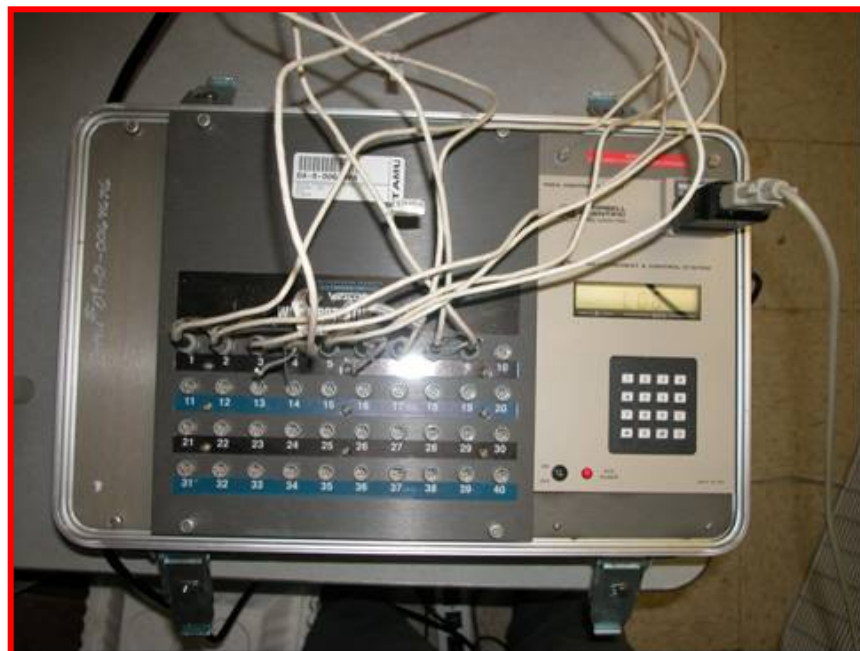


Fig. 29. CR-7 Datalogger with 40 Openings for Psychrometers



Fig. 30. Psychrometers Connected to CR-7 Datalogger



Fig. 31. Computer Connected to CR-7 Datalogger

### 3.3 Results and Analysis

#### 3.3.1 Wetting Protocol

As opposed to published results for soils, this approach gave results with high variability. Weight measurements revealed that very small amounts of water penetrated into these specimens under the capillary action. This could be due to the small percent of connected air voids in HMA specimens compared to soil specimens. In addition, the lack of proper control of temperature in this protocol contributed to the high variability in suction measurements.

The wetting test setup is shown in Fig. 32 where, psychrometer (1) is the nearest to the water, psychrometer (2) is in the middle, and psychrometer (3) is the top one. Figures 33 through 38 show examples of the relationship between the total suction in pF and time for a number of HMA specimens. Specimen 1 was prepared using granite aggregate; specimens 2, 4, and 6 were prepared from limestone aggregate, and specimens 3, 5, and 7 were prepared using crushed gravel, manufactured sand, and limestone screening. HR-33T microvoltmeter was used to obtain the results shown in Figs 33 to 38.

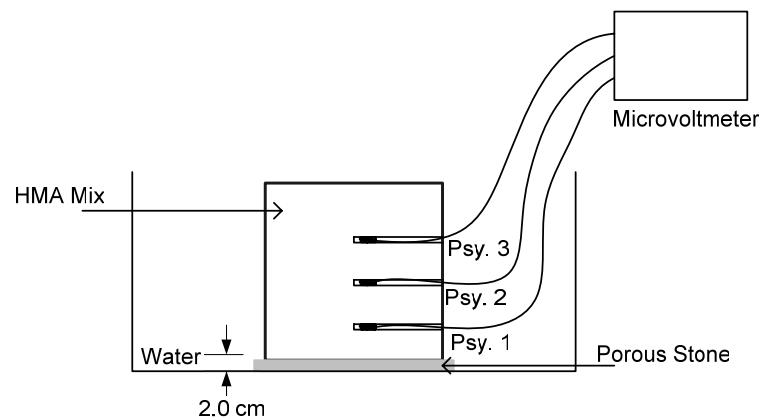


Fig. 32. Wetting Test Setup

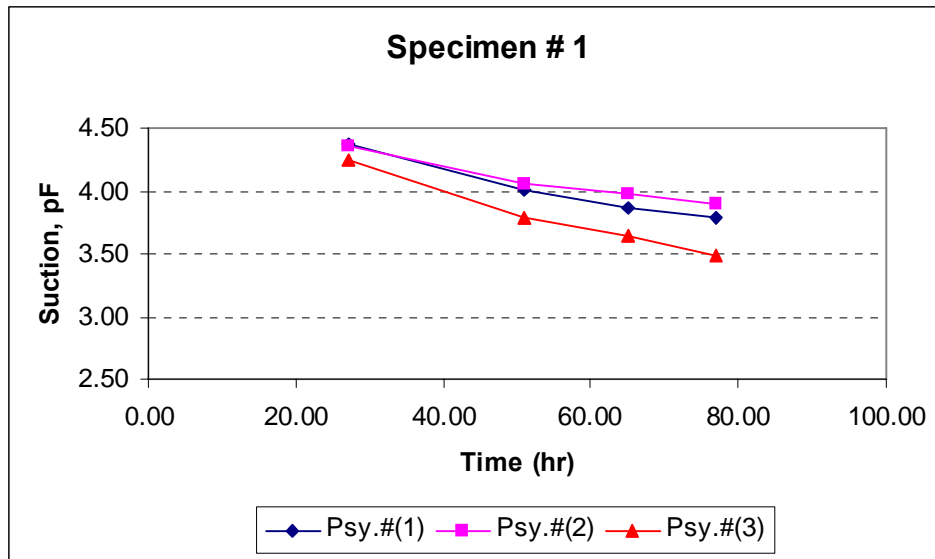


Fig. 33. Total Suction versus Time (Specimen 1)

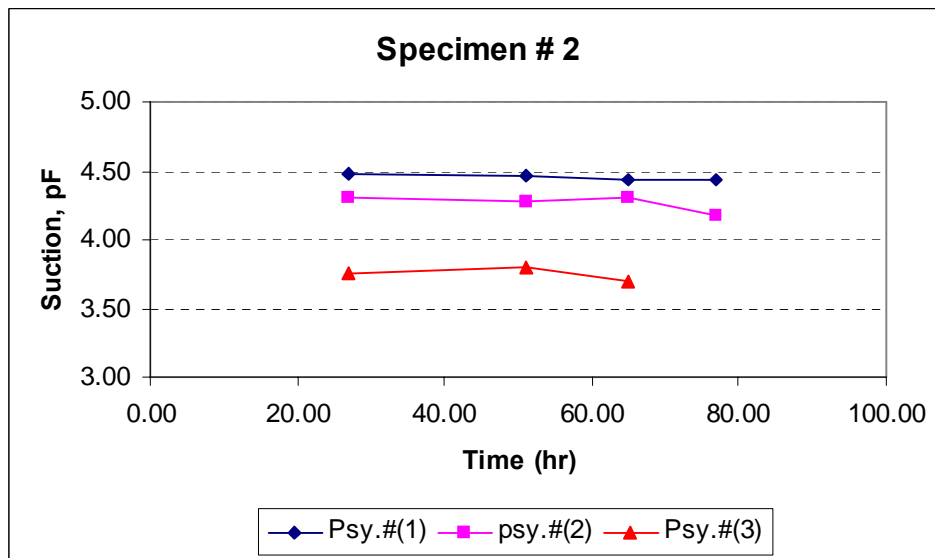


Fig. 34. Total Suction versus Time (Specimen 2)

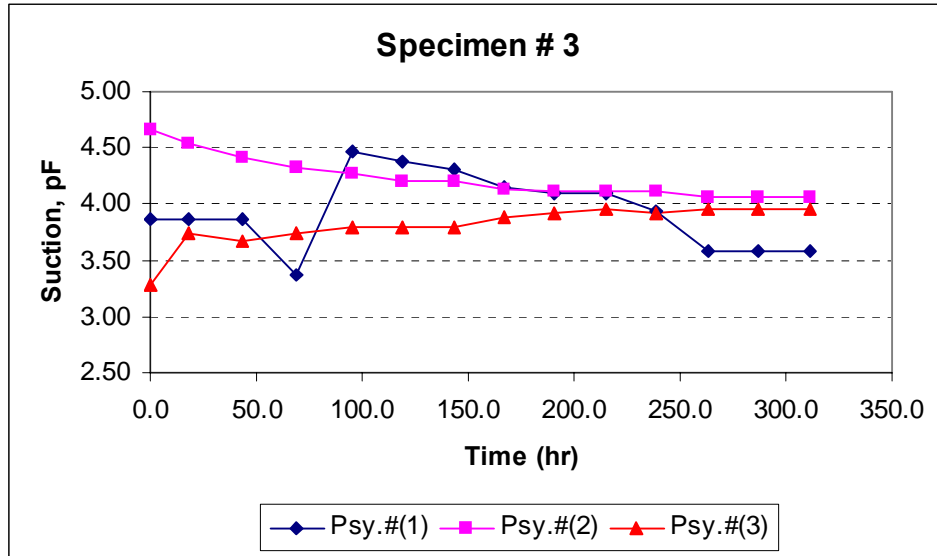


Fig. 35. Total Suction versus Time (Specimen 3)

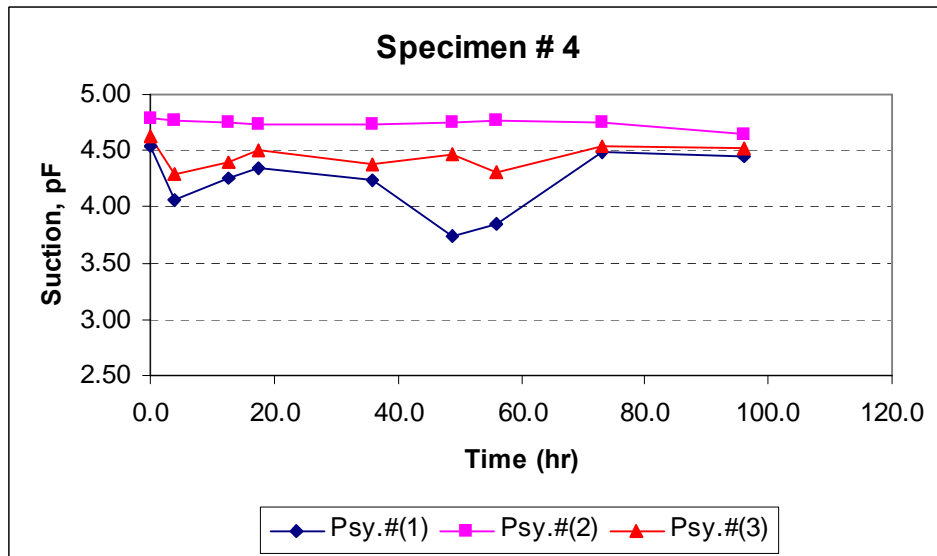
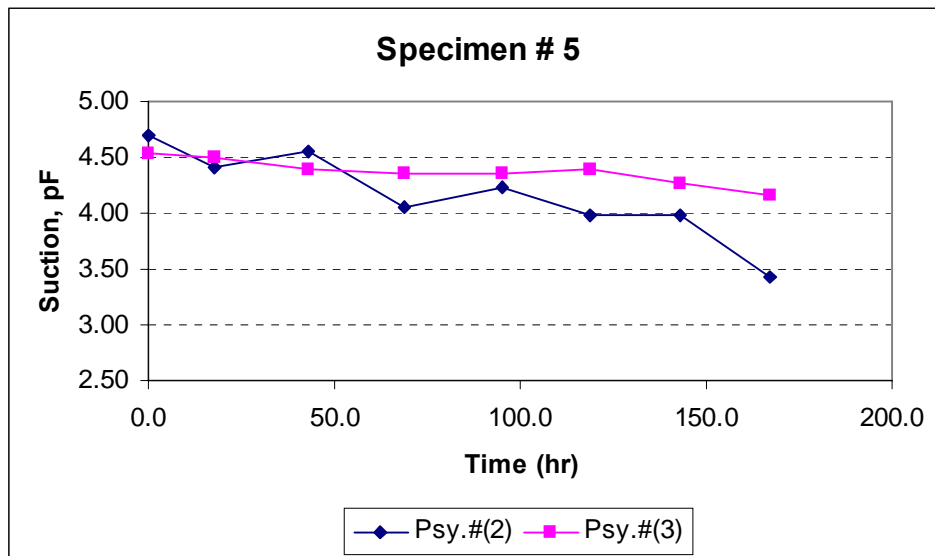


Fig. 36. Total Suction versus Time (Specimen 4)



Note: No response for Psy. 1

Fig. 37. Total Suction versus Time (Specimen 5)

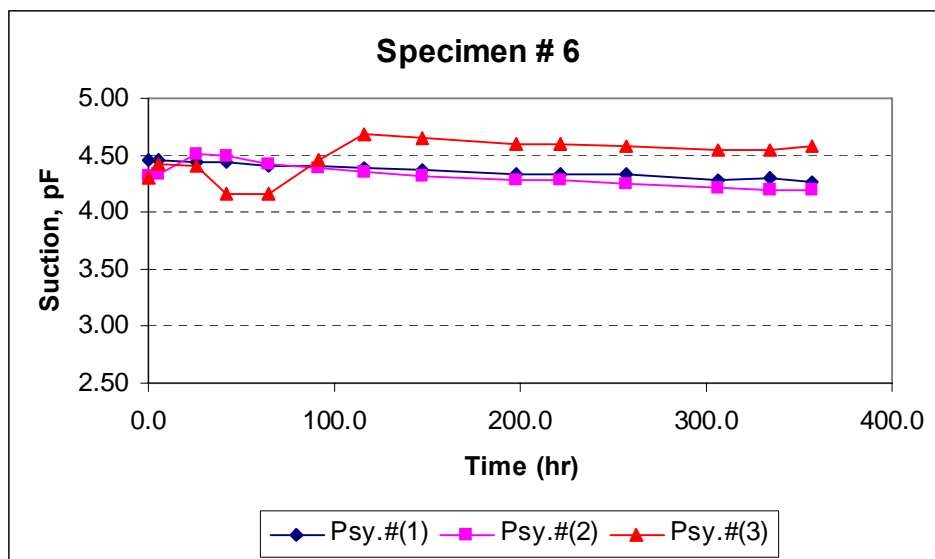


Fig. 38. Total Suction versus Time (Specimen 6)

As shown in Figs. 33 to 38, measurements were in 24-hour increments. Therefore, the high variability in the measurements could have been also caused by the low number of readings. Consequently, the CR-7 datalogger was used instead of the HR-33T to record the microvolt outputs every 10 minutes. Unfortunately, the measurements were out of range of the psychrometer (higher than 4.67 pF), indicating that specimens were dry most of the time, and the penetration of water was too small to reduce suction to values within the psychrometer range. Examples of the results using CR-7 are shown in Figs. 39 through 41. The results are presented in microvolt instead of pF since the suction level was out of the psychrometer's range and some of the readings were negative; it is not possible to convert the microvolt values to suction for negative microvolt values. Based on the experimental results, it was concluded that this protocol is not suitable to measure suction in HMA.

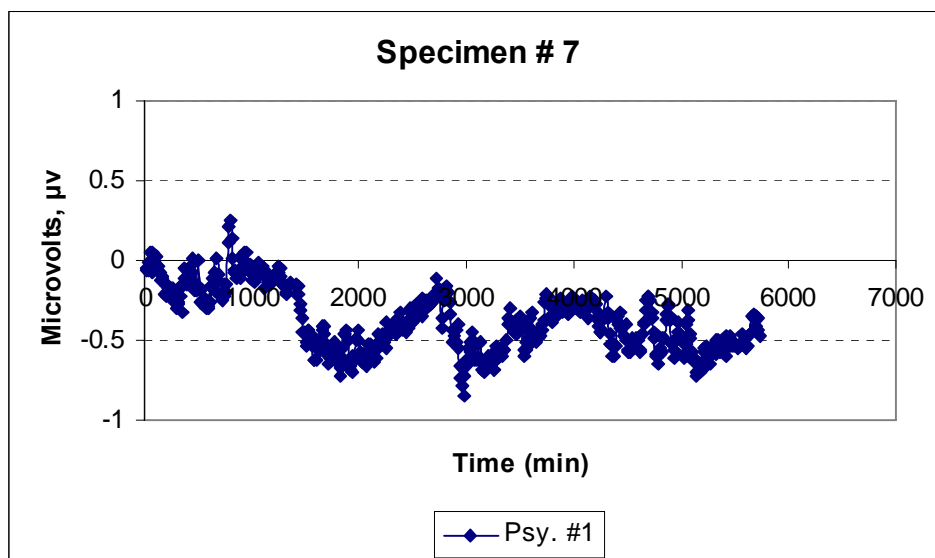


Fig. 39. Microvolt Outputs Recorded by Psychrometer 1

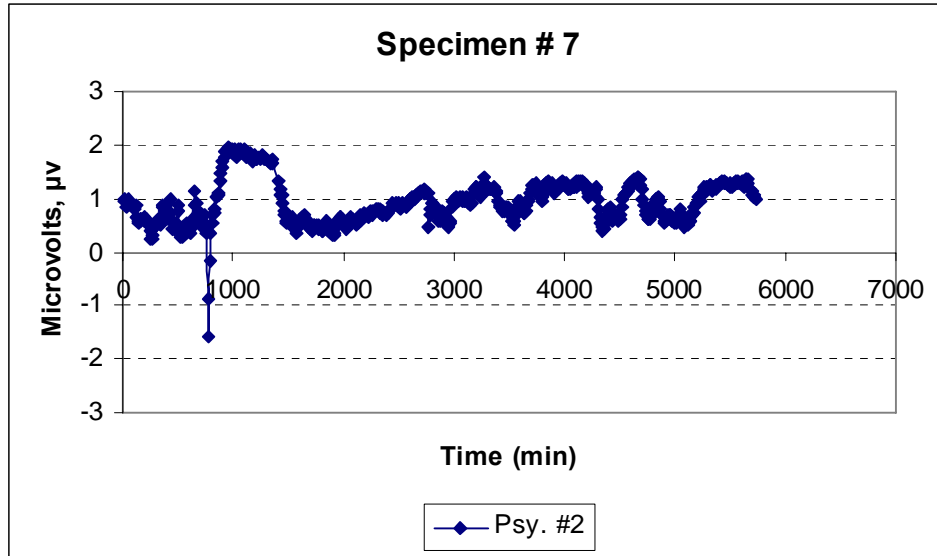


Fig. 40. Microvolt Outputs Recorded by Psychrometer 2

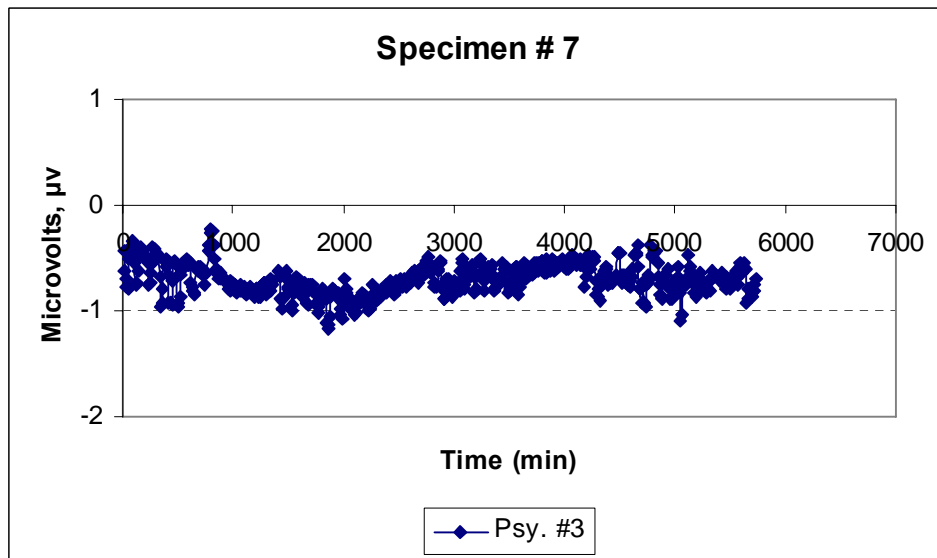


Fig. 41. Microvolt Outputs Recorded by Psychrometer 3



### **3.3.2 Drying Test under Room Temperature**

Unfortunately, this protocol did not yield any meaningful results. Even after seven days of drying under room temperature, the psychrometers did not record any change in microvolt outputs. This meant that the HMA specimens were still wet or did not lose enough moisture to reach suction values within the psychrometers' range. Therefore, it was concluded that this protocol was not suitable to measure HMA suction or differentiate among different HMA mixtures in terms of suction.

### **3.3.3 Drying Test Using Temperature-Controlled Room**

#### **3.3.3.1 Description of HMA Specimens**

These specimens were prepared at the University of Florida as part of a study on moisture damage and its relationship to mix design and material properties (Birgisson et al. 2003, Birgisson et al. 2004). At Texas A&M University, Castelblanco (2004) evaluated these specimens to investigate the relationship between HMA moisture damage and air void structure.

The first set of specimens was prepared using the Georgia granite aggregate (GA) with different gradations as shown in Table 5; while the second set of HMA specimens was prepared using Florida limestone aggregate (WR) with different gradations as shown in Table 6. Field experience showed that the granite mix has poor performance, while the limestone mix has good performance in terms of resistance to moisture damage (Birgisson et al. 2004, Castelblanco 2004). In Tables 5 and 6, the letter F stands for a fine-graded mixture, where the gradation passes above the restricted zone; C refers to a coarse-graded mixture. The F/C actually passes below the restricted zone, but it was

given the dual designation since it was modified from a fine-graded mix that was used in the state of Florida. Each specimen had a percent air voids around 7 percent.

Table 5. Granite Mixture Gradation (Castelblanco 2004).

Sieve Size (mm)	Granite: Percent Passing					
	GA-C1	GA-C2	GA-C3	GA-F1	GA-F2	GA-F3/C4
19	100	100	100	100	100	100
12.5	97.4	90.9	97.3	94.7	90.5	94.6
9.5	89	72.9	89.5	84	77.4	85.1
4.75	55.5	45.9	55.4	66.4	60.3	65.1
2.36	29.6	28.1	33.9	49.2	43.2	34.8
1.18	19.2	18.9	23	32.7	34	26
0.6	13.3	13.2	16	21	23	18.1
0.3	9.3	9.2	11.2	12.9	15.3	12.5
0.15	5.4	5.6	6.8	5.9	8.7	7.7
0.75	3.5	3.9	4.7	3.3	5.4	5.8

Table 6. Limestone Mixture Gradation (Castelblanco 2004).

Sieve Size (mm)	Limestone: Percent Passing					
	WR-C1	WR-C2	WR-C3	WR-F1	WR-F2	WR-F3/C4
19	100	100	100	100	100	100
12.5	97	91	98	96	91	95
9.5	90	74	89	85	78	85
4.75	60	47	57	69	61	67
2.36	33	30	36	53	44	37
1.18	20	20	24	34	35	26
0.6	15	14	18	23	24	20
0.3	11	10	13	15	16	14
0.15	7.6	6.7	9.2	9.6	9.1	8.6
0.75	4.8	4.8	6.3	4.8	6.3	5.8

X-ray computed tomography (CT) imaging analysis was used to analyze the air void distribution for these mixes (Castelblanco 2004). Table 7 shows a statistical analysis for the size of the air voids for both the granite and limestone specimens. Fig. 42 shows the difference between the sizes of the air voids in these specimens, where a positive difference refers to higher sizes of air voids in granite specimens. The air void analysis revealed that the granite specimens had larger air voids than the limestone specimens at the corresponding gradations as shown in Fig. 43 (Castelblanco 2004).

Table 7. Quartiles of Air Void Size Distribution (Castelblanco, 2004)

Specimen	Diameter (mm)		
	1 <sup>st</sup> Quartile	2 <sup>nd</sup> Quartile	3 <sup>rd</sup> Quartile
GA-C1	0.804	1.283	2.048
GA-C2	0.673	1.094	1.778
GA-C3	0.581	0.918	1.450
GA-F1	0.456	0.706	1.091
GA-F2	0.421	0.665	1.051
GA-F3/C4	0.531	0.850	1.359
WR-C1	0.602	0.957	1.522
WR-C2	0.554	0.890	1.429
WR-C3	0.488	0.780	1.246
WR-F1	0.425	0.655	1.009
WR-F2	0.387	0.609	0.958
WR-F3/C4	0.473	0.756	1.207

The relationship between resistance to moisture damage measured in the laboratory and air void size is shown in Fig. 44. The y axis is the ratio of the number of cycles required to fail moisture-conditioned specimens in the indirect tension test to the number of cycles required to fail specimens under dry condition. The resistance to moisture damage increases as this ratio increases. These results has lead Castelblanco

(2004) to conclude that there is a critical air void size “pessimum” at which the water gets into the mix and becomes difficult to get out, causing moisture damage. This critical air void size depends on the type of the mix. The air void distributions for the HMA mixes used in this study are attached in Appendix C.

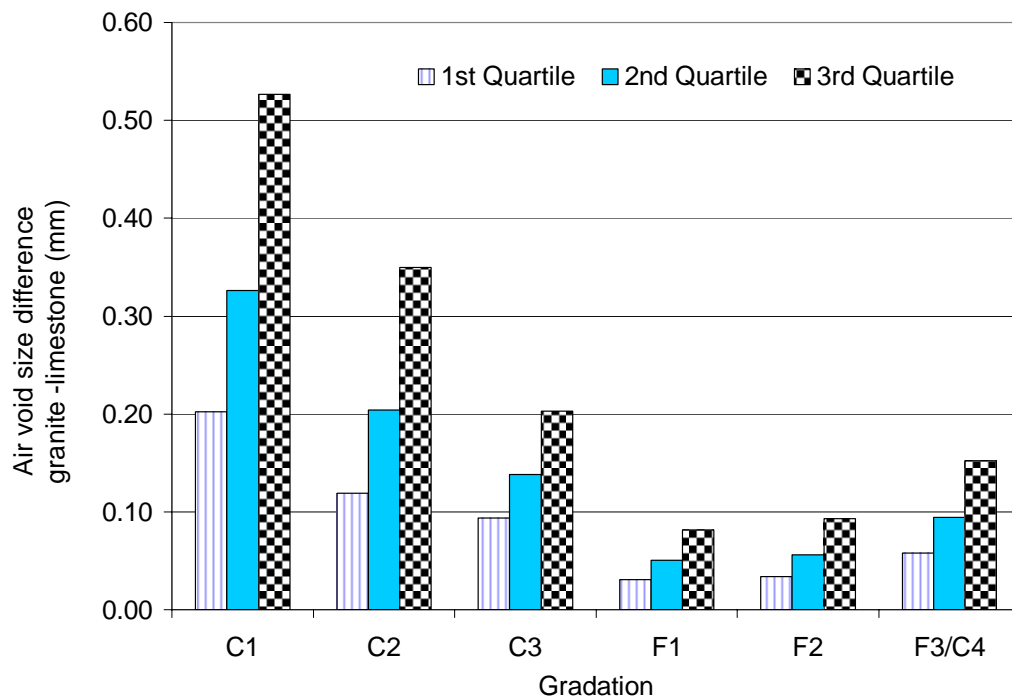
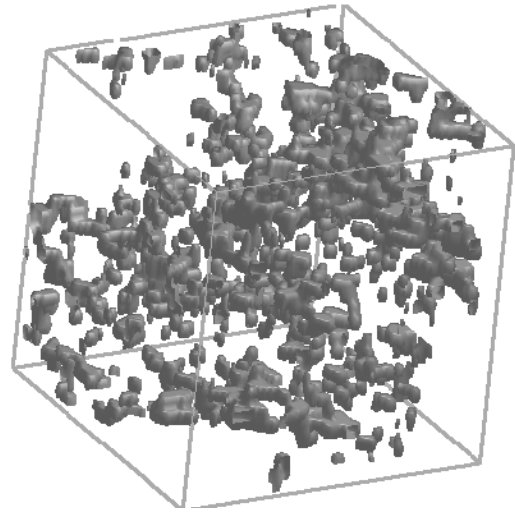
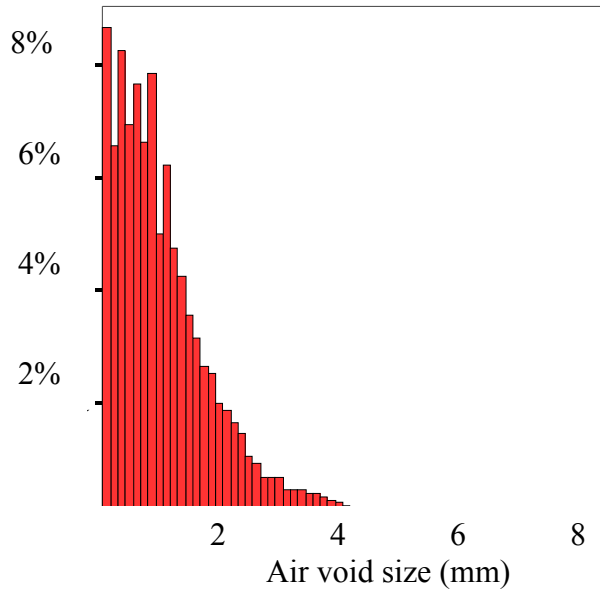
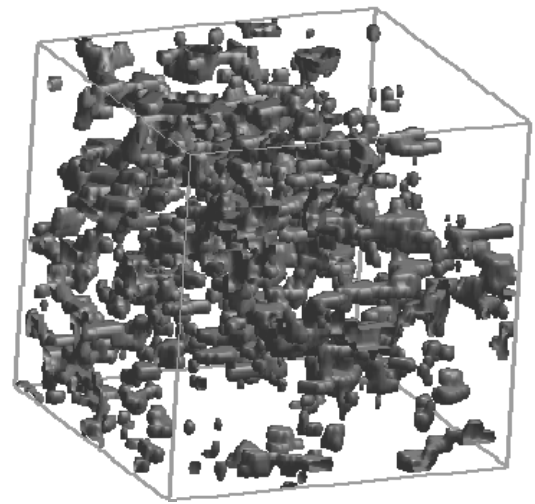
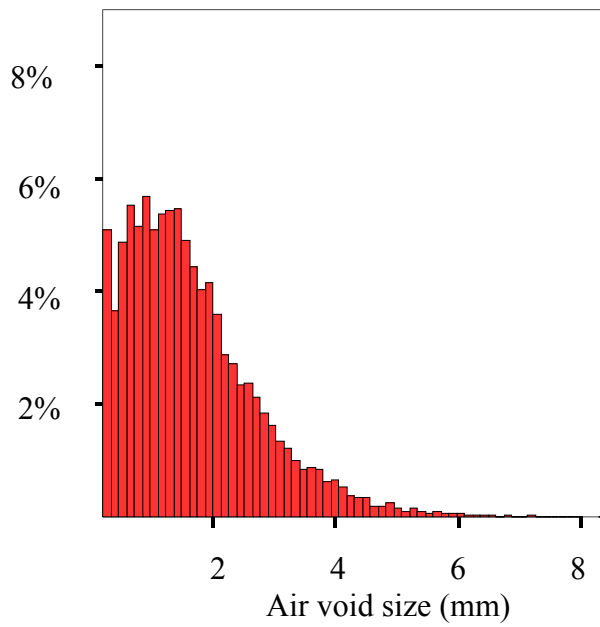


Fig. 42. Quartile Air Void Size Difference between Granite and Limestone (Castelblanco 2004)

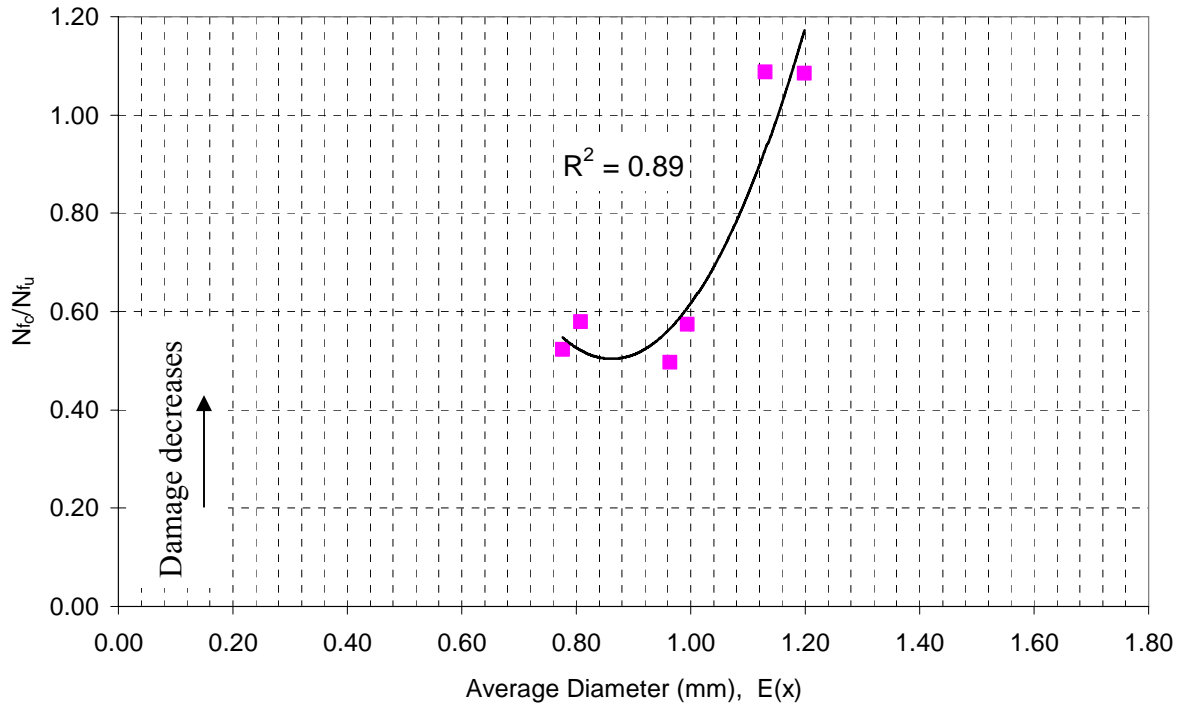


(a)

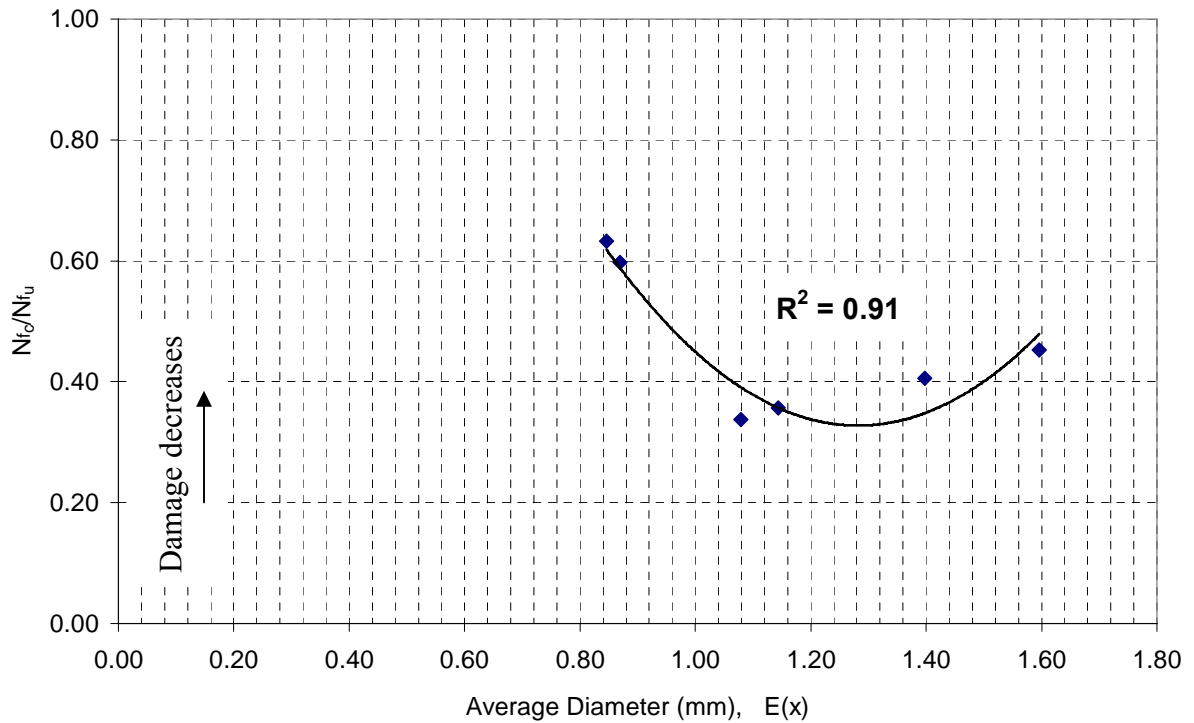


(b)

Fig. 43. Distributions and Three-Dimensional Visualization of Air Voids (a) WR-C1 and (b) GA-C1 (Castelblanco 2004)



(a)



(b)

Fig. 44.  $N_f$  Ratio and Average Diameter: (a) Limestone and (b) Granite (Castelblanco 2004)

### 3.3.3.2 Interpretation of Microvolt Outputs

The analysis of microvolt outputs depends on understanding the relationship between microvolts and total suction values as illustrated in Fig. 15. The approach used to analyze the microvolts-suction relationship is presented here with the aid of some experimental measurements obtained in this study.

Fig. 45 shows the recorded microvolt outputs versus time after stage 1 (60 minutes in the TCR). The recorded microvolts were negative, indicating that the total suction in this specimen was out of the psychrometer's range. This in turn means that the specimen was still wet and the suction was less than 3.67 pF. Therefore, it was decided to consider the total suction value to be equal to zero bar. The recorded microvolt measurements shown in Fig. 46 are for stage 2 (75 minutes in the TCR). The measurements were still negative, which means that this specimen was still wet and the total suction was less than 3.67 pF. Again, the total suction was considered to be equal to zero after stage 2.

As shown in Fig. 47, the specimen started to lose some water after stage 3 (180 minutes in the TCR), which caused the total suction to increase. The microvolt measurement reached  $6 \mu V$ , which allowed the calculation of the total suction using the calibration curve of this thermocouple psychrometer. The total suction was found to be 3.96 pF after this stage.

In stage 4, the specimen lost more water and suction increased. The recorded microvolt output after 1500 min (proposed equilibrium time) was  $17 \mu V$  as shown in Fig. 48, which is the maximum limit of this psychrometer. Hence the total suction was calculated to be 4.60 pF in this stage.

After stage 5 (480 minutes in the TCR), the recorded microvolt output shown in Fig. 49 was found to be  $0.5 \mu V$ , which was less the previous reading in stage 4 ( $17 \mu V$ ). This indicates that the specimen became dry enough for suction to be higher than the psychrometer range (see Fig. 15). Consequently, it was decided to consider the total suction value to be equal to the maximum limit of each psychrometer (about 4.68 pF).

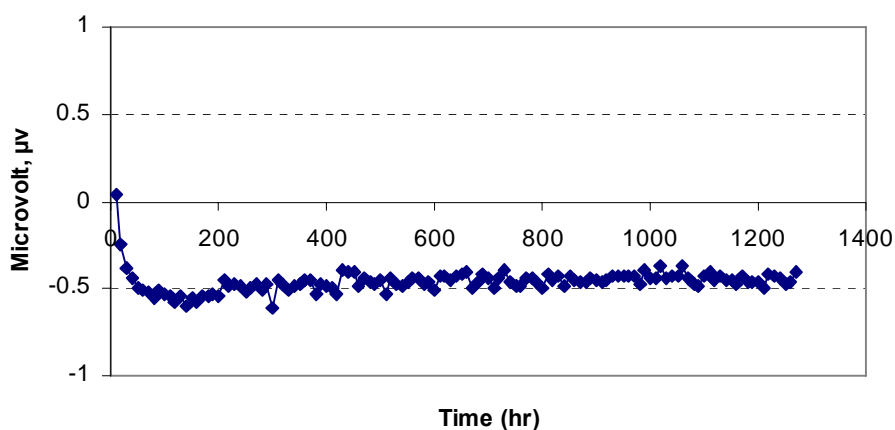


Fig. 45. Microvolt Outputs after Stage 1

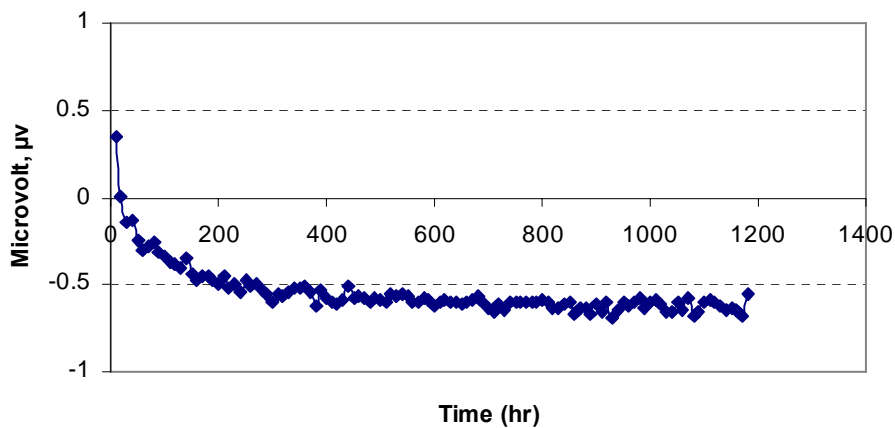


Fig. 46. Microvolt Outputs after Stage 2



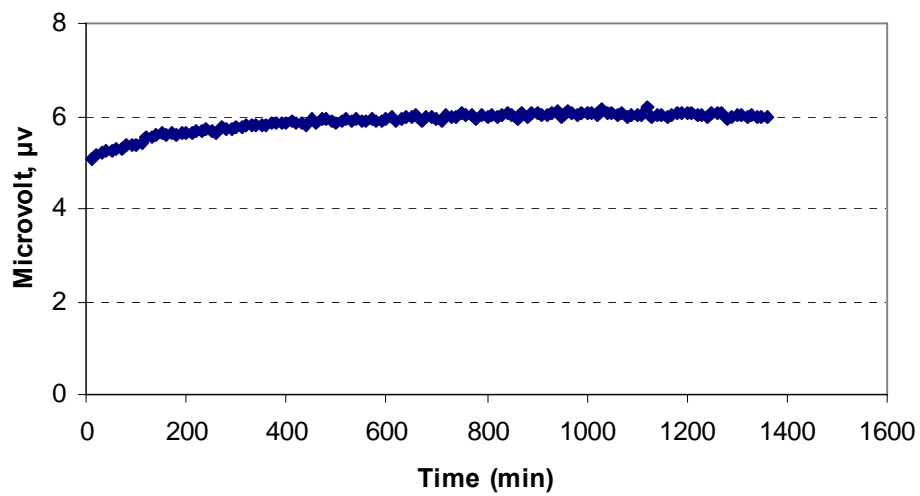


Fig. 47. Microvolt Outputs after Stage 3

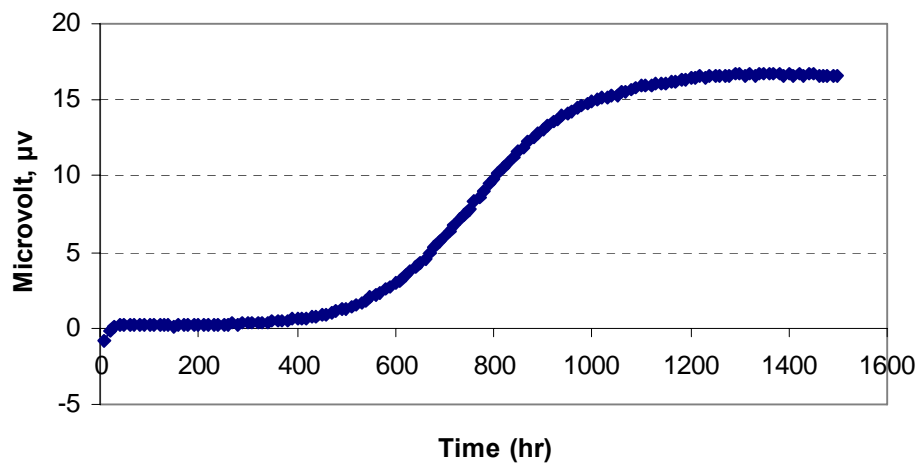


Fig. 48. Microvolt Outputs after Stage 4

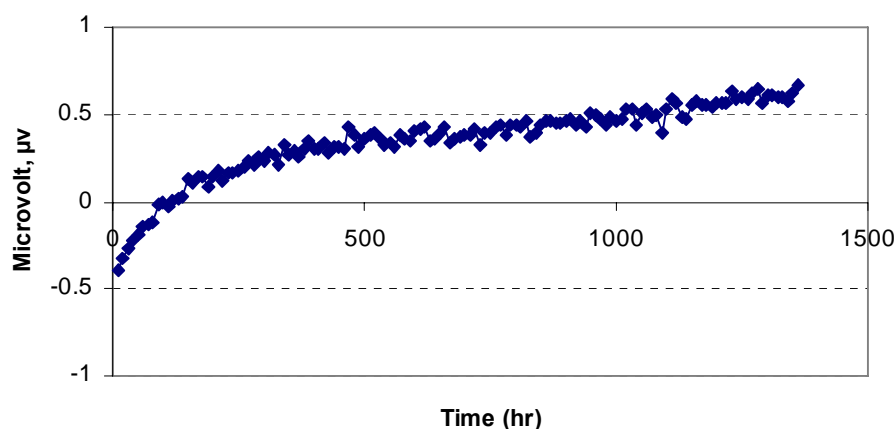


Fig. 49. Microvolt Outputs after Stage 5

### 3.3.3.3 Total Suction Results

The average of the measurements by the three psychrometers was taken as the suction after each stage. The results of the average total suction measurements for the limestone and granite specimens are presented in Tables 8 and 9, respectively. During the drying test, one specimen from the granite specimens (GA-C1) was damaged, and its results are not included in this thesis. A suction value of 0 in Tables 8 and 9 means that suction is less than 3.67 pF (4.5 bar), which indicates that suction is out of the psychrometer's range. Specimen WR-C1 went from a wet condition to a dry condition in stage 3.

Table 8. Average Total Suction Values in Bar for Limestone Specimens

Specimen #	Stage #				
	1	2	3	4	5
<b>WR-C1</b>	0	0	44.03	44.03	44.03
<b>WR-C2</b>	0	0	10.10	33.41	41.12
<b>WR-C3</b>	1.06	1.42	16.88	23.15	31.55
<b>WR-F1</b>	0	0	19.24	39.71	45.22
<b>WR-F2</b>	0	0	5.62	25.56	41.84
<b>WR-F3/C4</b>	0	0	12.93	29.53	44.98

Table 9. Average Total Suction Values in Bar for Granite Specimens

Specimen #	Stage #				
	1	2	3	4	5
<b>GA-C2</b>	0	0	0.33	1.29	4.37
<b>GA-C3</b>	0	0	0	3.74	10.10
<b>GA-F1</b>	5.31	6.06	15.09	15.09	19.23
<b>GA-F2</b>	0	0	0	3.40	8.01
<b>GA-F3/C4</b>	0	0	3.43	13.70	23.64

### 3.3.3.4 Water Content

Water content was measured after each stage in order to establish a relationship between the water content and total suction for each specimen. The water content equals to the weight of water divided by the dry weight of the specimen as shown in Eq. (8):

$$w = W_w / W_d \quad (8)$$

where

$w$  = water content

$W_w$  = weight of water

$W_d$  = specimen dry weight

The weight of water  $W_w$  equals to the weight of a wet specimen minus the dry weight of this specimen as illustrated in Eq. (9):

$$W_w = W_s - W_d \quad (9)$$

where

$W_s$  = specimen weight after each stage

$W_d$  = weight of the specimen

The water contents of the limestone and granite specimens after each stage are presented in Tables 10 and 11, respectively.

Table 10. Water Content in Percent in Limestone Specimens

Specimen #	Stage #				
	1	2	3	4	5
<b>WR-C1</b>	1.57	1.27	1.08	0.90	0.73
<b>WR-C2</b>	1.59	1.25	1.09	0.90	0.75
<b>WR-C3</b>	1.47	1.22	1.01	0.81	0.57
<b>WR-F1</b>	2.00	1.81	1.59	1.37	1.19
<b>WR-F2</b>	1.23	0.98	0.80	0.62	0.45
<b>WR-F3/C4</b>	2.30	2.10	1.85	1.56	1.32

Table 11. Water Content in Percent in Granite Specimens

Specimen #	Stage #				
	1	2	3	4	5
<b>GA-C2</b>	1.41	1.21	1.00	0.78	0.59
<b>GA-C3</b>	2.01	1.75	1.54	1.34	1.15
<b>GA-F1</b>	1.86	1.67	1.52	1.38	1.19
<b>GA-F2</b>	1.86	1.64	1.46	1.27	1.08
<b>GA-F3/C4</b>	1.84	1.55	1.39	1.22	1.08

Fig. 50 shows the amount of the initial absorbed water after vacuum saturation, water lost as a result of the drying process, and water remaining in each specimen after stage 5.

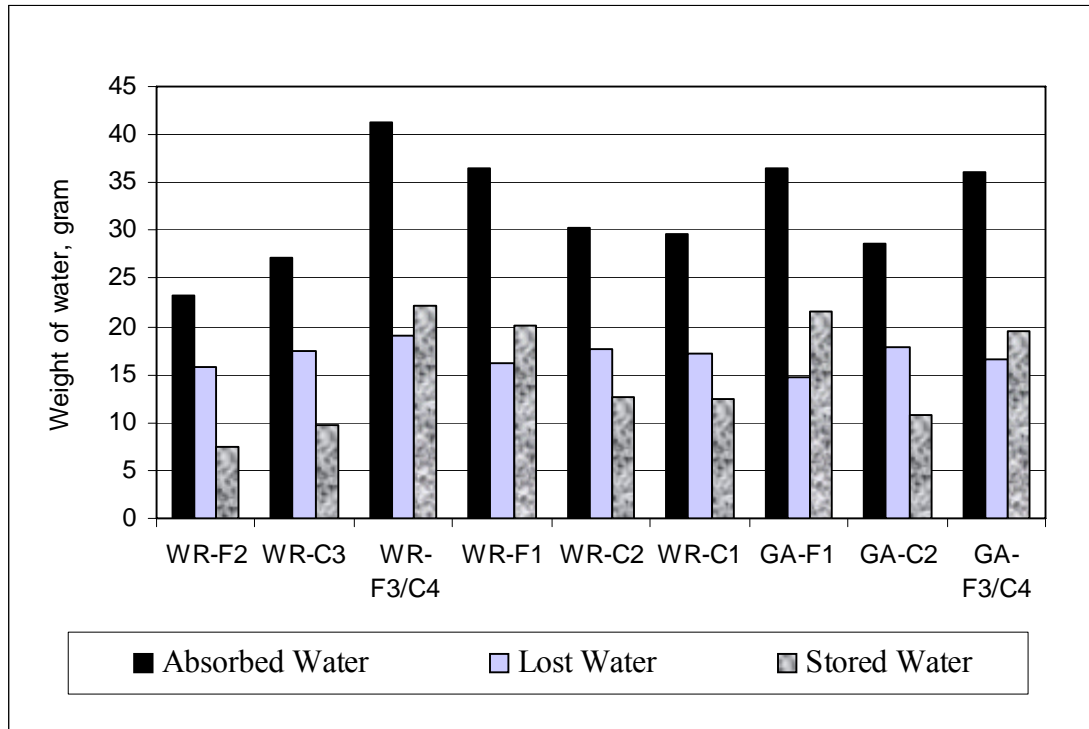


Fig. 50. Weights of Absorbed Water, Lost Water, and Stored Water in Mixes

### 3.3.3.5 Analysis of Total Suction Measurements

The relationships between moisture content and total suction for the limestone and the granite specimens are presented in Figs. 51 and 52, respectively. It is observed that both F1 and F3 specimens in the limestone and granite mixes had the highest suction. This is attributed to the fact that these two mixes had small air voids as evident in the

results in Table 7. Small air voids correspond to high specific surface area, and high suction as shown in Eq. (10) (Lytton 2005b).

$$(U_a - U_w) = \frac{T_s * SSA * \rho_w}{w} \quad (10)$$

where

$(U_a - U_w)$  = matric suction

$T_s$  = surface tension

$SSA$  = specific surface area

$\rho_w$  = density of water

$w$  = water content

However, the results from F2 did not have high suction as was expected from the air void sizes shown in Table 7. Careful evaluation of the aggregate and air void size distributions for F2 revealed useful information for explaining the results. The gradation was divided into a fine fraction and a coarse fraction. It was found that F2 had the largest average size for the coarse fraction, and the smallest average aggregate size for the fine gradations among all the other gradations. This mix exhibited the largest standard deviations of aggregate size distribution as well as air void size distribution. It is theorized that the suction measurements were more influenced by the coarse fraction of the gradation rather than the fine fraction.

By comparing the total suction measurements of both Figs. 51 and 52, it can be seen that the total suction measurements of limestone specimens were higher than the measurements of granite specimens. The total suction values reached the limit of thermocouple psychrometer in the case of the limestone specimens before the granite

specimens. From the air void distribution in Table 7, it can be seen that the granite mixes had in general larger air void sizes than the limestone mixes. The larger air voids are associated with smaller suction. The influence of air void size on suction is shown in Fig. 53. The radius of curvature is proportional with the diameter or the pore water size, and the radius of curvature is inversely proportional to the difference between the air and the water pressures across the surface (i.e.,  $[U_a - U_w]$ ) which is termed matric suction (Fredlund and Rahardjo 1993). This indicates that the radii of curvature of granite specimens were greater than the radii of curvature of limestone specimens, and hence the matric suction in granite mixes was less than the matric suction in limestone mixes.

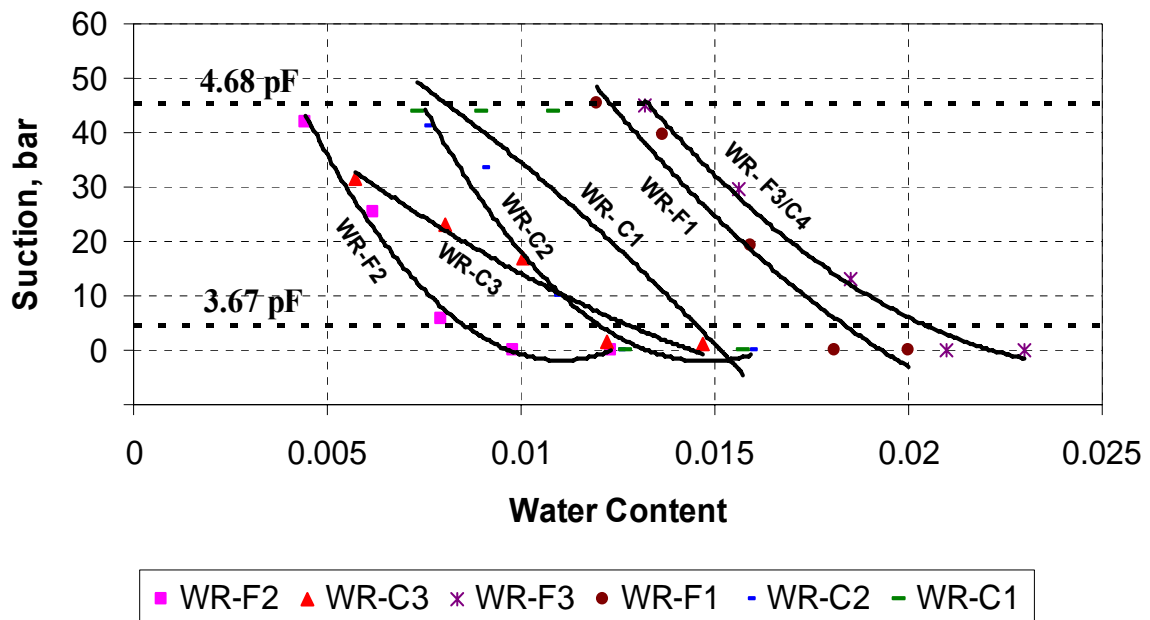


Fig. 51. Relationship between Water Content and Total Suction in Limestone Specimens

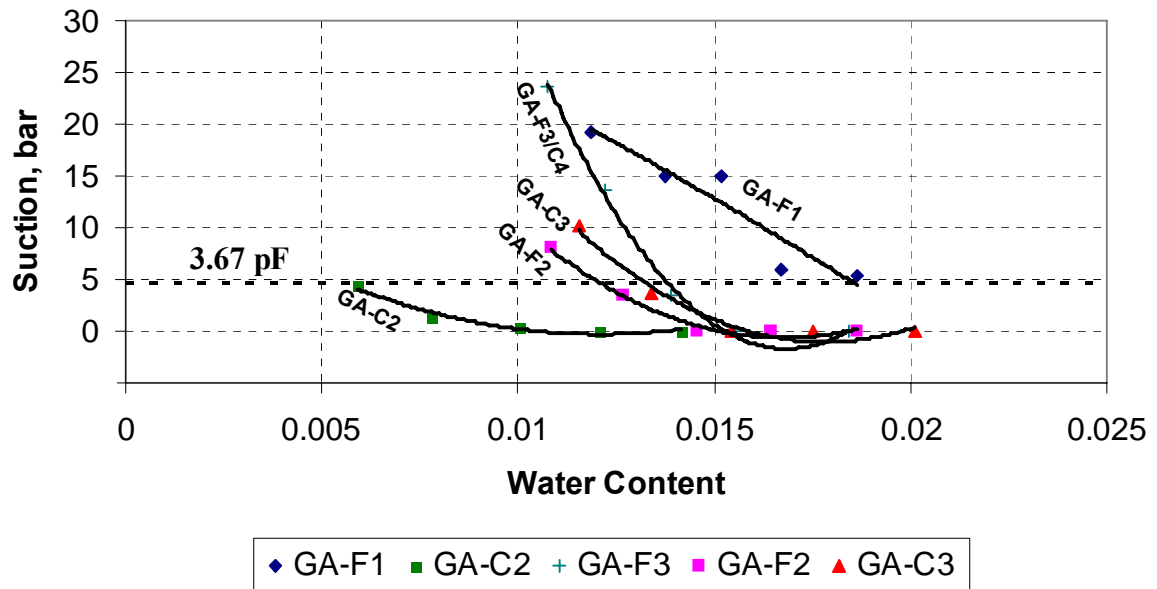


Fig. 52. Relationship between Water Content and Total Suction in Granite Specimens

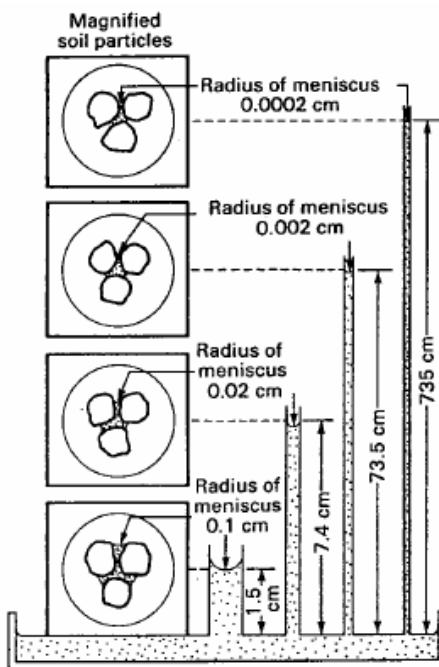


Fig. 53. Effect of Tube Radii on Radius of Curvature (Fredlund and Rahardjo 1993)



### **3.3.3.6 The Relationship between Total Suction and Moisture Damage**

The relationship between moisture damage and total suction is illustrated in Figs. 54 and 55 for the limestone and granite specimens, respectively. As discussed earlier, an increase in the value in the y axis indicates less moisture damage (Castelblanco 2004). It is interesting to note that a parabolic relationship exists between suction and moisture damage for the limestone specimens. It can be hypothesized that some specimens had low suction, which made it easier for air voids to lose moisture to the asphalt, causing more moisture damage. On the other hand, some specimens had very high suction, which made it difficult for the specimens to lose moisture to the environment, causing more moisture damage. It seems that there exists an optimum suction value at which moisture damage was minimal.

The granite specimens did not exhibit a relationship between suction and moisture damage. This can be caused by the large air voids in granite specimens and the poor bonding between granite aggregate and binder as reported by Castelblanco (2004). Consequently, significant moisture damage was caused even at small amounts of moisture, rendering no relationship between suction and moisture damage.

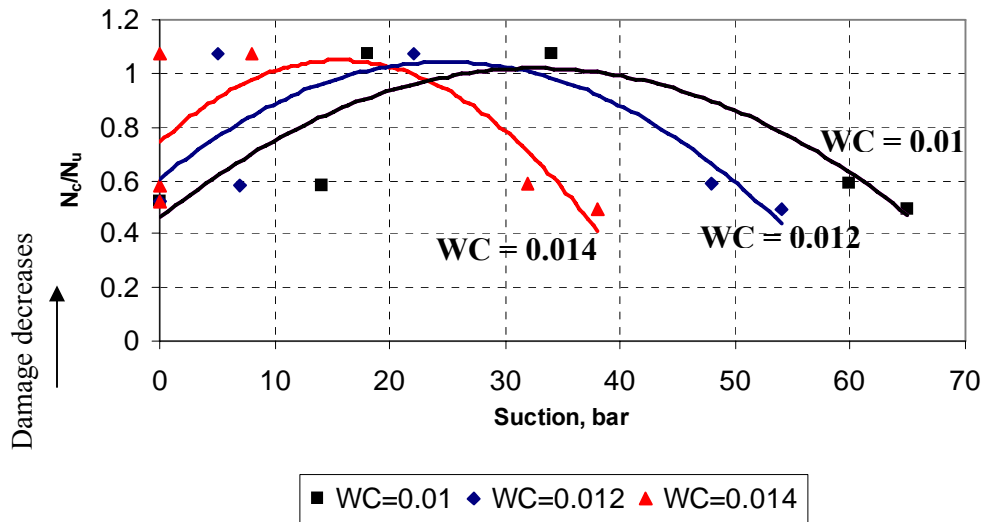


Fig. 54. Relationship between Moisture Damage and Total Suction in Limestone Mixes

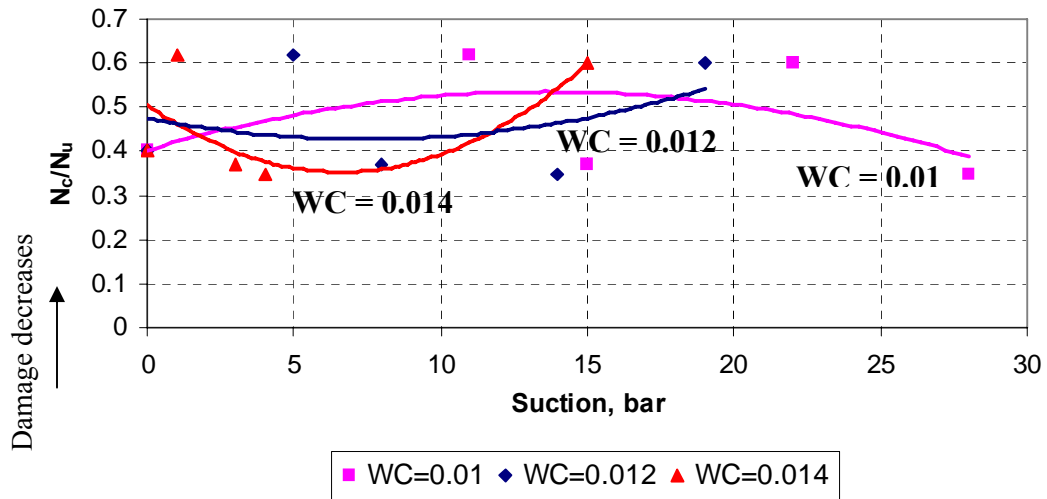


Fig. 55. Relationship between Moisture Damage and Total Suction in Granite Mixes

### **3.4 Using TST to Assess the Moisture Susceptibility in HMA Mixes**

The TST, which was discussed in Chapter II, has been used to evaluate the moisture susceptibility of granular bases in pavements (Scullion and Saarenketo 1997). Therefore, it was decided to investigate the ability of TST to assess the moisture susceptibility of HMA. As was done for the psychrometers, TST was used to assess the moisture susceptibility under drying and wetting protocols.

The wetting protocol consisted of the following steps:

- 1) A dry HMA specimen was wrapped with two layers of plastic clear wrap and with one layer of aluminum foil as shown in Figs. 56 and 57, respectively.
- 2) Plastic tape was used to tighten the wrap around a specimen, and the top and the bottom surfaces of the specimens were kept uncovered. In addition, about 1.30 cm from the bottom of a specimen was kept uncovered as shown in Fig. 58.
- 3) HMA specimens were placed over 0.65 cm thick porous stone as shown in Fig. 59 and in 1.9 cm bath of water as illustrated in Fig. 60
- 4) A percometer device, as shown in Fig. 10, was used to record the dielectric values of the HMA mixes every 24 hours. Six measurements were taken, one at the center of the specimen and five around the center as illustrated in Fig. 61.



Fig. 56. Specimen Wrapped with Plastic Wrap



Fig. 57. Specimen Wrapped with Aluminum Foil



Fig. 58. Plastic Tape Is Used to Fasten the Wrap



Fig. 59. Porous Stones Placed in Bath of Water



Fig. 60. HMA Mixes Placed over Porous Stones in Bath of Water



Fig. 61. Percometer Used to Record Dielectric Values

The drying protocol started by saturating specimens with water under vacuum saturation for about 20 minutes. Specimens were wrapped as was done in the wetting protocol. Then, specimens were placed in a room at 25 °C. The dielectric values were

measured by the percometer every 24 hours for one week. Six specimens were tested, four specimens (1, 2, 3, and 4) using the wetting protocol and two specimens (5 and 6) using the drying protocol. The six specimens were prepared from the same materials: crushed gravel, manufactured sand, and limestone screening. Specimen 1 had 5 percent air void, and specimens 2, 4, and 6 had 9.2 percent air void; specimens 3 and 6 had 6.3 percent air void.

### **3.4.1 Results of the TST**

The results of the TST, as shown in Fig. 62, showed very small change in dielectric values. In the wetting protocol, the dielectric values increased on average from 4.3 to 4.8, while in the drying protocol the dielectric values dropped from 5.3 to 4.8. It was concluded that the dielectric values of HMA mixes were between 4.3 to 5.3, and this range is not sufficient to assess the moisture damage in HMA mixes. In soils as discussed earlier in Fig. 11 the dielectric values are higher than the dielectric values in HMA, and it is found that the maximum acceptable dielectric values for the good-quality aggregate is 16 (Scullion and Saarenketo 1997)

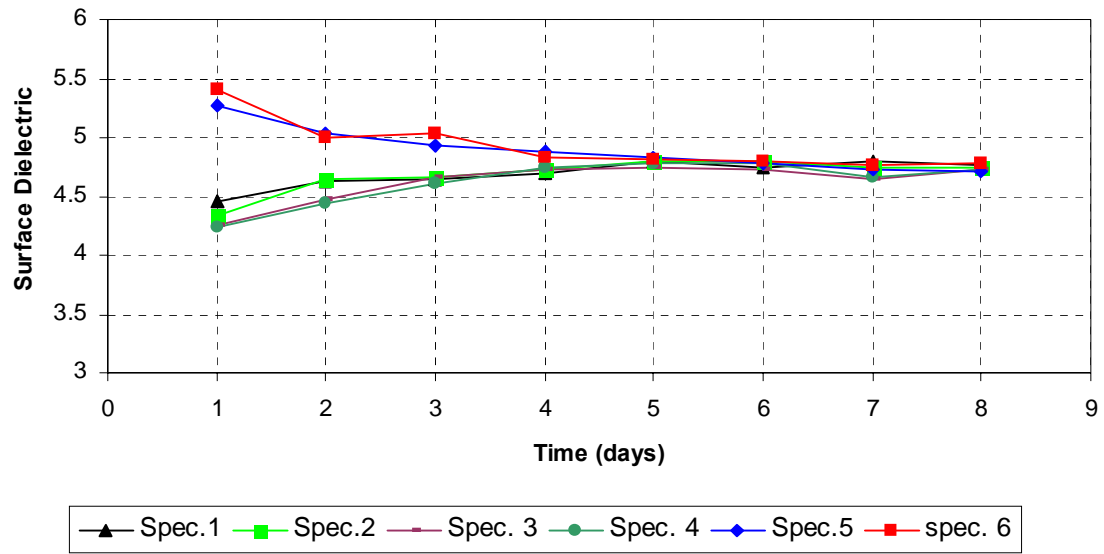


Fig. 62. TST Results of HMA Mixes



## CHAPTER IV

### DETERMINATION OF THE DIFFUSION COEFFICIENT

#### 4.1 Introduction

In this part of the study, sand asphalt specimens were prepared from combinations of aggregate and binders with different bond energies and field performance in terms of resistance to moisture damage. Suction measurements were conducted on these specimens, and the results were used to calculate the diffusion coefficient, which quantifies the movement of moisture in sand asphalt. The calculated diffusion coefficients were related to the sand asphalt resistance to moisture damage. This chapter includes a brief introduction on the moisture diffusion and the proposed test for measuring the diffusion coefficient.

#### 4.2 The Moisture Diffusion Concept

Mitchell (1979) used the Laliberte and Corey's permeability equation (Laliberte and Corey 1967) as shown in Eq. (11), and the mass balance equation for unsteady fluid flow to develop a simplified formulation of moisture diffusion. Mitchell (1979) assumed  $n$  value in Eq. (11) to be 1.

$$k = k_0 \left( \frac{h_0}{h} \right)^n \quad (11)$$

where

$k_0$  = saturated permeability

$h_0$  = a reference value of total suction, taken to be 100 cm

$h$  = total suction

$n$  = positive constant depending on the material's type

The permeability  $k$  from Eq. (11) is then substituted into Darcy's law given in Eq. (12) to get Eq. (13):

$$v = -k \left( \frac{dh}{dx} \right) \quad (12)$$

where

$v$  = flow velocity

$k$  = permeability

$\frac{dh}{dx}$  = head gradient

$$v = -k_0 \left( \frac{h_0}{h} \right) \left( \frac{dh}{dx} \right) \quad (13)$$

Eq. (13) can be rearranged to become:

$$v = -k_0 h_0 \left( \frac{dh/h}{dx} \right) \quad (14)$$

where

$$\frac{dh}{h} = d(\log_e h) = \frac{1}{0.432} d \log_{10} h \quad (15)$$

Substituting Eq. (15) into Eq. (14) gives:

$$v = -\frac{k_0 h_0}{0.434} \frac{d \log_{10} h}{dx} \quad (16)$$

where  $\log_{10} h$  = the total suction in  $pF$  units, which is termed  $u$ . Therefore, Eq. (16) can

be written as:

$$v = -\frac{k_0 h_0}{0.434} \frac{du}{dx} \quad (17)$$

i.e., 
$$v = -p \frac{du}{dx} \quad (18)$$

where  $p = \frac{k_0 h_0}{0.434}$  is a constant.

In Fig. 63 Mitchell (1979) considered an incremental section of the material with the dimensions  $\Delta x$ ,  $\Delta y$ , and  $\Delta z$ . The proposed section by Mitchell has a source of moisture generated in the soil at a rate per unit volume defined by  $f(x, t)$ .

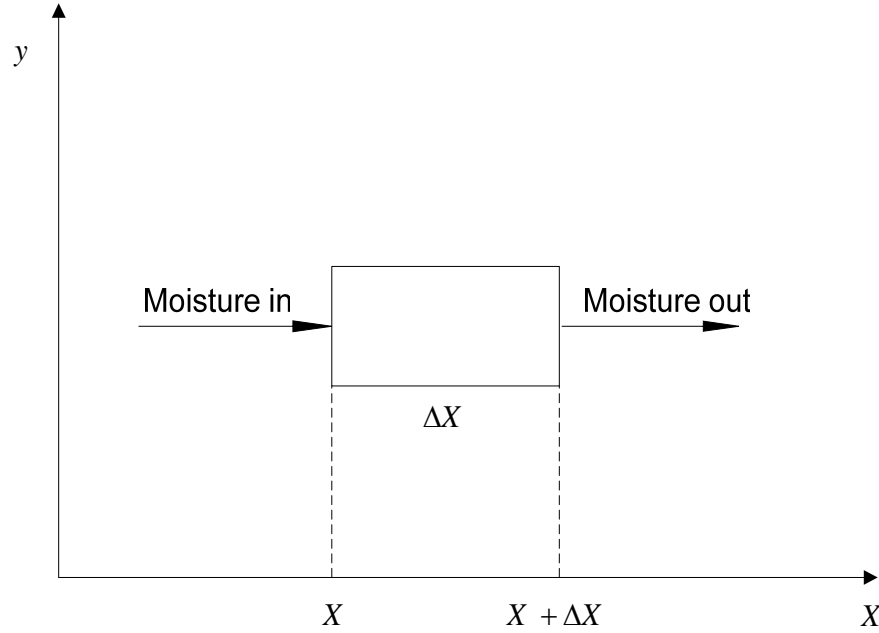


Fig. 63. Incremental Section with Dimensions  $\Delta x$ ,  $\Delta y$ , and  $\Delta z$

For the case of one dimensional flow in the  $x$  direction, the net flow into the body can be represented by Eq. (19):

$$\Delta Q = v_x \Delta y \Delta z \Delta t \Big|_x - v_x \Delta y \Delta z \Delta t \Big|_{x+\Delta x} + f(x, t) \Delta x \Delta y \Delta z \Delta t \quad (19)$$

Substituting  $v_x$  from Eq. (18) into Eq. (19) gives:

$$\Delta Q = -p \Delta y \Delta z \left( \frac{\partial u}{\partial x} \right)_x \Delta t - \left\{ -p \Delta y \Delta z \left( \frac{\partial u}{\partial x} \right)_{x+\Delta x} \Delta t \right\} + f(x, t) \Delta x \Delta y \Delta z \Delta t \quad (20)$$

$$= p \Delta x \Delta y \Delta z \frac{\left( \frac{\partial u}{\partial x} \right)_{x+\Delta x} - \left( \frac{\partial u}{\partial x} \right)_x}{\Delta x} \Delta t + f(x, t) \Delta x \Delta y \Delta z \Delta t \quad (21)$$

$$\Delta Q_{\Delta x \rightarrow 0} = p \Delta x \Delta y \Delta z \frac{\partial^2 u}{\partial x^2} \Delta t + f(x, t) \Delta x \Delta y \Delta z \Delta t \quad (22)$$

Mitchell (1979) defined the relationship between moisture content and suction as shown in Eq. (23):

$$c = \frac{dw}{du} \quad (23)$$

where

$c$  = moisture characteristic

$w$  = gravimetric water content

$u$  = suction, pF

If the suction is in the range of 2 pF to 4 pF, the moisture characteristic ( $c$ ) is assumed by Mitchell (1979) to be constant and the hysteresis can be neglected. The water content is defined as:

$$w = \frac{W_w}{W_s} \quad (24)$$

where

$W_w$  = weight of water

$W_s$  = weight of solids

The amount of stored moisture can be expressed by Eq. (25):

$$\Delta Q = \frac{\Delta W_w}{\gamma_w} = \frac{\Delta w W_s}{\gamma_w} = \Delta x \Delta y \Delta z (\Delta u c \frac{\gamma_d}{\gamma_w}) \quad (25)$$

where

$\gamma_d$  = dry density

$\gamma_w$  = water density

The amount of stored moisture given in Eq. (25) is equal to the net flow into the body given by Eq. (22). Hence, Eqs. (22) and (25) can be combined to give:

$$p \Delta x \Delta y \Delta z \Delta t \frac{\partial^2 u}{\partial x^2} + f(x, t) \Delta x \Delta y \Delta z \Delta t = \Delta x \Delta y \Delta z (\Delta u c \frac{\gamma_d}{\gamma_w}) \quad (26)$$

$$p \frac{\partial^2 u}{\partial x^2} + f(x, t) \frac{\gamma_d c}{\gamma_w} \frac{\partial u}{\partial t} \quad (27)$$

Eq. (27) can be written as:

$$\frac{\partial^2 u}{\partial x^2} + \frac{f(x, t)}{p} = \frac{\gamma_d c}{\gamma_w p} \frac{\partial u}{\partial t} \quad (28)$$

or

$$\frac{\partial^2 u}{\partial x^2} + \frac{f(x, t)}{p} = \frac{1}{\alpha} \frac{\partial u}{\partial t} \quad (29)$$

Eq. (29) is the diffusion equation, where  $\alpha = \frac{\gamma_w p}{\gamma_d c}$  is the diffusion coefficient. If the

moisture flow is in three directions, Mitchell (1979) defined general form of the diffusion equation as:

$$\frac{\partial^2 u}{\partial x^2} + \frac{\partial^2 u}{\partial y^2} + \frac{\partial^2 u}{\partial z^2} + \frac{f(x, y, z, t)}{p} = \frac{1}{\alpha} \frac{\partial u}{\partial t} \quad (30)$$

The movement of the moisture through unsaturated medium is defined by the diffusion equation, Eq. (30), and the diffusion coefficient is considered to be constant.

### 4.3 Determination of Diffusion Coefficient, $\alpha$

There are two different experimental procedures proposed by Mitchell for the determination of the diffusion coefficient. The first procedure is the soaking test, and the second procedure is the evaporation test. In this study the soaking test is used for the determination of the diffusion coefficient in sand asphalt.

#### 4.3.1 The Soaking Test Procedure for Determination of $\alpha$

The diffusion coefficient can be measured by what is called the soaking test in which the change of the total suction in a specimen is monitored as a function of time. In this test, a specimen is kept in a cylindrical container where it is sealed from all sides except one surface which is exposed to a liquid as shown in Fig. 64. This liquid has a known suction,  $u_l$ , while the specimen is originally at suction  $u_0$ .

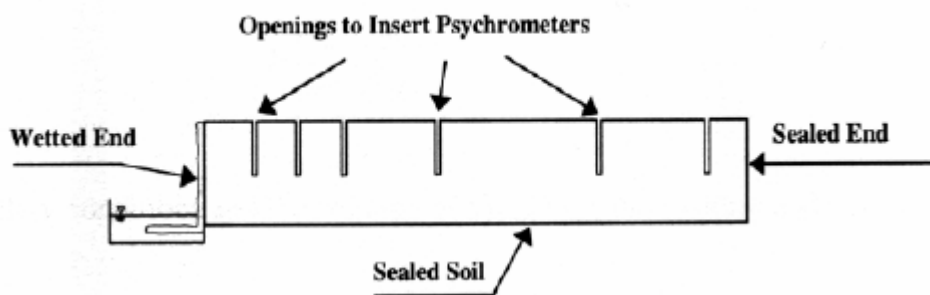


Fig. 64. Soaking Test Setup for Determination of  $\alpha$  (Tang 2003)

Mitchell (1979) developed a solution for Eq. (30) using the boundary conditions of the experiment. Substituting  $f(x, y, z, t)$  as zero, Eq. (30) is simplified to Eq. (31):

$$\alpha \frac{\partial^2 u}{\partial x^2} = \frac{\partial u}{\partial t} \quad (31)$$

The boundary conditions for this problem are:

Sealed boundary:

$$\frac{\partial u(0,t)}{\partial x} = 0 \quad (32)$$

Boundary exposed to the liquid with known suction:

$$u(l,t) = u_l \quad (33)$$

Initial suction:

$$u(x,0) = u_0 \quad (34)$$

Using the Laplace Transform method, the solution of Eq. (31) is given in Eq. (35):

$$u = u_l + \frac{4(u_l - u_0)}{\pi} \sum_{n=1}^{\infty} \frac{(-1)^n}{2n-1} \exp\left(-\frac{(2n-1)^2 \pi^2 t \alpha}{4l^2}\right) \cos\frac{(2n-1)x}{2l} \quad (35)$$

where

$u$  = suction as a function of the position and the time

$t$  = time

$x$  = distance from closed end

$l$  = the total length of the sample

#### 4.4 Determination of the Diffusion Coefficient in Sand Asphalt

##### 4.4.1 Specimens Preparation

The diffusion coefficient can be determined by measuring the change of the total suction with time using Mitchell's soaking test. The sand asphalt specimens were prepared from different combinations of aggregates and binders with different bond

energies and field performance in terms of resistance to moisture damage. Zollinger (2005) conducted a study on six different sand asphalt mixes using the dynamic mechanical analyzer (DMA) to develop an experimental protocol to evaluate the susceptibility of asphalt mixes to moisture damage. Zollinger (2005) compared the DMA results to the surface energies of aggregates and binders, and the field performance of pavement sections where these mixes were used. Three of the mixes that were tested by Zollinger were included in this study. These mixes were referred to by Zollinger as 4, 7, and 8. In order to avoid any confusion in the description of these mixes, the labels that were used in the original study will be maintained here. The aggregate gradations for mixtures 4, 7, and 8 are shown in Tables 12, 13, and 14, respectively. The descriptions of these mixes are given in Table 15. Based on careful field evaluation of these mixtures, mixture 8 had “poor” resistance to moisture damage, mixture 7 had “fair to poor” resistance to moisture damage, and mixture 4 had “very good” resistance to moisture damage among all the mixes evaluated by Zollinger (2005).

The sand asphalt specimens were prepared using the fine portion of the aggregate gradation mixed with the binder. The finer portion has been considered the portion of the aggregate passing sieve number 16 (1.18 mm) to the pan. Zollinger (2005) used the job mix formula to calculate the aggregate gradation proportions as shown in Tables 16, and 17. The sand asphalt from mixtures 7 and 8 consisted of natural sand and limestone, while sand asphalt mixture 4 consisted of sandstone screening, igneous screening, and hydrated lime. The percentages of these aggregates are shown in Table 18.

The method used by Zollinger (2005) to prepare the specimens was followed in this study. The filler was mixed with pure binder at the binder mixing temperature, and



then the asphalt-filler material was mixed with the remaining fine aggregate. The mixture was placed in an oven for two hours for short-term oven aging. The temperature was turned to the compaction temperature for one hour prior to the compaction. The theoretical maximum specific gravity was determined before placing the mixture in a 6-inch diameter gyratory mold. Then, the mix was compacted to the targeted air void using a Superpave gyratory compactor. In this study the target percent air void was 15 percent at a specimen height of 85 mm. Each side of a specimen was trimmed about 17.5 mm to get the final specimen height of 50 mm. Then, a coring bit was used to obtain a 50 mm diameter by 50 mm height specimen. A gyratory specimen after coring is shown in Fig. 65, while the test specimens are shown in Fig. 66.

Table 12. Mixture 4 Gradation

Sieve Size (mm)	MER	MER	MER	ARK Granite	Texas TY A
	C-Rock	D-Rock	Screenings	Donnafill	Lime
	22%	57%	12%	8%	1%
	%passing	%passing	%passing	%passing	%passing
50.8	100.00	100.00	100.00	100.00	100.00
37.5	100.00	100.00	100.00	100.00	100.00
25.4	100.00	100.00	100.00	100.00	100.00
19.5	100.00	100.00	100.00	100.00	100.00
12.7	64.00	100.00	100.00	100.00	100.00
9.5	17.00	96.00	100.00	100.00	100.00
4.75	1.00	49.00	99.00	100.00	100.00
2.36	0.80	20.00	72.00	100.00	100.00
1.18	0.50	12.00	54.00	100.00	100.00
0.6	0.40	10.00	37.00	96.00	100.00
0.3	0.30	8.00	32.00	67.00	100.00
0.15	0.20	6.00	22.00	40.00	100.00
0.075	0.10	4.00	11.00	24.00	100.00
<b>Binder Source</b>	<b>Wright PG 76-22</b>				
<b>Optimum % Binder</b>	<b>5.1</b>				

Table 13. Mixture 7 Gradation

Sieve Size (mm)	# 8 Limestone	# 8 Gravel	Limestone Sand	Natural Sand
	27.50%	27.50%	12.50%	32.50%
	%passing	%passing	%passing	%passing
50.8	100.00	100.00	100.00	100.00
37.5	100.00	100.00	100.00	100.00
25.4	100.00	100.00	100.00	100.00
19.5	100.00	100.00	100.00	100.00
12.7	100.00	100.00	100.00	100.00
9.5	88.00	95.00	100.00	100.00
4.75	18.00	20.00	100.00	100.00
2.36	2.00	2.00	90.00	92.00
1.18	2.00	2.00	63.00	67.00
0.6	2.00	2.00	40.00	44.00
0.3	2.00	2.00	20.00	18.00
0.15	2.00	2.00	9.00	5.00
0.075	2.00	2.00	6.40	4.30
<b>Binder Source</b>	<b>Tri-State PG 64-22</b>			
<b>Optimum % Binder</b>	<b>5.4</b>			

Table 14. Mixture 8 Gradation

Sieve Size (mm)	#8 Gravel	Natural Sand	Limestone Sand
	65%	18%	17.50%
	%passing	%passing	%passing
50.8	100.00	100.00	100.00
37.5	100.00	100.00	100.00
25.4	100.00	100.00	100.00
19.5	100.00	100.00	100.00
12.7	100.00	100.00	100.00
9.5	95.00	100.00	100.00
4.75	20.00	100.00	100.00
2.36	2.00	92.00	90.00
1.18	2.00	67.00	63.00
0.6	2.00	44.00	40.00
0.3	2.00	18.00	20.00
0.15	2.00	5.00	9.00
0.075	2.00	4.30	6.40
<b>Binder Source</b>	<b>Marthon/Ashland PG 64-28</b>		
<b>Optimum % Binder</b>	<b>5.0</b>		

Table 15. Mixture Descriptions (Zollinger 2005)

<b>Mix #</b>	<b>Highway</b>	<b>Location</b>	<b>Reported Performance</b>	<b>Aggregate Type</b>	<b>Binder Grade</b>
<b>4</b>	Texas IH 20 Test Section 2	Atlanta, TX	Good	Sandstone	PG 76-22
<b>7</b>	Ohio SR 511	Ashland County, OH	Fair to Poor	Gravel Limestone, Rap	PG 64-22
<b>8</b>	Ohio SR 226	Wayne County, OH	Poor	Gravel, Rap	PG 64-28

Table 16. Aggregate Gradation for Sand Asphalt Mixtures 7 and 8

<b>Sieve Size mm</b>	<b>Mix 7 and Mix 8</b>	
	Limestone Sand	Natural Sand
1.18	100.0	100.0
0.6	60.1	64.0
0.3	25.4	23.3
0.15	6.3	2.9
0.075	1.8	1.8

Table 17. Aggregate Gradation for Sand Asphalt Mixture 4

<b>Sieve Size mm</b>	<b>Mix 4</b>		
	Sandstone Screenings	Granite Donnafill	Hydrated Lime
1.18	100.0	100.0	100.0
0.6	61.1	94.8	100.0
0.3	49.7	57.3	100.0
0.15	26.9	22.4	100.0
0.075	1.7	1.7	100.0

Table 18. Aggregate Composition of Test Specimens

Aggregate Type	Mix 7	Mix 8	Mix 4
Limestone Sand	28	50	-
Natural Sand	72	50	-
Sandstone Screening	-	-	57
Igneous Screenings	-	-	38
hydrated Lime	-	-	5



Fig. 65. Gyrotory Specimen after Coring of Test Specimens

#### 4.4.2 Testing Apparatus and Measurement Setup

The following steps were followed to measure suction in sand asphalt specimens:

- 1) Test specimens were drilled with a 0.95 cm (3/8 inch) diameter bit. The depth of the hole was 4.5 mm from the top of the specimen, i.e., the distance between the base and the end of the hole was 5 mm as illustrated in Figs. 67 and 68.



Fig. 66. Sand Asphalt Specimens after Coring Gyrotory Compacted Mixes

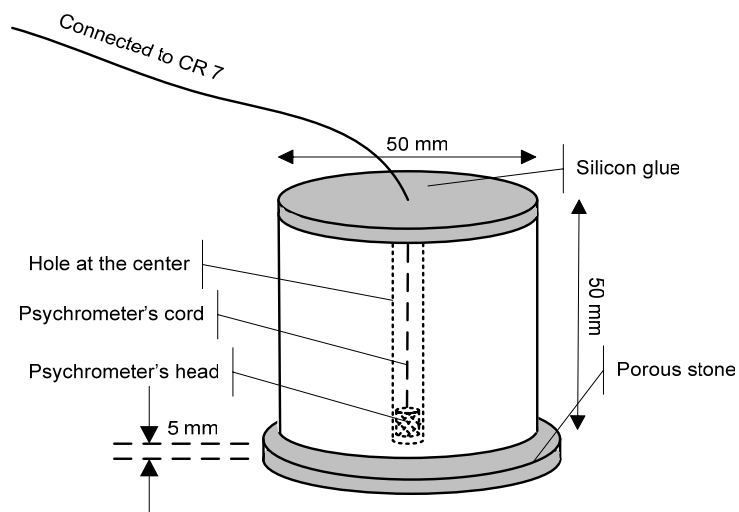


Fig. 67. Schematic View of Drilled Sand Asphalt Specimen

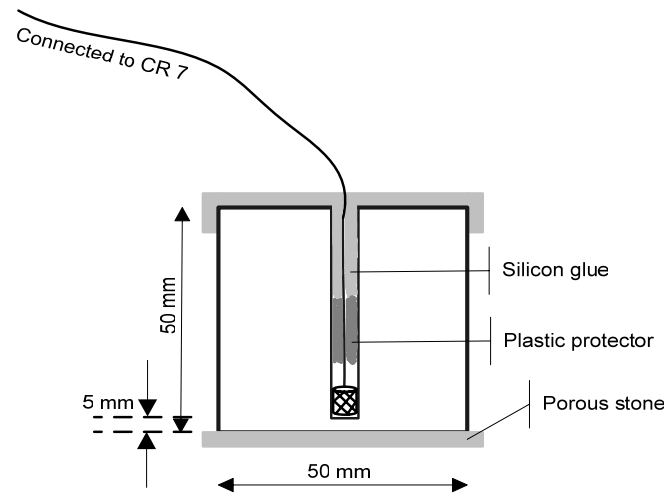


Fig. 68. Cross Section at Center of Drilled Sand Asphalt Specimen

2) The psychrometer was inserted to the end of the hole as shown in Fig. 69.



Fig. 69. Inserting Psychrometer



Fig. 70. Sealing Hole and Covering Upper Side with Silicon Glue

- 3) A small piece of plastic filler was placed in the hole without covering the psychrometer's head. The rest of the hole and upper side of the specimen were filled and covered with silicon glue to prevent any moisture flow as shown in Fig. 70. The plastic filler was used to protect the psychrometer from the liquid glue.
- 4) The silicon glue was allowed to dry for about 12 hours. Then, the specimens were placed on porous stones in a bath of water. The water temperature was maintained at 25 °C by using a temperature controller. The purpose of using porous stones underneath the specimens was to ensure uniformity of water distribution underneath a specimen's base.

### **4.4.3 Results and Analysis**

#### **4.4.3.1 Suction Measurements**

The first step for measuring the diffusion coefficient was to determine the change in suction with time. Based on the calibration curve, the thermocouple psychrometer was used to measure the total suction from 3.67 pF to 4.68 pF.

The psychrometer reading during the test is illustrated here with the aid of the example results shown in Fig. 71. Initially, the asphalt sand specimen was dry, and the suction value was out of the psychrometer's range (i.e., higher than 4.68 pF). This response is given by part 1 in Fig. 71. This response was for the period when a specimen was outside the water bath, and the glue was drying. Once a specimen was placed in the water bath, water started to diffuse into the mix and suction started to decrease. However, as shown in part 2 of Fig. 71, suction remained outside the psychrometer range. This part is equivalent to part 3 in Fig. 15. As water continued to diffuse, suction dropped

to a point within the psychrometer's range (around 4.68 pF). This point is the maximum point in Fig. 71 after which suction continued to decrease. Part 3 represents the true suction measurement within the psychrometer's range. All total suction measurements for the different mixes are given in Appendix D.

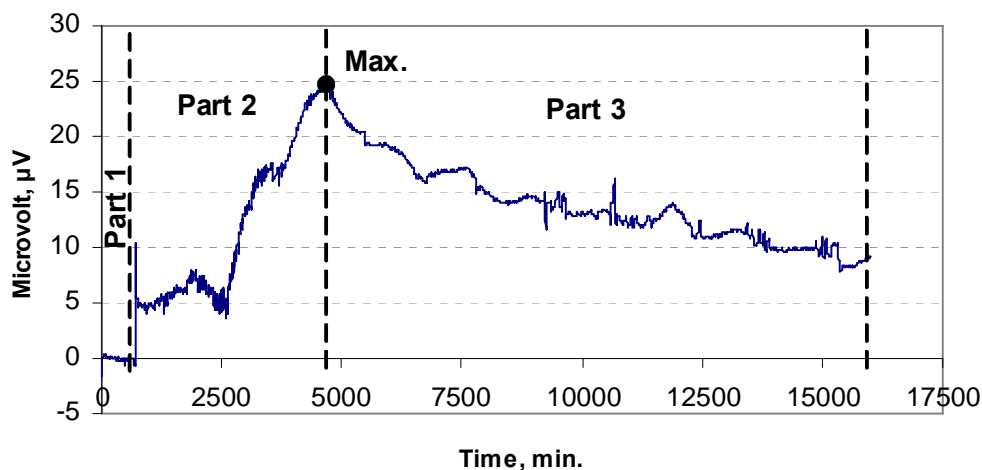


Fig. 71. Microvolt Outputs from Soaking Test versus Time

#### 4.4.3.2 Analysis of Suction Measurements

Based on the results of suction measurements in Appendix D, the elapsed time for total suction to drop from the oven dry range to the maximum psychrometer's range time was calculated and summarized in Table 19. This time corresponds to part 2 of Fig. 71 when the specimen was placed in water. Suction in mix 8 dropped from the oven dry range, over 5.5 pF, to the upper limit of the psychrometer's range (4.68 pF) in 43.13 hours, while it took 137.8 hours for mix 7, and 177.7 hours for mix 4.



Table 19. Average Elapsed Time for Total Suction to Drop to Psychrometer's Range

Mix. #	Average Time, hours
<b>8</b>	43.13
<b>7</b>	137.8
<b>4</b>	177.7

The diffusion coefficient was calculated by using Mitchell's equation for the soaking test (Eq. [35]). Although a test specimen was not sealed on the circumference, an assumption was made that moisture flow can be considered one dimensional. This was motivated by the fact that the distance between the psychrometer and the base of the specimen was 5 mm, while the distance between the psychrometer and the circumference was about 25 mm. Therefore, it was assumed that moisture will diffuse from the base much faster than from the circumference. Test specimens were cut after testing, and it was found that the portion underneath the psychrometer was wet, while the portion from the circumference to the psychrometer was dry.

The diffusion coefficient was calculated using the procedure developed by Aubeny and Lytton (2003), which can be outlined as follows:

- 1) An initial value of diffusion coefficient is assumed, and by using this value, the theoretical suction value can be calculated by Eq. (35). Eq. (35) requires the following:
  - $u_1$  = the suction of the liquid (water). It is taken to be 2.75 pF (Mitchell 1979)
  - $x$  = the distance from the closed end, equal to the length of the specimen (50 mm) subtracting the distance between the

psychrometer and the base (5 mm). The distance between the psychrometer and the base should be measured accurately by cutting the specimen after the test, and if it is not equal to 5 mm, the exact distance should be used. This distance varied between 5 mm to 7 mm in this study.

- $l$  = sample length
- $u_0$  = initial suction value, it is taken the maximum limit of each psychrometer.
- $u$  = measured suction as a function of the time and the distance  $x$ .  
First, the suction, pF–time curve is fitted using the polynomial, and the equation of this polynomial is obtained. The time between the initial suction until the time at the end of the test, or the time until suction dropped to the lower limit of the psychrometer, is divided into 10 equal periods. Using the equation of the polynomial, the total suction at these selected times is determined.
- $t$  = time at each suction measurement (ten values)

- 2) The difference between the theoretical suction value calculated from Eq. (35) and the measured suction  $E$  is calculated as follows:

$$E = u_{Theoretical} - u_{measured} \quad (36)$$

- 3) The square  $E$  is summed for all suction measurements:

$$E^2 = (u_{Theoretical} - u_{measured})^2 \quad (37)$$

- 4) The diffusion coefficient was determined such that the square error is minimized.

This step can be performed by any software program such as solver in Excel or

Matlab. In this study, two Matlab programs were modified from the one developed by Sood (2005) for the evaporation (drying) test to fit the soaking test that was used in this study. The first program, “alphawettingtest,” is used to calculate the diffusion coefficient, and the second one, “wetest,” is used to calculate the theoretical suction based on the calculated diffusion coefficient. Both of the programs are given in Appendix E.

The diffusion coefficient was calculated for mixes 4, 7 and 8, and the results are presented in Table 20 and Fig. 72.

Table 20. Diffusion Coefficient  $\alpha$  for Mixes 8, 7, and 4

<b>Mix #</b>	<b>Range of <math>\alpha</math>, cm<sup>2</sup>/sec</b>	<b>Average <math>\alpha</math>, cm<sup>2</sup>/sec</b>	<b>Standard Deviation</b>
<b>8</b>	1.18E-05 to 3.40E-05	2.10E-05	8.34E-11
<b>7</b>	2.80E-06 to 6.40E-06	4.20E-06	3.52E-12
<b>4</b>	1.60E-06 to 7.30E-06	4.78E-06	4.62E-12

#### **4.4.3.3 Relationship of Suction and Diffusion Coefficient to Surface Energy and**

##### **DMA Results**

Zollinger (2005) calculated the surface energy components of aggregates and asphalts as shown in Tables 21 and 22, respectively.

Table 21. Surface Energy Components of Aggregates (Zollinger 2005)

Mix	Aggregate Type	Surface Energy Components (Ergs/cm <sup>2</sup> )				
		$\Gamma$	$\Gamma^{LW}$	$\Gamma^{AB}$	$\Gamma^+$	$\Gamma^-$
4	Light Limestone	105.05	62.43	42.55	2.033	222.67
4	Dark Limestone	167.88	63.96	103.93	8.52	316.92
7 & 8	Limestone	111.14	58.05	53.01	1.77	401.18
7 & 8	Gravel	193.21	63.42	129.74	7.74	546.37

Note:  $\Gamma$  = the total bond Gibbs free energy of the material surface per unit surface area  
 $\Gamma^{LW}$  = the nonpolar, Lifshitz-van der Waals bond Gibbs free energy of the material surface  
 $\Gamma^{AB}$  = the polar, Acid-Base bond Gibbs free energy of the material surface  
 $\Gamma^+$  = the acid component of the surface energy of a material  
 $\Gamma^-$  = the base component of the surface energy of a material

Table 22. Surface Energy Components of Asphalts for Wetting (Zollinger 2005)

Mix	Asphalt Grade	Surface Energy Components (Ergs/cm <sup>2</sup> )				
		$\Gamma$	$\Gamma^{LW}$	$\Gamma^{AB}$	$\Gamma^+$	$\Gamma^-$
4	76-22	15.71	12.17	3.59	1.13	2.88
7	64-22	30.07	29.95	0.05	0.01	1.02
8	64-28	19.68	18.72	0.83	0.01	2.75

Zollinger (2005) ranked the three mixes by dividing the adhesive wet bond energy ( $\Delta G^{aW}$ ) by the adhesive dry bond energy ( $\Delta G^{aD}$ ). A decrease in the absolute value of  $\Delta G^{aW} / \Delta G^{aD}$  indicates a decrease in the ability of moisture to damage the asphalt-aggregate bond. As shown in Table 23, mix 4 had the best resistance to moisture damage followed by mixes 7 and then 8.

Zollinger (2005) also ranked those mixes based on DMA results as shown in Table 24. The DMA is a torsional device that was used to measure the number of loading cycles to failure with moisture conditioning (Wet  $N_f$ ) and the number of cycles to failure without moisture conditioning (Dry  $N_f$ ). A picture of a DMA specimen mounted in the

device is shown in Fig. 73. The results in Table 24 indicate that mix 4 is superior to mixes 7 and 8 in the resistance to moisture damage.

Table 23. Mixture Rankings According to Adhesive Wetting Bond Energy under Both Dry and Wet Conditions (Zollinger 2005)

Mix	Binder	Material	$\Delta G^a$ Wet	$\Delta G^a$ DRY	$\frac{ \Delta G^a Wet }{ \Delta G^a Dry }$
4	Wright PG 76-22	Light Sandstone	-61.99	91.57	0.6769684
4	Wright PG 76-22	Dark Sandstone	-95.25	103.38	0.9213581
7	Tri-State PG 64-22	Limestone	-115.58	87.49	1.3210653
8	Marathon/Ashland PG 64-28	Limestone	-119.82	81.27	1.4743448
7	Tri-State PG 64-22	Gravel	-160.22	94.56	1.6943739
8	Marathon/Ashland PG 64-28	Gravel	-161.87	90.92	1.7803564

Table 24. Mixture Rankings According to Average Fatigue Life in Both Dry and Wet Conditions

Mix	Average Fatigue Life ( $N_f$ )		$\frac{Wet N_f}{Dry N_f}$
	Dry	Wet	
4	16349	14671	0.9
7	3159	803	0.25
8	8767	2231	0.25

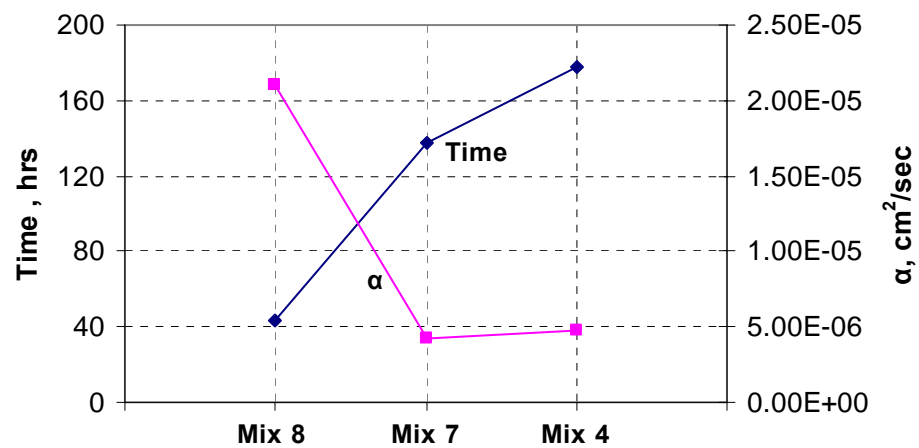


Fig. 72. Elapsed Time for Total Suction to Drop to Psychrometer's Range, and Average Diffusion Coefficient,  $\alpha$



Fig. 73. Asphalt Sand Specimen Mounted in DMA (Zollinger 2005)

The rate of moisture diffusion into HMA could be attributed to the moisture ability to break the cohesive and adhesive bonds in the mix. Following this notion, a shorter time for suction to reach the psychrometer's range (Table 19) corresponds to more moisture damage. Therefore, mix 4 is expected to exhibit more resistance to moisture damage than mixes 7 and 8. Also, mix 7 is expected to be better than mix 8 in resisting moisture damage. The diffusion coefficient  $\alpha$  values in Table 20 also support that mix 8 had a higher diffusion coefficient than the other two mixes and, consequently, is expected to have poor resistance to moisture damage. The ranking of the three mixes based on suction measurements correlate very well with the field performance as shown in Fig. 72. It also has very good correlation bond energy ratio parameters as shown in Fig. 74 and a good correlation with the DMA results as shown in Fig. 75.

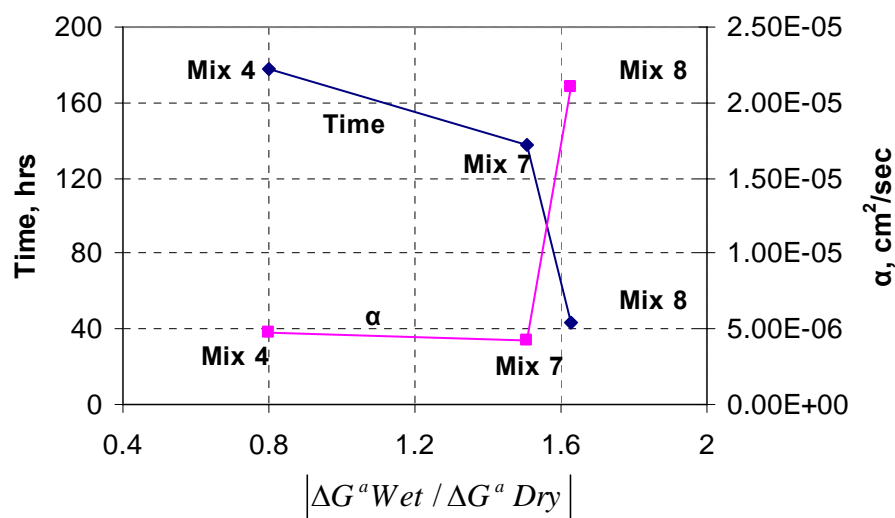


Fig. 74. Elapsed Time, Diffusion Coefficient ( $\alpha$ ), and Adhesive Wetting Bond Energy

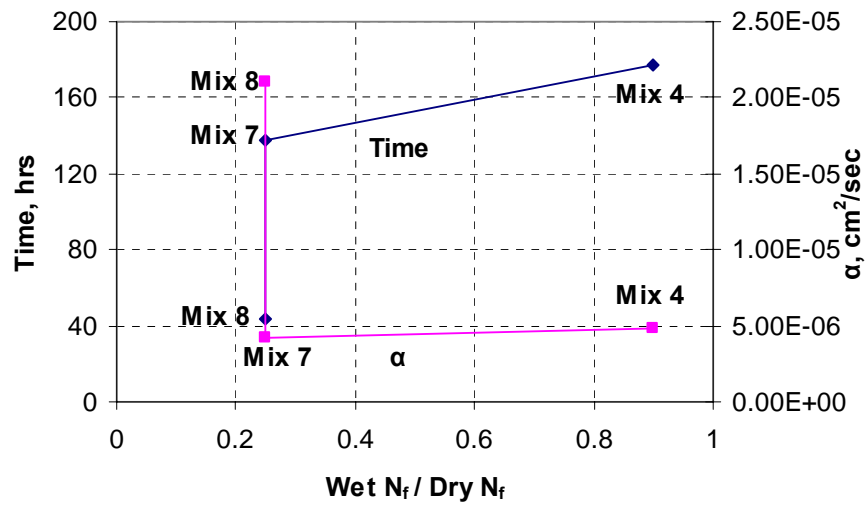


Fig. 75. Elapsed Time, Diffusion Coefficient ( $\alpha$ ), and DMA Results



## CHAPTER V

### CONCLUSIONS AND RECOMMENDATIONS

#### 5.1 Conclusions

Suction has been studied for many years; however this is a new concept for HMA, and there is no experimental method for measuring suction in HMA. The first objective of this study was achieved by developing a procedure to measure the total suction in HMA mixes. Thermocouple psychrometers were used to measure total suction. After conducting many tests with different setups, it was found that the drying test using a 60 °C temperature-controlled room is the proper setup for measuring the total suction using thermocouple psychrometers. Suction measurements for limestone and granite specimens revealed that fine specimens had the highest suction. This is attributed to the fact that these mixes had small air voids that correspond to high specific surface area and high suction. Also, it was found that the total suction measurements of limestone specimens were higher than the measurements of granite specimens. The total suction values of limestone specimens reached the limit of thermocouple psychrometer before those of the granite specimens. This is because the granite mixes in general had larger air void sizes than the limestone mixes. It is interesting to note that a parabolic relationship exists between suction and moisture damage in limestone specimens. It can be hypothesized that some specimens had low suction, which made it easier for the air voids to lose moisture to the asphalt, causing more moisture damage. On the other extreme, some specimens had high suction, which made it difficult for the specimens to lose moisture to the environment, which caused moisture damage. It seems that there exists an optimum suction value at which the moisture damage was minimal. The granite

specimens did not exhibit a relationship between suction and moisture damage. This can be caused by the large air voids in granite specimens, and the poor bonding between granite aggregate and binder, as reported from the field.

In the second part of this study, the total suction was measured in sand asphalt specimens. The soaking test was used to measure the change of total suction with time. The results showed that water diffused into sand asphalt specimens that are known to have poor resistance to moisture damage faster than those that are known to have good resistance to moisture damage. The diffusion coefficient was calculated in sand asphalt, which depends on the change of total suction with time. The results revealed that the diffusion coefficient can be used to differentiate between mixes with poor and good resistance to moisture damage.

## **5.2 Recommendations**

- More experimental measurements should be conducted to define the range of suction associated with poor resistance to moisture damage. The drying test setup that was developed to measure the total suction in HMA in this study should be used.
- More diffusion coefficient measurements should be taken to define the range associated with poor resistance to moisture damage.

## REFERENCES

- Aitchison G. D., Ed., (1965). *Moisture equilibria and moisture changes in soils beneath covered areas, A Symp.*, Butterworths, Australia.
- Aubeny, C., and Lytton, R. L. (2003). "Estimating strength versus location and time in high plasticity clays." *Research Report No. FHWA/TX-03/2100-PI*, Texas Transportation Institute, College Station, Texas.
- Birgisson, B., Roque, R., and Page G. (2003). "Evaluation of water damage using hot mix asphalt fracture mechanics." *Journal of the Association of the Asphalt Paving Technologists*, 72, 424-462.
- Birgisson, B., Roque, R., and Page G. (2004). "The use of a performance-based fracture criterion for the evaluation of moisture susceptibility in hot mix asphalt." *Transportation Research Record* 3431, TRB, 55-61.
- Bulut, R., Lytton, R. L, and Wray, W. K (2001), "Soil suction measurement by filter paper." *ASCE Geotechnical Special Publication Number 115*, 243-261.
- Campbell Scientific, Inc. (1997). *CR7 measurement and control system instruction manual*, Campbell Scientific, Inc., Logan, Utah.
- Campbell Scientific, Inc. (2001). *PC208W datalogger support software instruction manual*, Campbell Scientific, Inc., Logan, Utah.
- Castelblanco, A. (2004). "Probabilistic analysis of air void structure and its relationship to permeability and moisture damage of hot mix asphalt." M.S. Thesis, Department of Civil Engineering, Texas A&M University, College Station, Texas.
- Edlefsen, N. E, and Anderson, A. B. C. (1943). "Thermodynamics of soil moisture." *Hilgardia*, 15, 31-298.

- Fredlund, D. G., and Rahardjo, H. (1993). *Soil mechanics for unsaturated soils*, John Wiley & Sons, Inc., New York.
- Krahn, J., and Fredlund, D. G. (1972). "On total matric and osmotic suction." *J. Soil Sci.*, 114(5), 339-348.
- Laliberte, G. E., and Corey, A. T. (1967). "Hydraulic properties of disturbed and undisturbed soils." *Permeability and capillary of soils*, ASTM, Philadelphia, 56-71.
- Lang, A. R. G. (1967). "Osmotic coefficients and water potentials of sodium chloride solutions from 0 to 40°C." *Australian Journal of Chemistry*, 20, 2017-2023.
- Lytton, R. (2005a), "Adhesive fracture in asphalt concrete mixtures." In *Asphalt technology handbook*, J. Youtcheff, ed., Marcel Dekker, Monticello, NY, (In Press).
- Lytton, R. (2005b). *Micromechanics of civil engineering materials*, Class Handouts, CVEN 613, Texas A&M University, College Station, Texas.
- Mitchell, P. W. (1979). "The structural analysis of footings on expansive soil." *Report Research No. 1*, K. W. G. Smith and Assoc. Pty. Ltd., Newton, South Australia.
- Scullion T., and Saarenketo T. (1997). "Using suction and dielectric measurements as performance indicators for aggregate base materials." *Transportation Research Record* 1577, 37-44.
- Sood, E. (2005). "Determination of diffusion coefficient for unsaturated soils." M.S. Thesis, Department of Civil Engineering, Texas A&M University, College Station, Texas.
- Syed, I., Scullion, T., and Randolph R. B. (2000). "Tube suction test for evaluating aggregate base material in frost and moisture-susceptible environments." *Transportation Research Record* 1709, 78-90.

Tang, D. (2003). "A simplified formulation for moisture diffusion through partly saturated clays." M.S. Thesis, Department of Civil Engineering, Texas A&M University, College Station, Texas.

Wescor, Inc. (2001). *HR-33T dew point microvoltmeter, instruction/services manual*, Wescor, Inc., Logan, Utah.

Zollinger, C. J. (2005). "Application of surface energy measurements to evaluate moisture susceptibility of asphalt and aggregates." M.S. Thesis, Department of Civil Engineering, Texas A&M University, College Station, Texas.

**APPENDIX A**  
**MACRO EXCEL FILE FOR CALCULATING CORRECTED**  
**MICROVOLT READINGS**

Sub copy\_col()

Dim val1 As Double

Dim val2 As Double

Dim pasterow As Integer

Dim pastecol As Integer

Dim row As Integer

Dim col As Integer

Dim startrow As Integer

Dim startrow1 As Integer

Dim val As Double

Dim Tval As Double

Dim Xval As Double

Dim Newval As Double

pasterow = 1

pastecol = 18

startrow = 3

Sheets("Sheet1").Select

```
For counter = startrow To 2720 Step 10
```

```
startrow1 = counter
```

```
For row = startrow1 To startrow1 + 7
```

```
For col = 4 To 17 Step 3
```

```
Cells(row, col).Select
```

```
Application.CutCopyMode = False
```

```
Selection.Copy
```

```
Cells(pasterow, pastecol).Select
```

```
ActiveSheet.Paste
```

```
val = Cells(pasterow, pastecol).Value
```

```
Tval = Cells(row, col - 2).Value
```

```
Xval = Cells(row, col - 1).Value
```

```
Newval = (val / (0.325 + (0.027 * Tval))) - Xval
```

```
Cells(pasterow, pastecol).Value = Newval
```

```
pastecol = pastecol + 1
```

```
Next col
```

```
Next row
```

```
pasterow = pasterow + 1
```

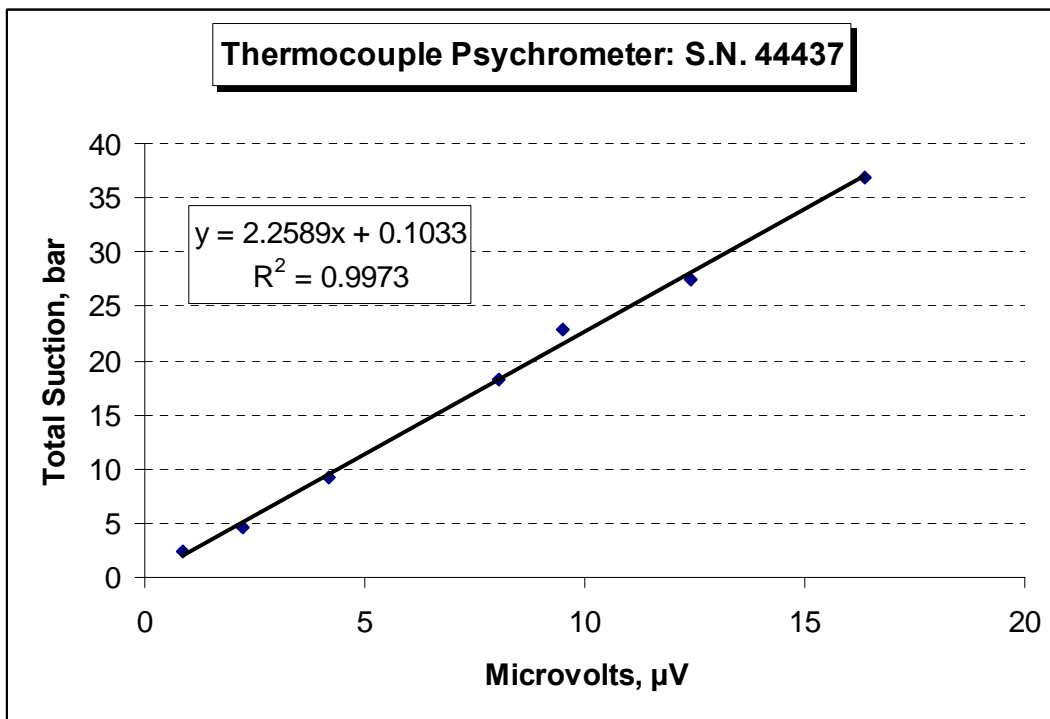
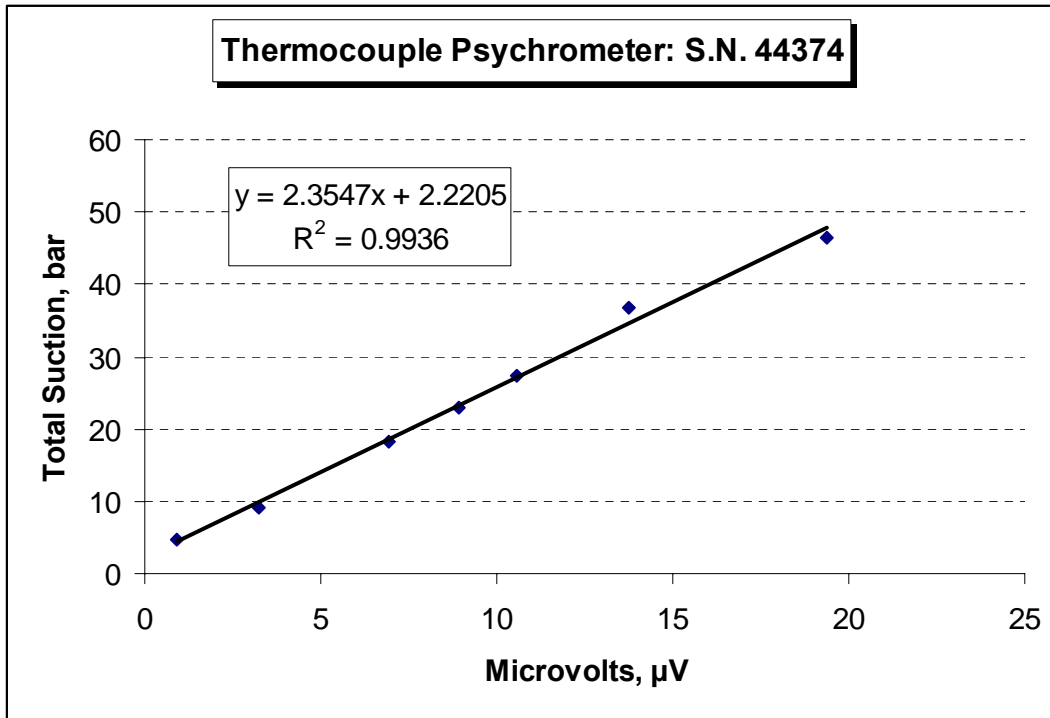
```
pastecol = 18
```

```
Next counter
```

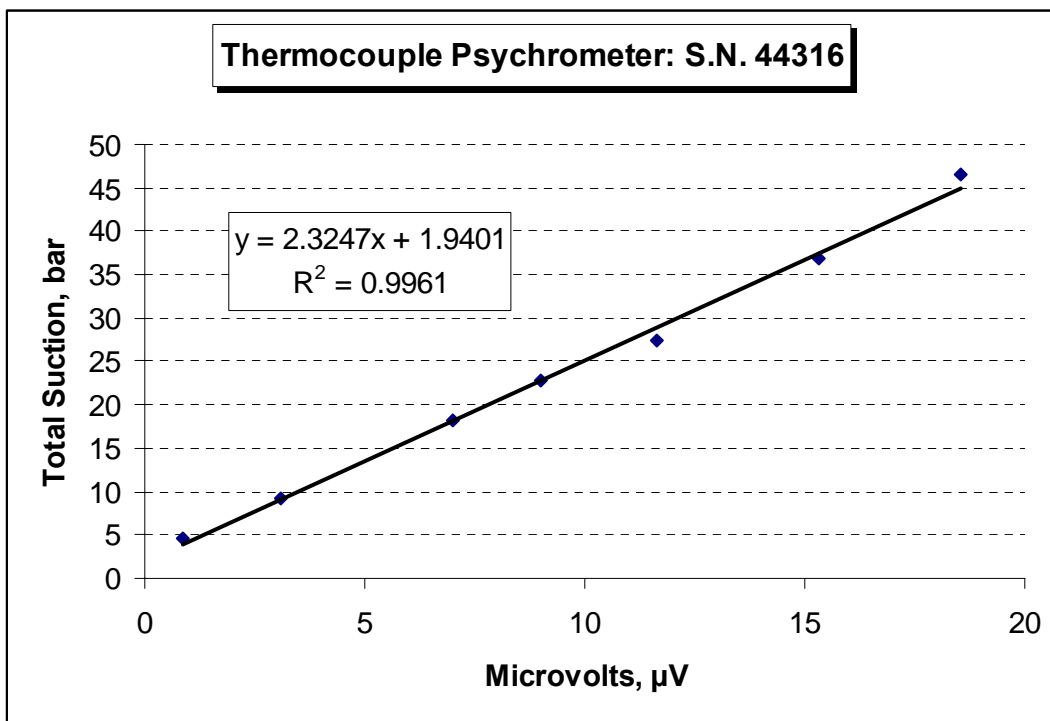
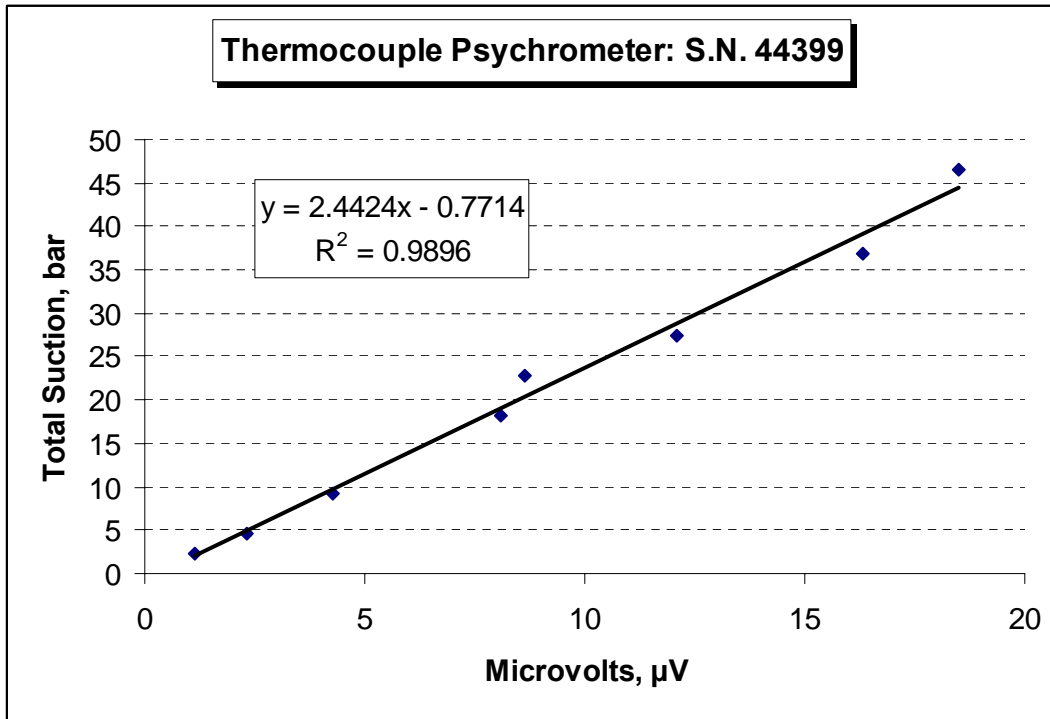
```
End Sub
```

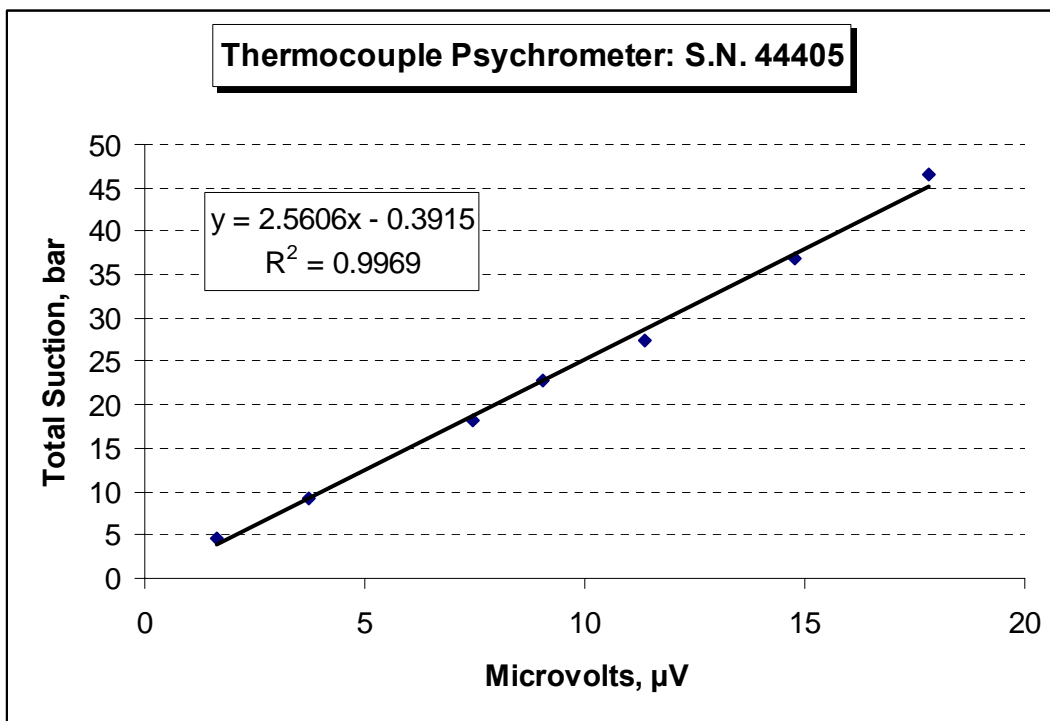
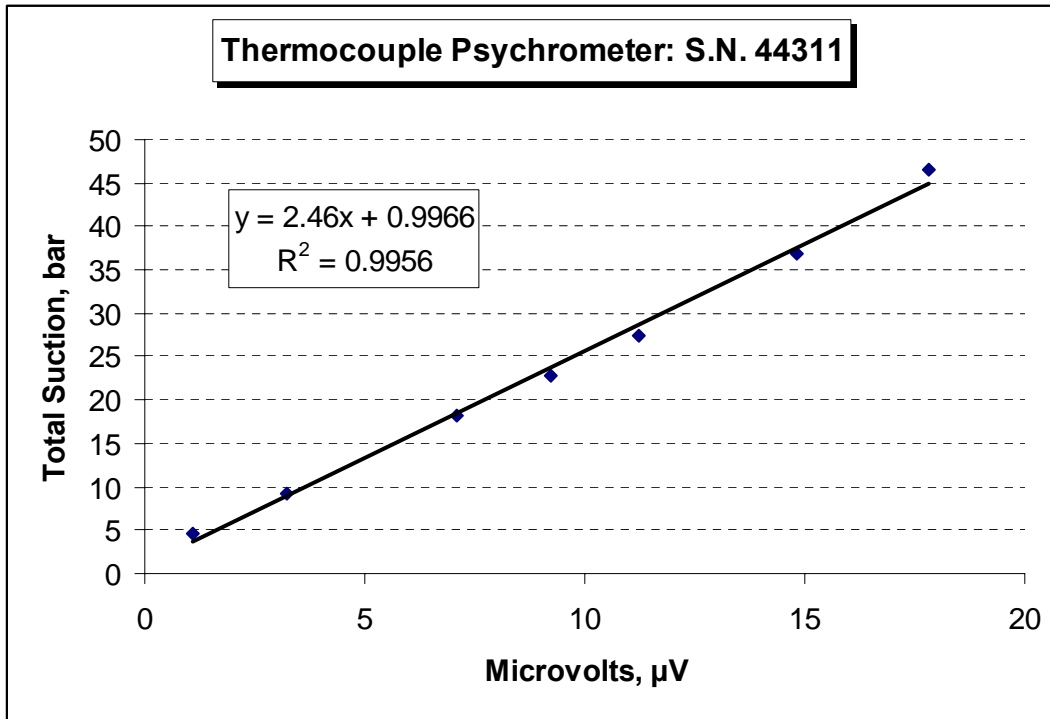
## APPENDIX B

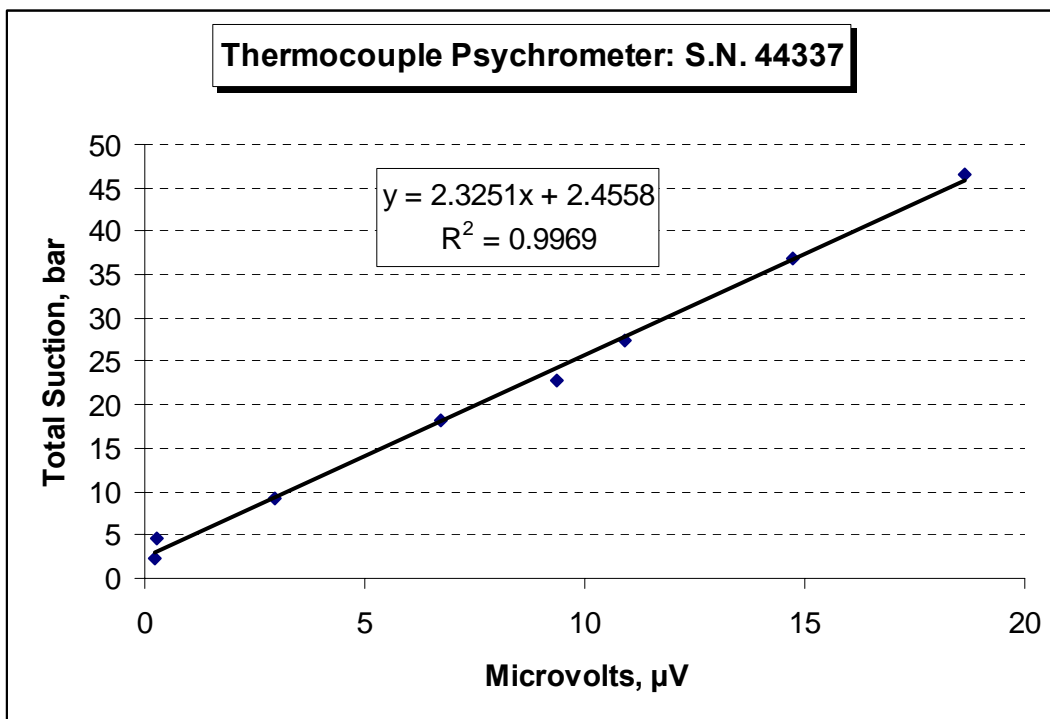
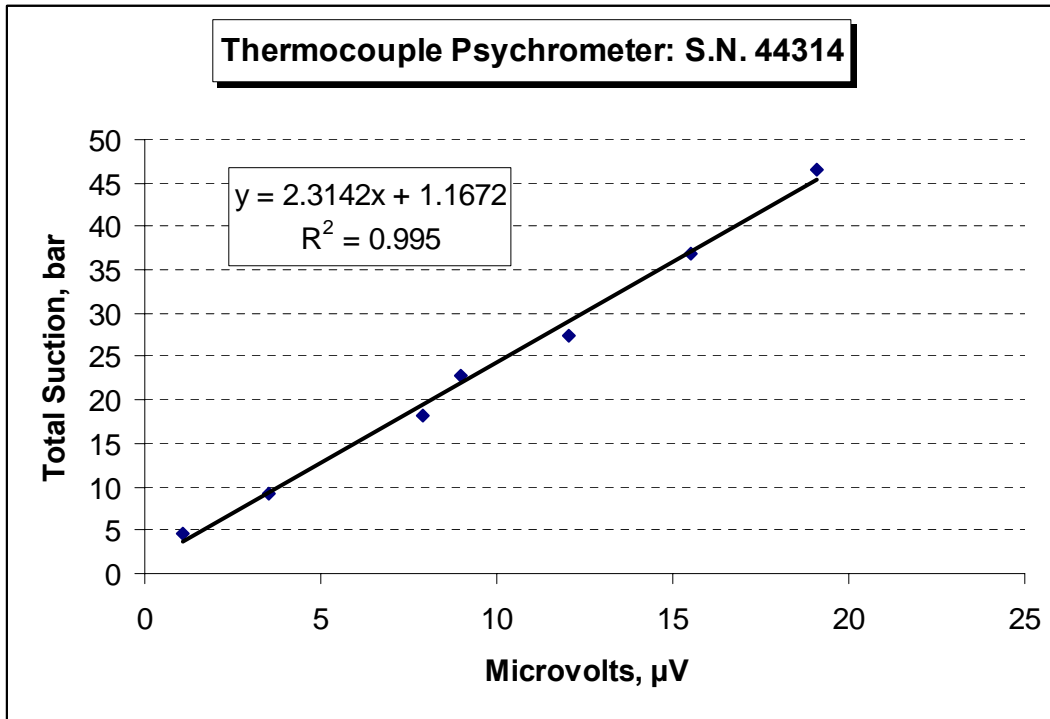
## CALIBRATION CURVES OF THERMOCOUPLE PSYCHROMETERS

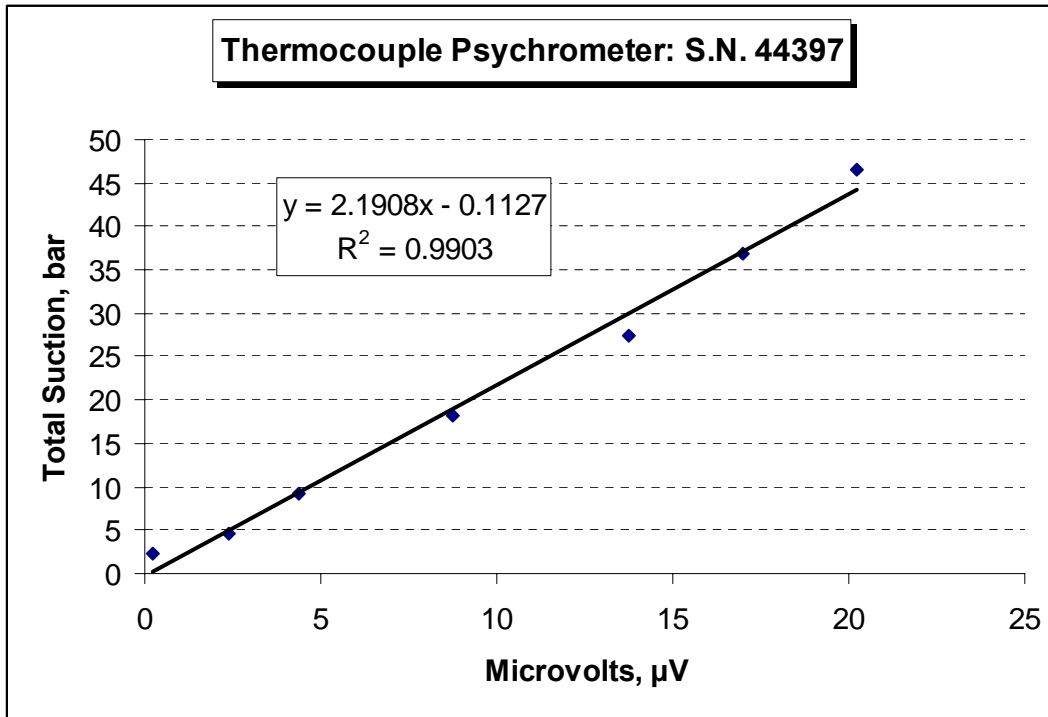




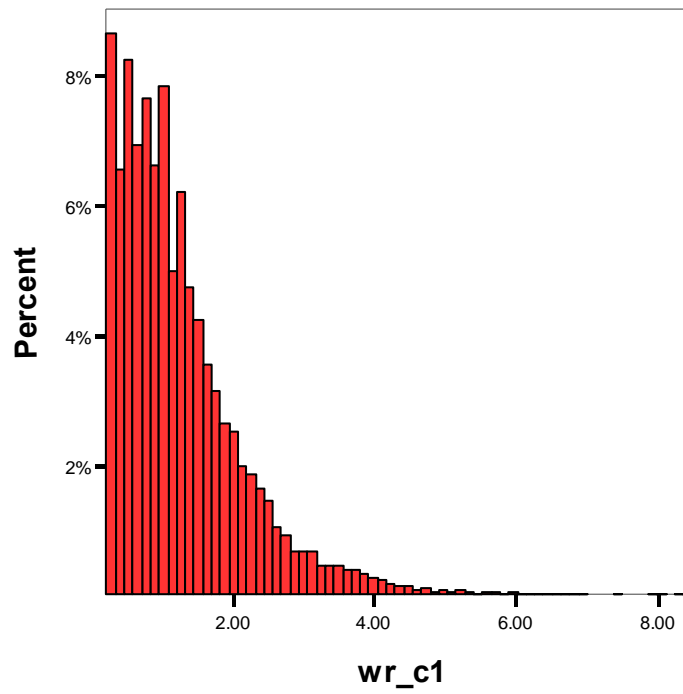


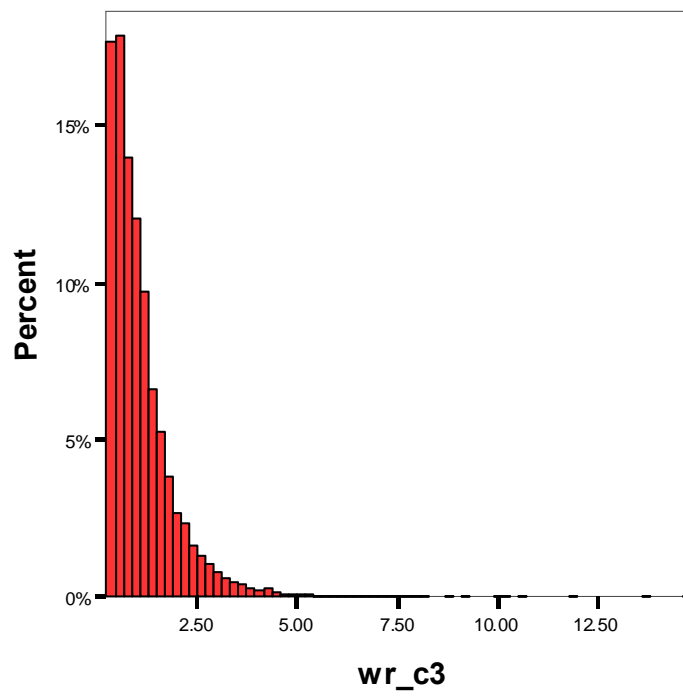
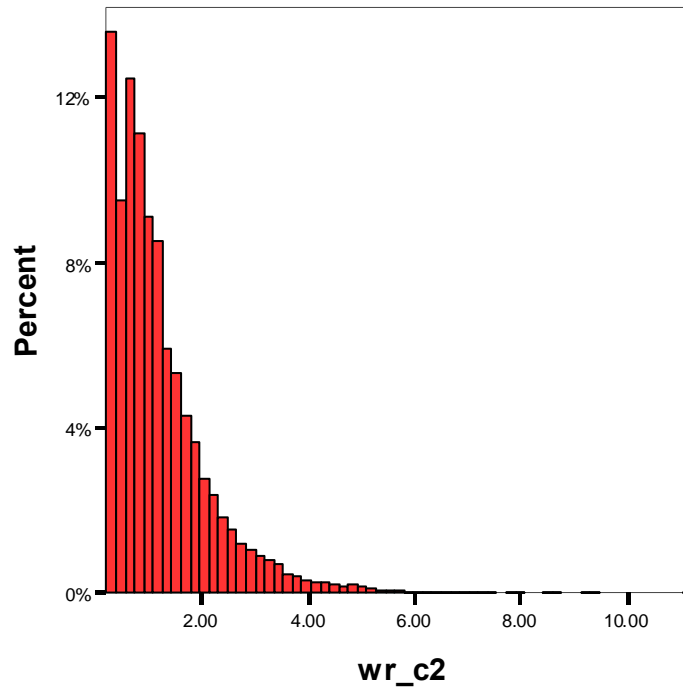


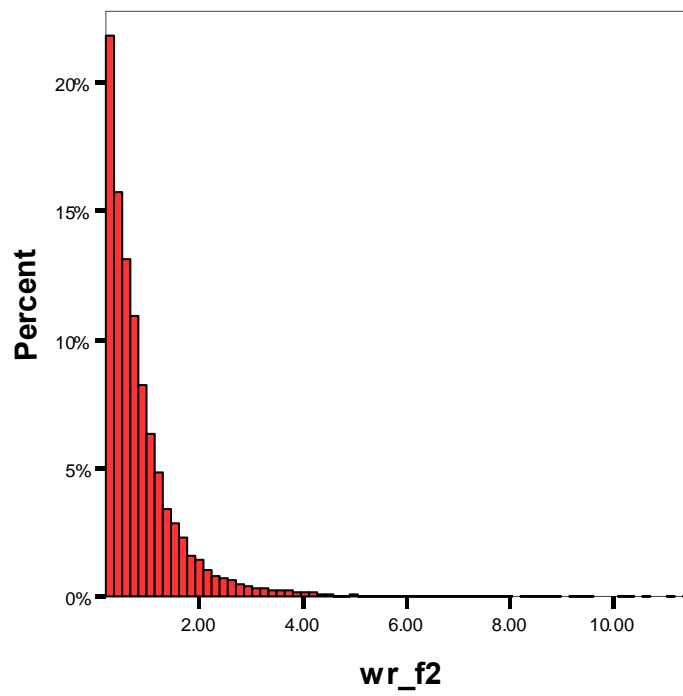
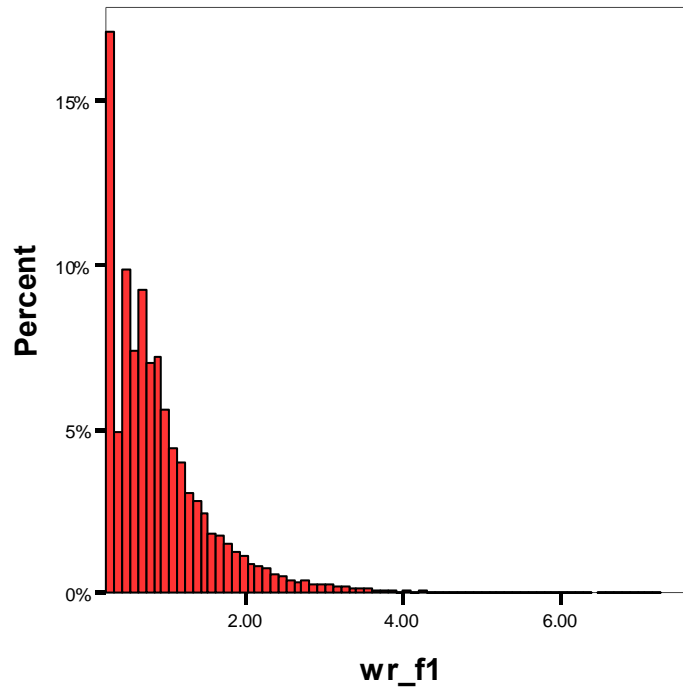


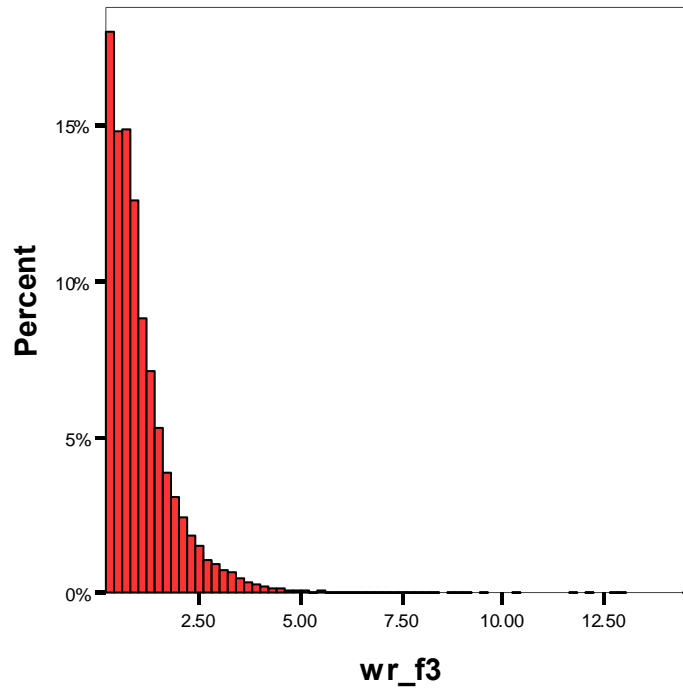


**APPENDIX C**  
**AIR VOID DISTRIBUTION FOR LIMESTONE SPECIMENS**  
**(CASTELBLANCO 2004)**



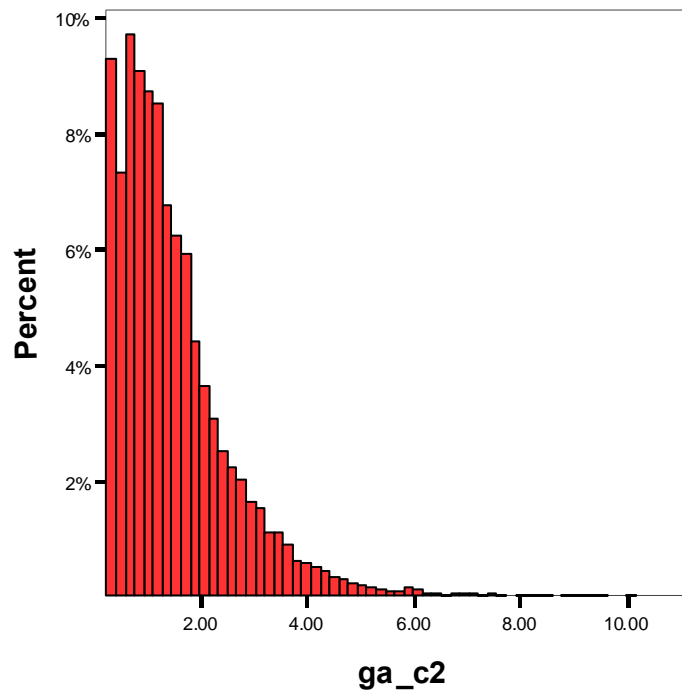


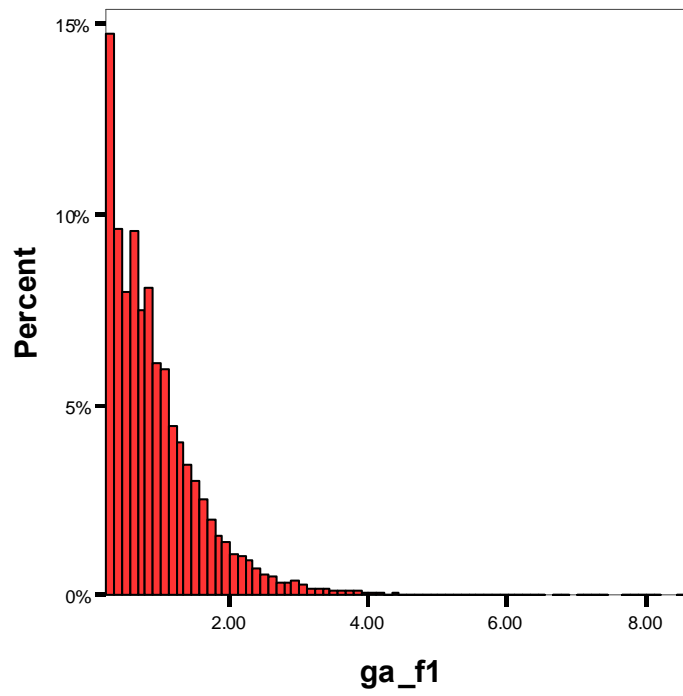
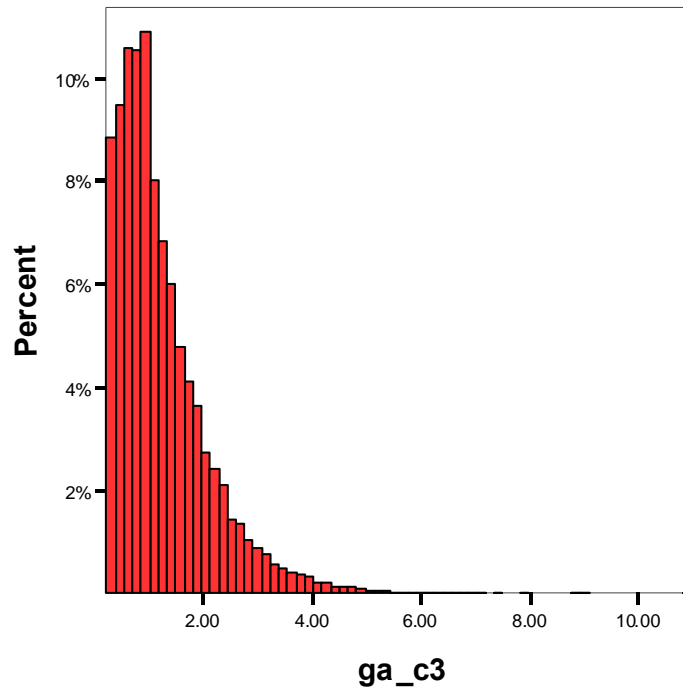


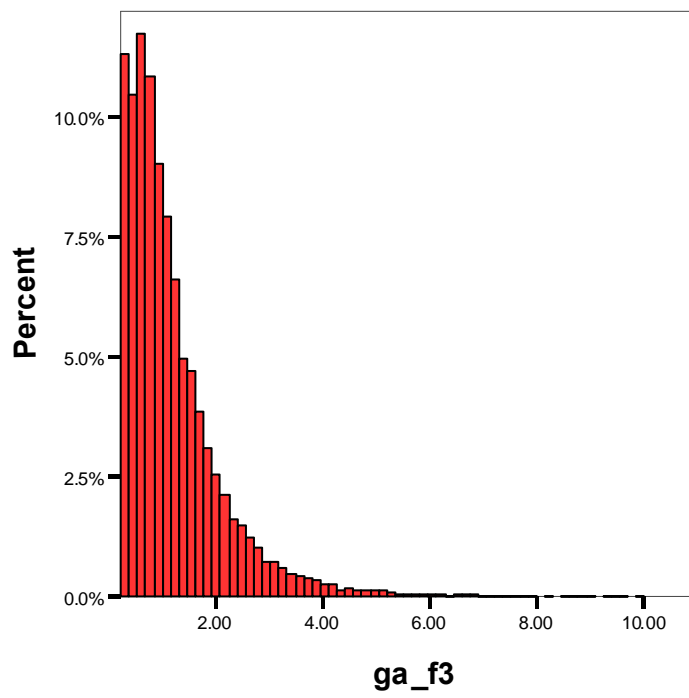
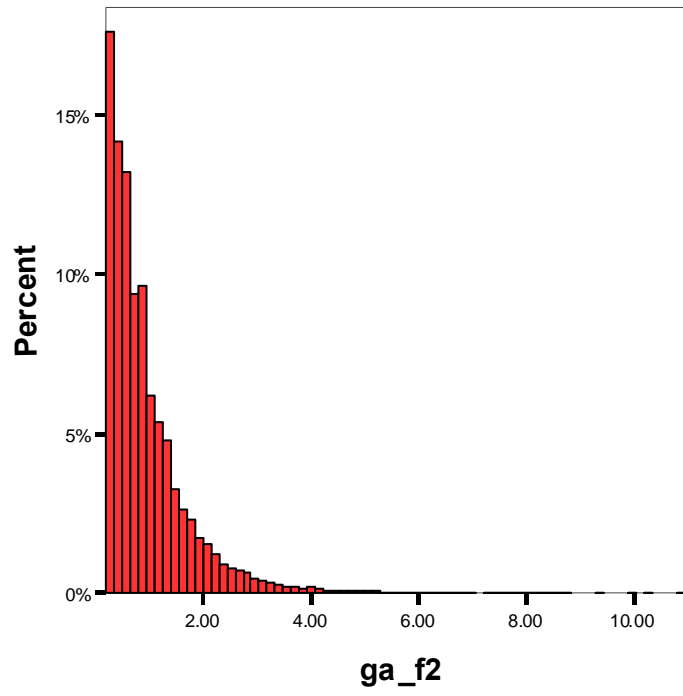




### Air Void Distribution for Granite Specimens (Castelblanco 2004)



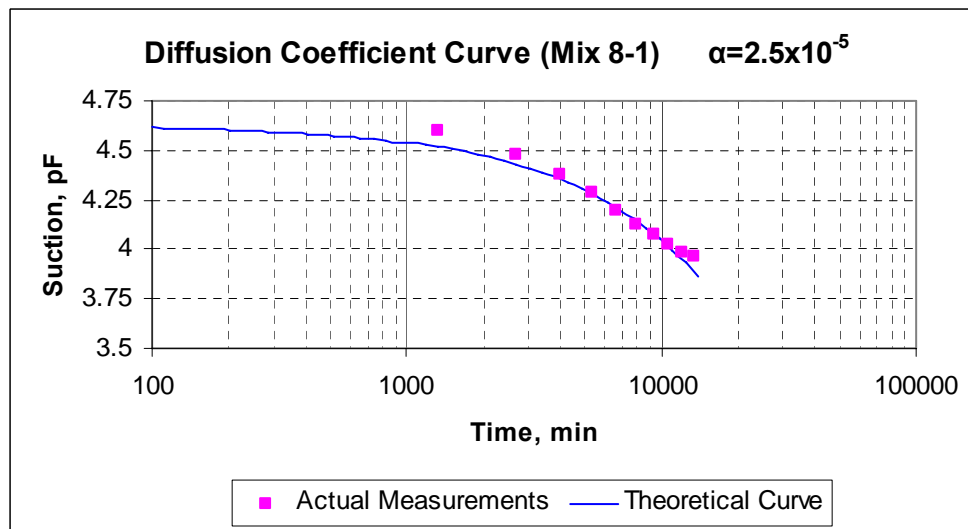
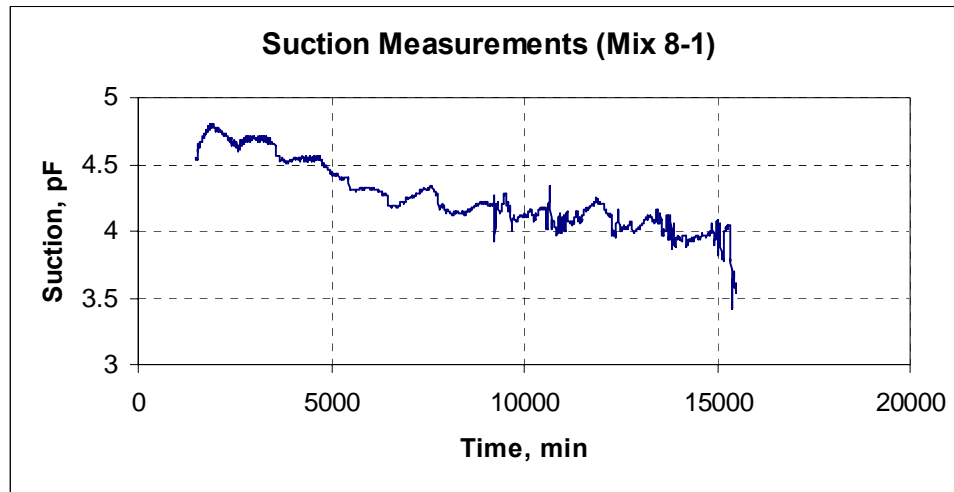




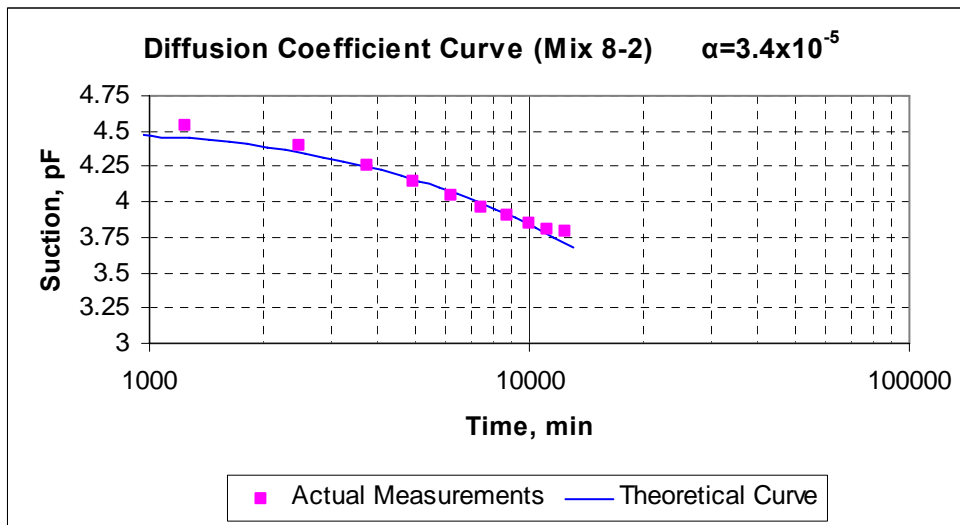
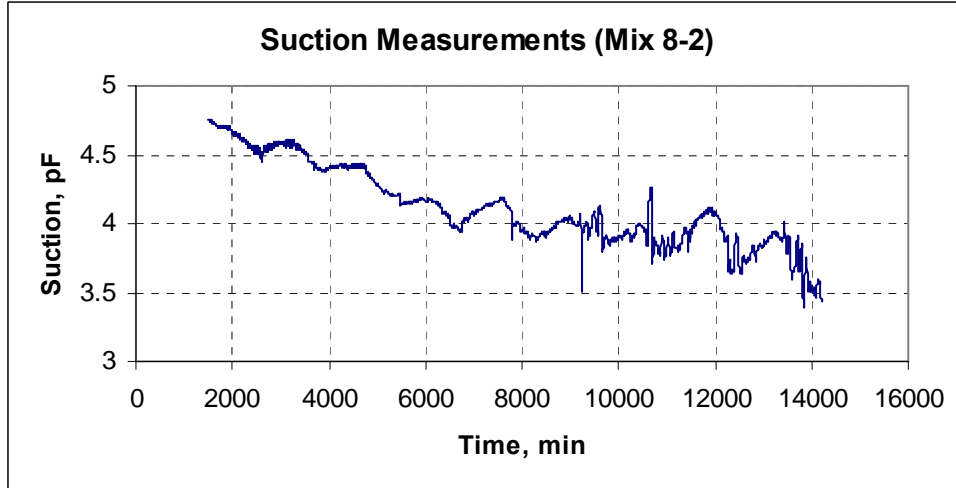
**APPENDIX D**

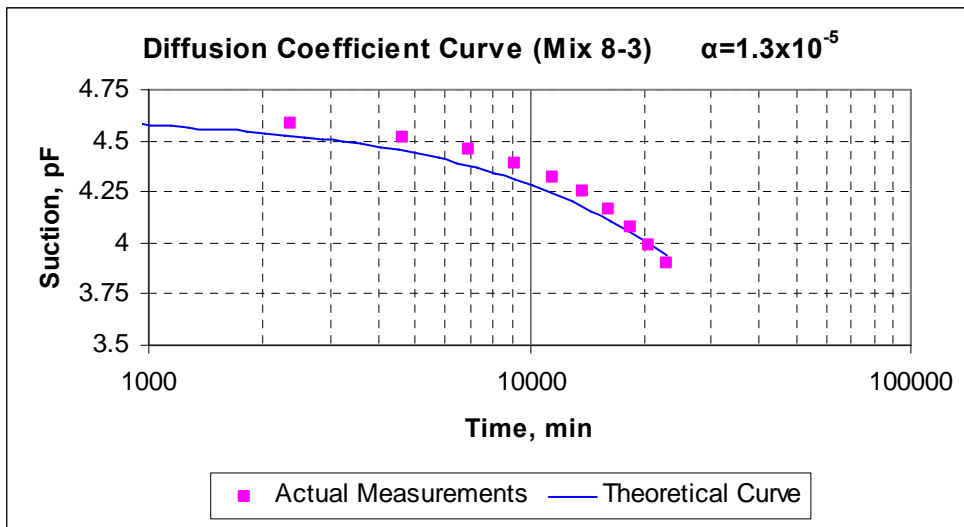
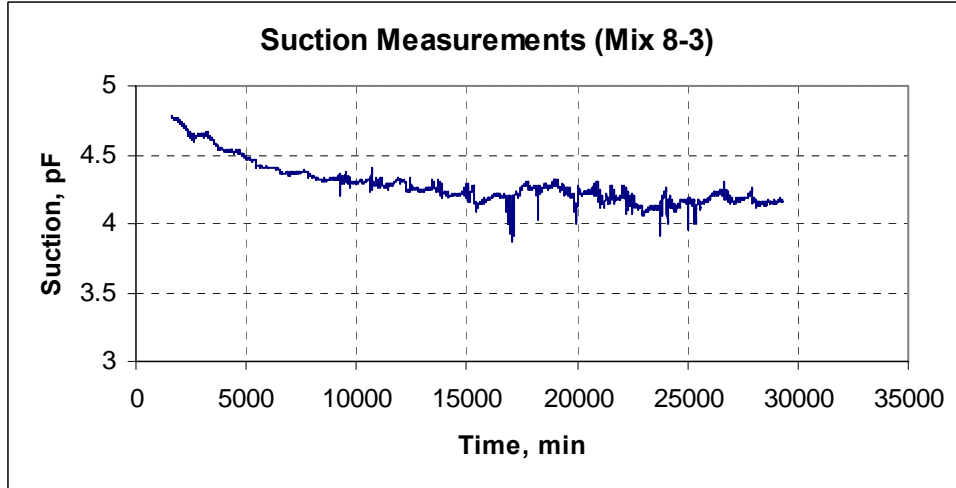
**TOTAL SUCTION MEASUREMENTS AND DIFFUSION**

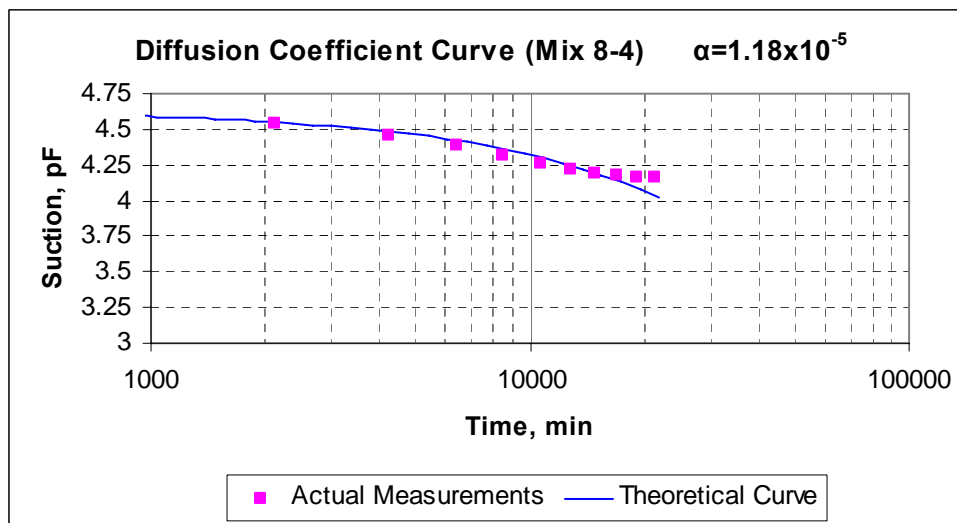
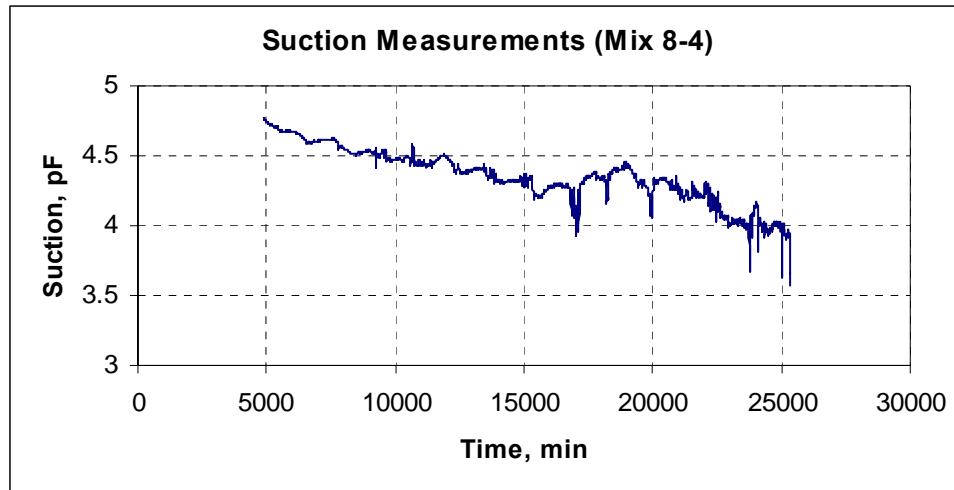
**COEFFICIENT CURVE**

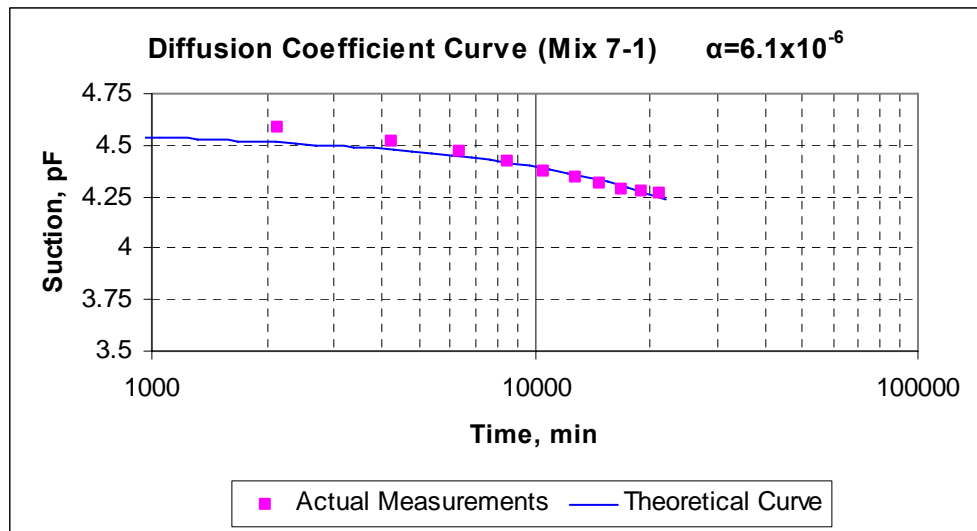
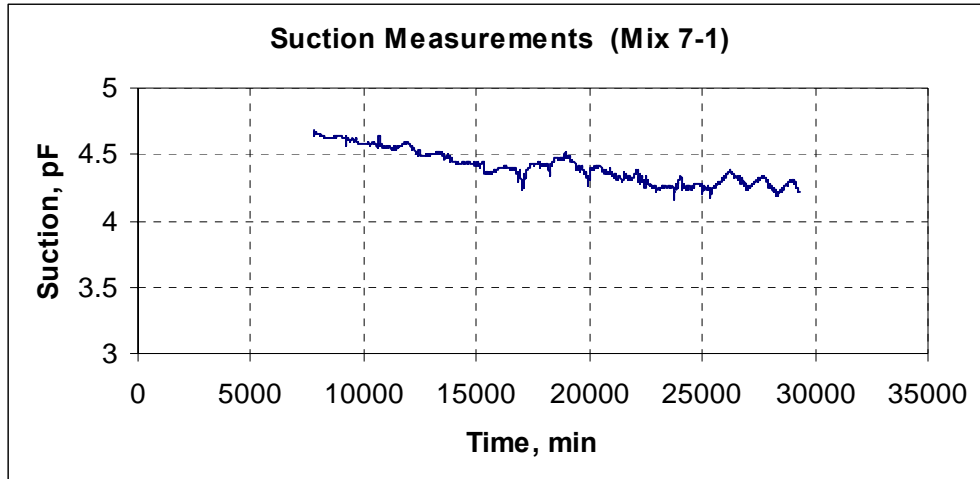


(Note:  $\alpha$ ,  $\text{cm}^2/\text{sec}$ )

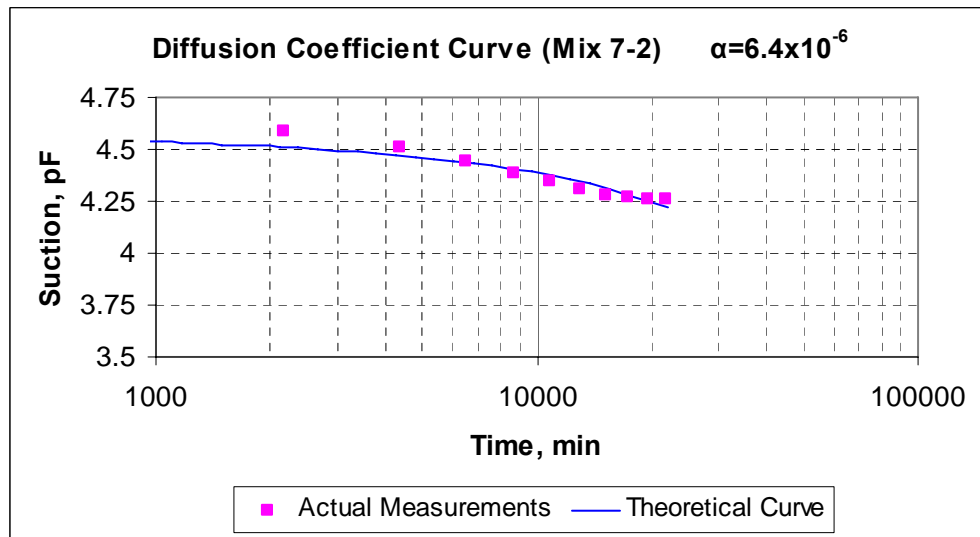
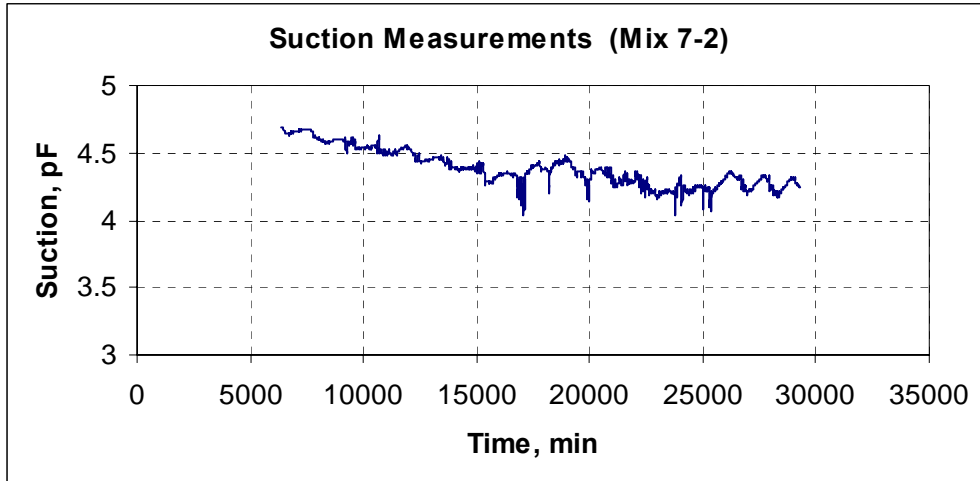


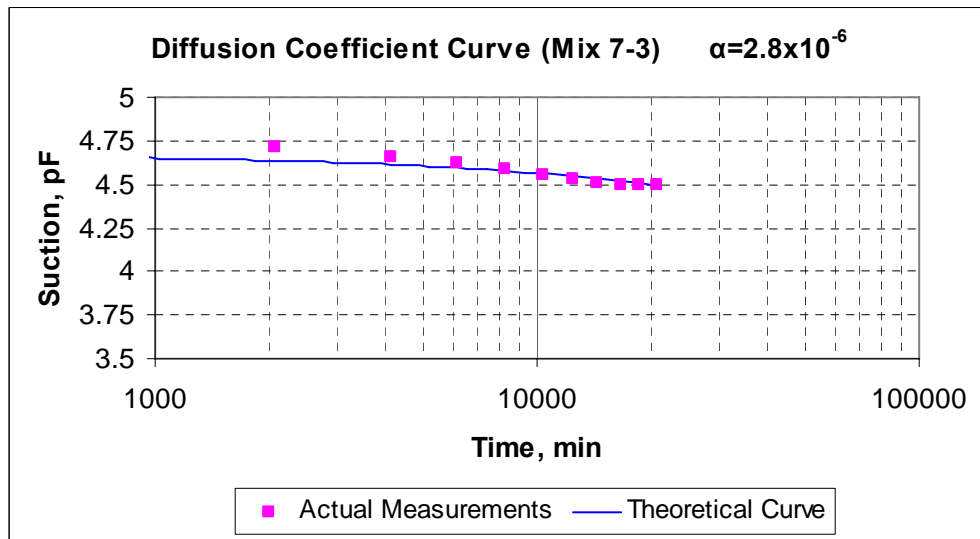
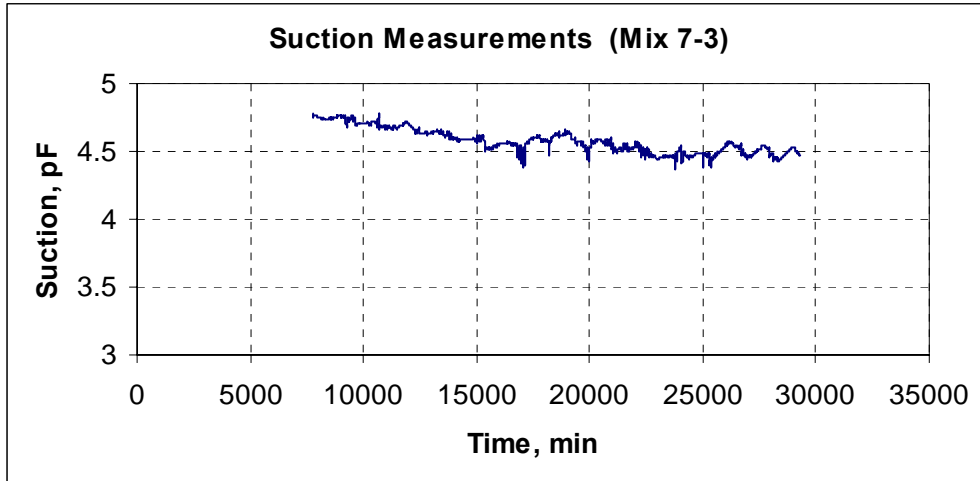


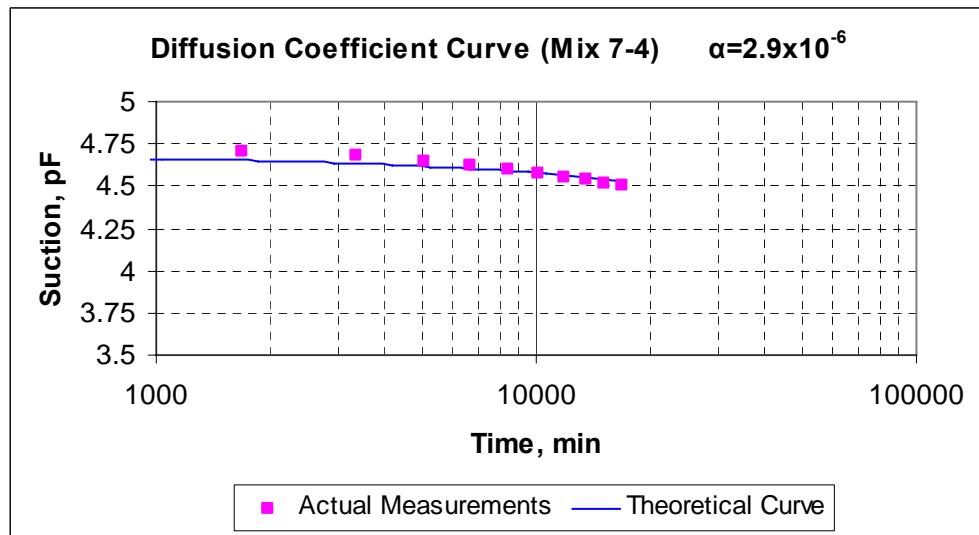
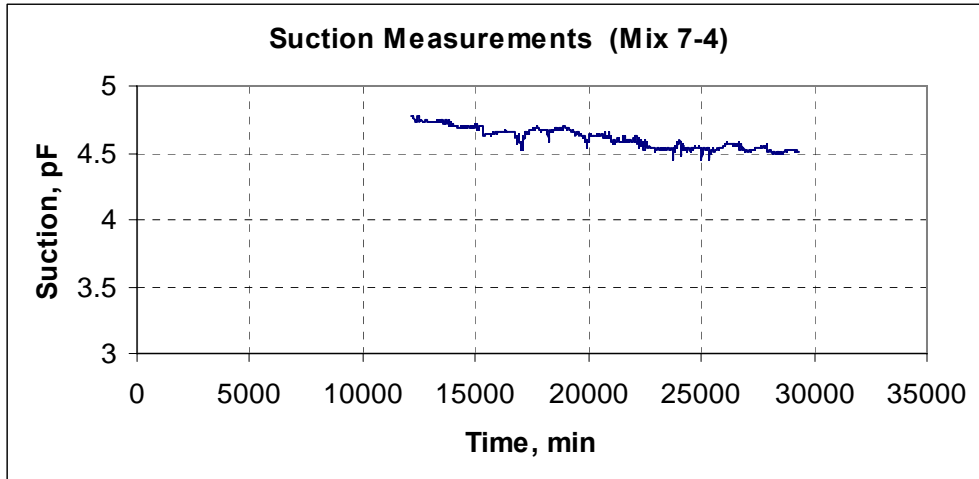


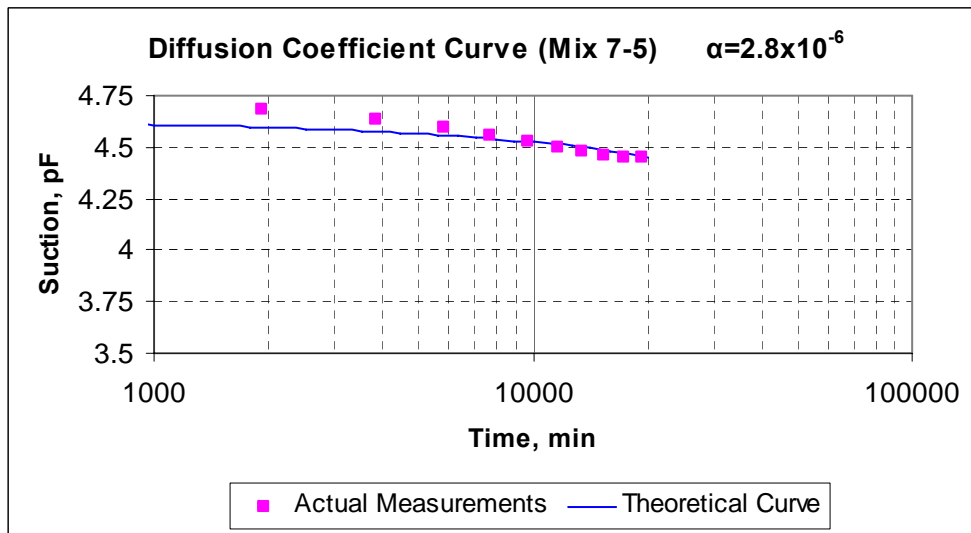
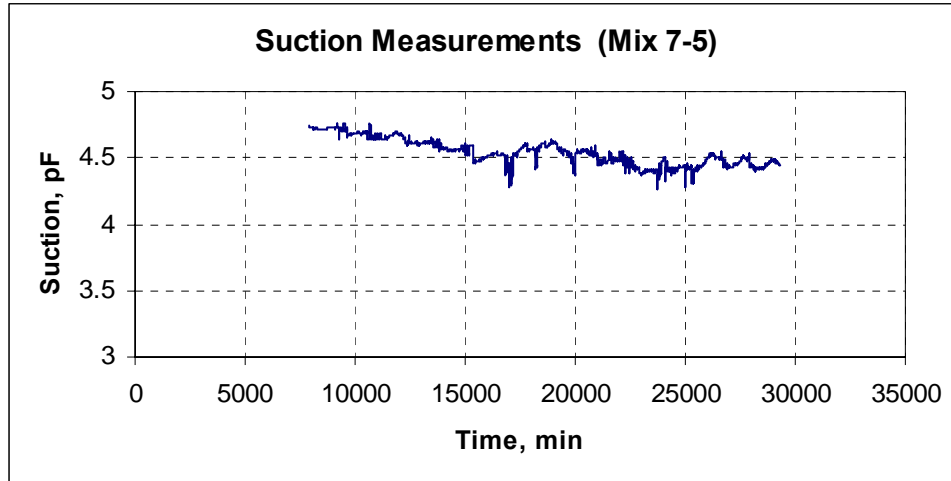


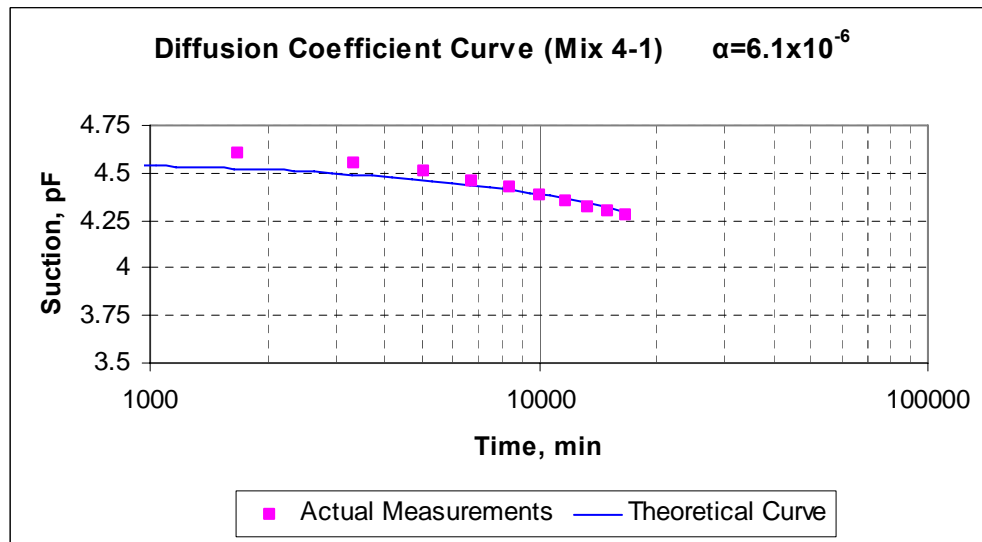
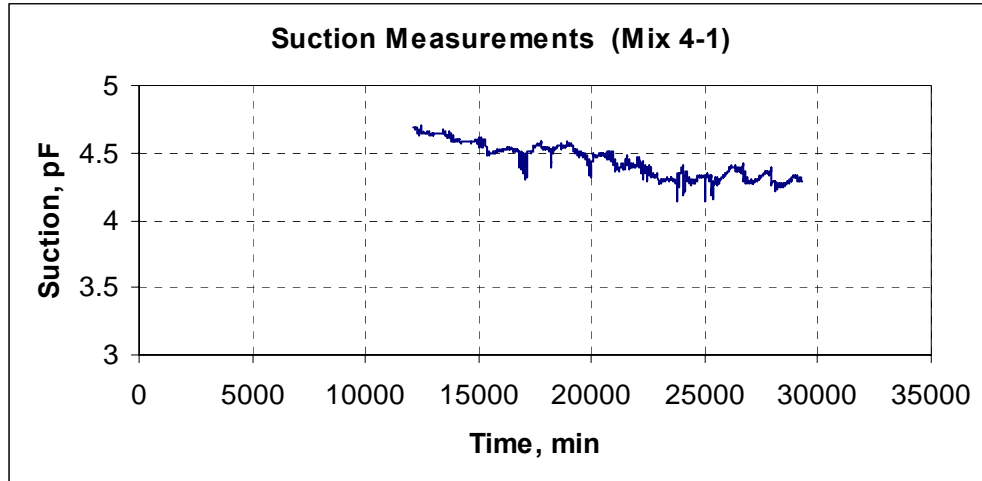


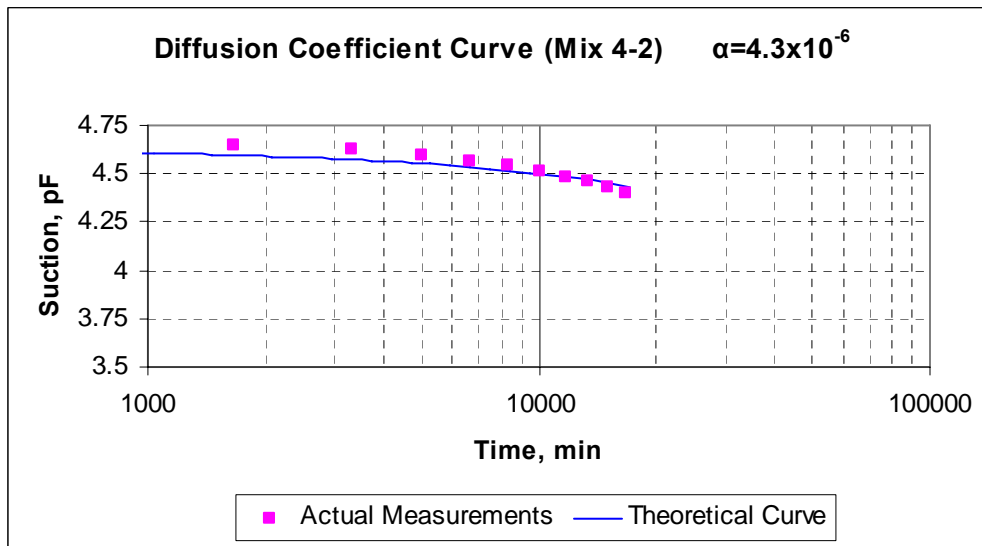
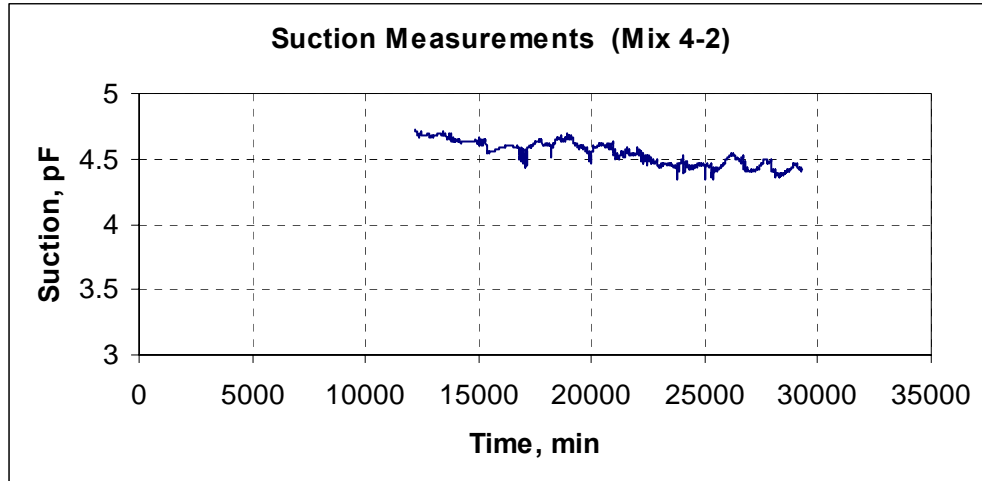


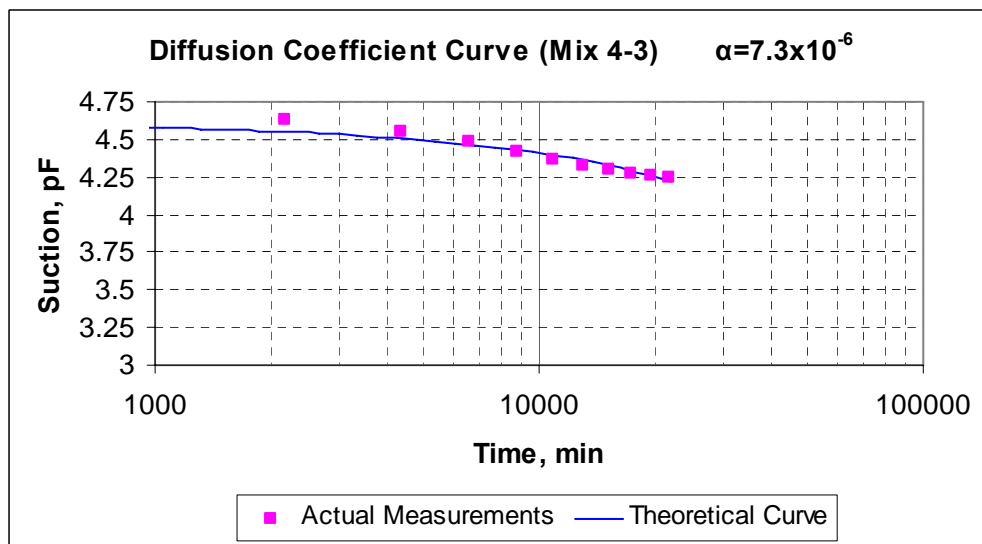
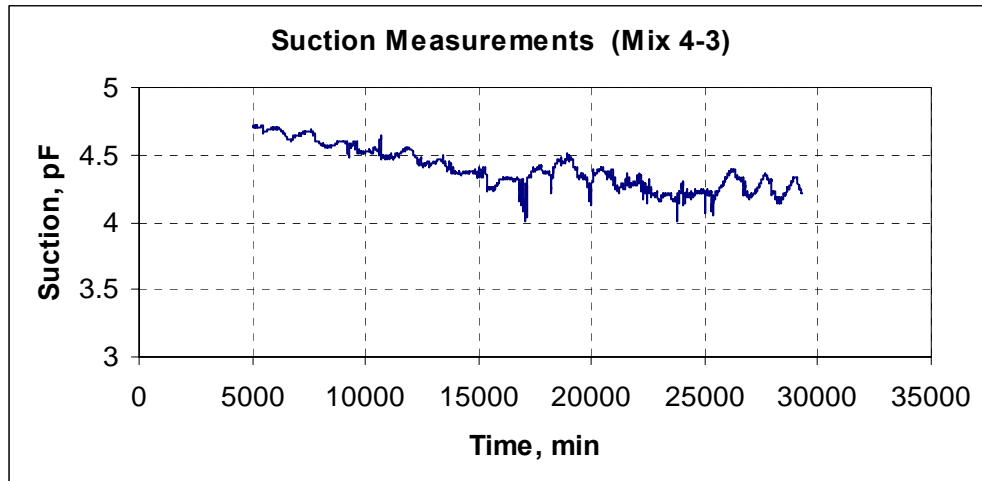


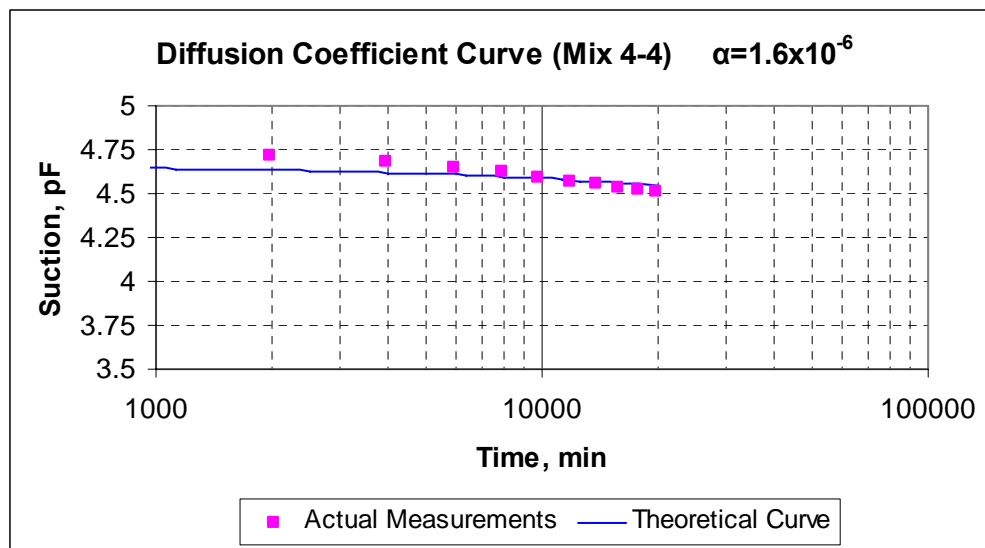
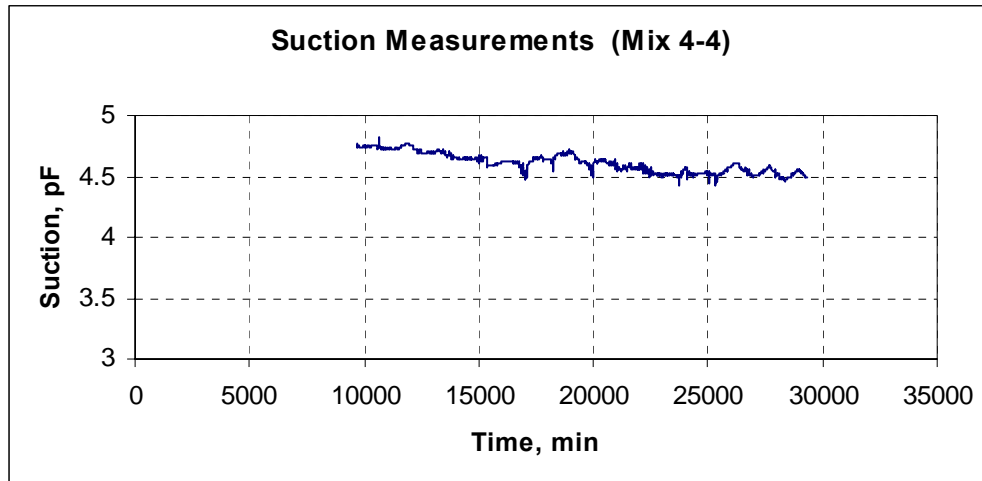




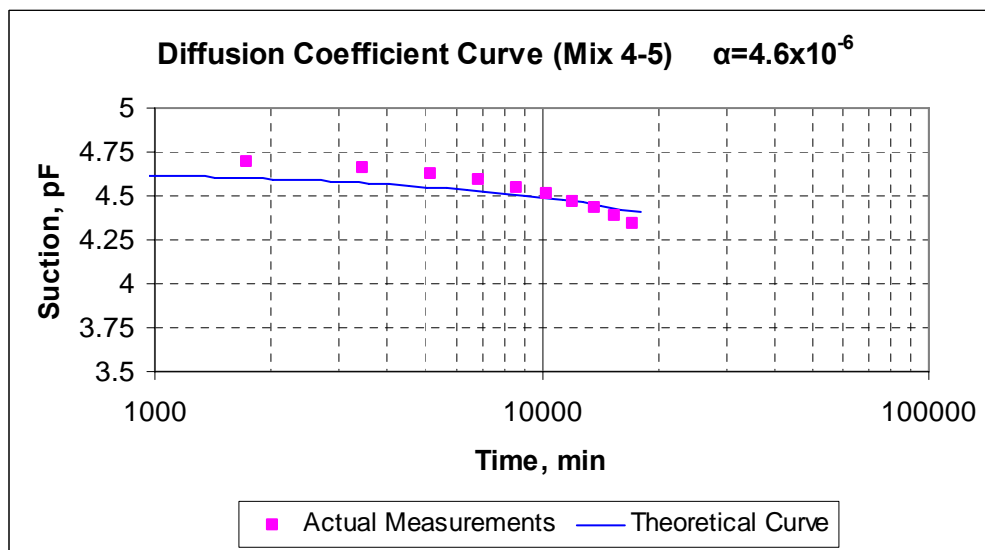
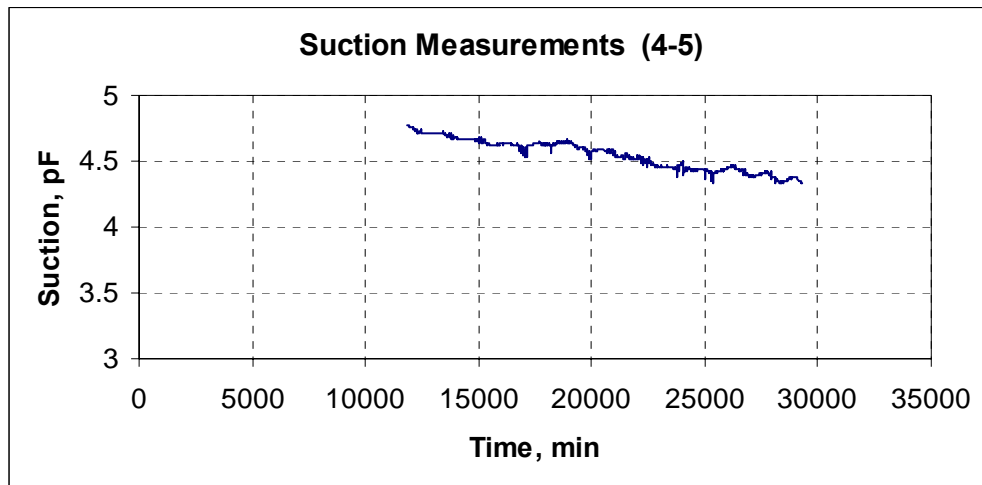












## APPENDIX E

### MATLAB PROGRAM “ALPHAWETTINGTEST”

```
%program to estimate alpha from wetting test
```

```
clear all
```

```
alpha0=input('starting alpha ');
```

```
alphaf=input('final alpha ');
```

```
nalpha=input('number of alpha trials ');
```

```
u1=input('suction of the liquid, pF ');
```

```
u0=input('initial suction, pF ');
```

```
x=input('coordinate of psychrometer ');
```

```
L=input('length of specimen ');
```

```
tm=input('measurement times ');
```

```
um=input('suction measurements ');
```

```
num=input('number of measurements ');
```

```
%compute error as function of alpha
```

```
dalpha=(alphaf-alpha0)/(nalpha-1)
```

```
err(1:nalpha)=0
```

```
alpha=alpha0
```

```
for k=1:nalpha
```

```
    alph(k)=alpha;
```

```
    u=linspace(u1,u1,num);
```

```

for n=1:20

    c1=((2*(n)-1)-x)/(2*L);

    c2=(((2*(n)-1)-x)^2*(22/7)^2*tm*alpha)/(4*(L)^2);

    c3=(-1)^(n)/((2*(n)-1);

    c4=(4*(u1-u0))/(22/7);

    du=c4*c3*exp(-c2)*cos(c1);

    u=u+du;

end

errvector=um-u;

err(k)=norm(errvector);

alpha=alpha+dalpha;

end

display(alph(1:nalpha)')

display(err(1:nalpha)')

```

### Matlab Program “wetttest”

```

%program to plot theoretical curves for Wetting test

clear all

alpha=input('alpha ');
u1=input('suction of the liquid, pF ');
u0=input('initial suction, pF ');
tstart=input('start time ');
tstop=input('end time ');
num=input('number of time increments per log cycle ');
x=input('coordinate of psychrometer ');
L=input('length of specimen ');

%select solution times
ncycle=log10(tstop/tstart);
num=num*ncycle+1;
logtstart=log10(tstart);
logtstop=log10(tstop);
logt=linspace(logtstart,logtstop,num);
t=10.^logt;

%solution for suction
u=linspace(u1,u1,num);

```

```
for n=1:20

    c1=((2*(n)-1)-x)/(2*L);

    c2=(((2*(n)-1)-x)^2*(22/7)^2*t*alpha)/(4*(L)^2);

    c3=(-1)^(n)/((2*(n))-1);

    c4=(4*(u1-u0))/(22/7);

    du=c4*c3*exp(-c2)*cos(c1);

    u=u+du;

end

display(t(1:num)')

display(u(1:num)')
```

## VITA

### **EMAD ABDEL-RAHMAN KASSEM**

Permanent Address:  
Damas, Mit-Ghamr  
Dakahlia, Egypt  
Email: emad.kassem@gmail.com

### **EDUCATIONAL BACKGROUND**

M.S., Civil Engineering, Texas A&M University, College Station, Texas, USA  
August 2005

B.S., Civil Engineering, Zagazig University, Zagazig, Egypt  
May 2001

### **WORK EXPERIENCE**

Research Assistant  
Texas Transportation Institute, College Station, Texas, USA  
January 2004 – August 2005

Full-Time Engineer  
Misr Consult (Environmental & Infrastructure Studies), Cairo, Egypt  
December 2002 – December 2003

Site Supervisor  
Military Duty, Cairo, Egypt  
October 2001 – November 2002

Intern, Part Time Engineer  
Misr Consult (Environmental & Infrastructure Studies), Cairo, Egypt  
Summer 2000

Intern, Training Engineer  
Al-Madaen Engineering Firm, Al-Mahala Al- Kobra, Egypt  
Summer 1999